



The Optically Dark Gamma Ray Burst Population

James Duke

Supervisors:

Prof. Nial Tanvir

Prof. Paul O'Brian

Thesis submitted for the degree of
Master of Philosophy
at the University of Leicester

X-ray & Observational Astronomy Group
Department of Physics and Astronomy
University of Leicester

February 14th, 2011

The Optically Dark Gamma Ray Burst Population

James Duke

ABSTRACT

The *Swift* satellite has now detected more than 500 long-duration gamma ray bursts (GRBs), but statistical analysis remains challenging because the sub-sample with redshifts is relatively small and potentially biased. In this work we construct a more homogenous sample by imposing selection criteria designed to remove bursts which were not easily observable by large ground-based telescopes.

The resulting fraction is more complete in terms of redshifts, with $\sim 89\%$ of bursts in our sample having spectroscopically or photometrically constrained redshifts as opposed to $\sim 25\%$ of the full *Swift* sample. Based on our sample, we find the fraction of *Swift* bursts occurring at redshifts of $z > 6$ to be in the range $2 - 23\%$. We use this sample to constrain the fraction of *Swift* bursts which are ‘dark’, i.e. those for which the optical emission seems to be suppressed relative to the X-ray. Defining a burst to be dark by the criteria of Jakobsson et al. (2004), we find a dark burst fraction in the range $16 - 58\%$. Of these, we find the fraction of dark bursts occurring at $z > 6$ to be in the range $4.5 - 28\%$, and thus the fraction of dark bursts occurring at redshifts of $z < 6$ to be $\sim 72\%$.

From this we conclude that only a small fraction of dark bursts are caused by suppression of the optical afterglow due to an extreme redshift, and that the dominant cause of dark GRBs is dust extinction.

Given that we have shown a substantial fraction of *Swift* GRBs are dark, and a substantial fraction of these are due to dust extinction, we conclude that a significant fraction of GRBs occur in dusty environments, despite a preference for low metallicity environments. In agreement with recent authors, we believe that most dark GRBs are caused by moderate levels of dust at moderate redshifts ($A_V = 0.5 - 2.0$, $z = 1 - 3$), and show from redshift distributions derived from our sample that the largest fraction of *Swift* GRBs (and dark GRBs) occur at these redshifts, coincident with the vigorous epoch of star formation believed to have taken place in dusty environments at these redshifts (Hopkins and Beacom 2006).

ACKNOWLEDGEMENTS

Right, there are a fair few people I need to thank for getting me to this stage and helping my through my time doing this, and a fair few people who have given me absolutely no help at all but are still getting a mention.

First off and in many ways the most important person to thank is my long suffering supervisor, Nial Tanvir. He has successfully dragged me kicking and screaming through the many trials and tribulations of data analysis, rescued me time and time again from the dark pits dug by such evils as 'IRAF' and Gemini image analysis, and been my guide through one ill fated burger-fuelled trip to Alabama. Despite the myriad projects he seems to permanently involved in, he has always throughout the last few years found time to sacrifice for me, even if I have not been the perfect student. I feel here that I should also acknowledge Nial's little commented upon but nonetheless phenomenal stealth capabilities, which are on-par with that of any Royal Marine Commando. If the light in his office is on but the door closed, this means he is somewhere within a 1km radius, but I have no doubt it would take the most skilled and experienced of aborigine trackers to constrain his position any further. There have been occasions when I have considered setting traps, but I feel he would have merely slipped past these unscathed. But despite these sometimes phantom like qualities, Nial is always but an email away, no matter where in the world he might be, and no matter what problem I've had, no matter how trivial. He has really never failed to help me in this regard, and for that Nial, I give you thanks.

Nial is not the only one who has helped me day by day, and credit needs to go to several people. I would first like to thank one Evert Rol (Rol tide!) for in my first few weeks he was given the unenviable task of teaching me how to use the horror known as IRAF, and also all the skills associated with image analysis. He probably deserves some form of prize for pulling that off. I'd like to thank Phil Evans (probably much to his surprise) for knowing everything it is possible to know about Linux, computing and British bird calls, and thank him for solving the many computing problems or otherwise I have thrown across the office during my time here. I would also greatly like to thank Klaas Wiersema, for knowing absolutely everything else, and always finding the time to answer whatever annoying question I should have. I must also commend Klaas's collection of fantastic internet virals, that have helped keep me sane (to a given value of sane anyway), with particular reference to the infamous 'Sledgehammer Explosives' video and the ingenious 'Flush Tracker'.

Whilst I am on the topic of Klaas and Phil, having spent 2 years in the office with them, I also think some kind of acknowledgment should go to each of their long suffering desks. Both Phil and Klaas adopt a similar 'organic' strategy to desktop management,

which in my opinion puts considerable strain on their desks super-structures, far exceeding the stress tolerances their original designers intended. Although this organic desk management strategy appears to a casual observer to be near identical for both Klaas and Phil, I can confirm through long term observations that there are subtle but significant differences.

Phil employs what I call the 'expansionist' method, whereby every available unclaimed office surface is eventually assimilated, whereas Klaas adopts a much more intensive approach, whereby the layers of paperwork on his desk now exceed over one foot in height in the worst hit regions. Although Phil claims to have in recent months 'tidied' his desk, it still distinctly resembles in my opinion a portion of the Battle of the Somme fought through a major paper mill. I should probably also confess to Phil at this juncture that on many occasions over the past few years that I have randomly moved the various paper-drifts around on his desk in an experiment to see if he would notice. Results have thus far been negative on all counts. Klaas has however shamelessly made no such attempts at tidying his desk since I have been here, and preliminary analysis of deep-core drilling samples from the mounds of paper indicate that tidying may not have occurred since some time in the early 90s. I also, thanks to Klaas, currently have a geology paper in-prep about my recent discovery of what I have named 'printoutite', a hard sedimentary rock created from hundreds of tonnes of compressed layers of printed paper, formed within the very lowest layers of Klaas's desk.

As well as Klaas and Phil who have been great helps to me, I must also thank my other office mates who have made my time here better. Well, most of the time anyway. I would like to thank Antonia, a grizzled ex-teacher, for putting up with my various antics, even if my attempts to teach her how to swear properly have not yet bore fruit. As a word of warning to anyone reading this, try not to set her off talking about teaching. If you were not present at the beginning of the conversation you would swear blind she was talking about her time in the SAS. Its like listening to Vietnam flashbacks. I would of course like to thank Owen, whom I constantly monitor to make sure his enthusiasm does not reach critical levels, presumably resulting in some form of super nova, and commend him for his dogged two year long defence of the welsh culture. He should also be commended for being the only person I know for being able to sustain a conversation at volumes I have never before thought possible, for durations I initially believed to be implausible. He is also the only person I know that has inside the same ten minutes been genuinely excited about both the office door and the his office chair, for reasons the rest of us may well have wrote off completely had he not been there to point them out. Kim is the latest edition to our office, and although I have not known him long I wish him the best of luck as Nial's new student.

There are many people in the department I would also like to thank that have helped me and put their hand in various projects over the years. I'd like to thank Rhaana Starling

and Kim Page for teaching which way up X-ray data goes and how to use Xspec, and to Rhaana for helping me with some analysis in the first few months I had here. I'd like to thank Dick Willingale for taking the time to process some data for me that eventually went into this work. I'd like to particularly thank Andrew Levan who was a constant source of advice, suggestions, data and frisbee to me, particularly in my first few years. Then of course I must thank Paul O'Brian, my second supervisor, who has helped me jump through many hoops of fire along the way. He also has an inflatable alien in his office which I believe is worth a mention. Then there is Kiri, our postgraduate secretary who has successfully coped with the administrative-disruption field I apparently radiate, and has put up with my unique brand of filling in highly official forms.

I couldn't possibly go without thanking all my fellow students that don't share my office. I would like to thank the two that started at the same time as me, Dave Baker (whom I give the 'most spectacular diagrams' and 'most diagrams' awards) and Lucy Heil ('most disorientated' and 'most descriptive'), the girls in the office at the other end of the corridor, Vicky Heard ('coolest', Heard 2011), Amy Scott ('most defensive of tea-time biscuits') and Naomi ('most unfortunate office'), those pesky theorists, David Cole ('most AGNs consumed during coffee time'), Chris Nixon ('most minions' award, 'most supervisors' award and 'least work directly done by self' award) and Kastytis ('most orcs slain by a longbow' award), to the guys and gals upstairs, Nathan ('most undergraduates killed 2009 and 2010') and Katherine ('best canadian' and 'most calm given the circumstances'), to the inhabitants of the SRC, Charly (special civic citation for single handedly keeping the shoe industry afloat) and Pippa ('most portable' and 'best rude puns'), and of course to my friends in the department that have since graduated and left, Alexander Hobbs ('best dressed by evening'), Chris Cottis ('poker player extraordinaire' and 'most likely to be mistaken for Jesus at a distance'), Fergus ('most surprising beard'), Paul Steele ('most entertaining drunkard' and 'most overworked kidneys' awards), Peter Cossins ('most erratic work hours' and 'most entertained by toad noises' awards) and of course Rich Owen ('most french', 'most contaminated' and 'most unfortunate' awards). Thankyou very much, and well done to you all.

It goes without saying that I would like to give a heartfelt thanks to everyone at the Karate club and especially Sensei Rick Jackson. Without your friendship, help and tuition I have no doubt that I would be a very different person today, and probably would not have got to this stage and be writing this now. The club means more to me than anything, and I'd like to thank everyone that has poured their hearts into it over the years and help in its running. I also feel I should say a big thankyou to Steph and Piyal, who have sacrificed what probably builds up to quite a significant amount of time (and petrol...) getting me there and back over recent years, and generally being prepared to help everyone out no matter what. Thank you all everyone.

Perhaps the biggest thankyou of all needs to go to my parents. Without them I would not even be here at all, I would never have met all the people I have thanked thus far and would not be where I am now and capable of doing what I can now do. They have given me everything and never failed to help. They have hauled my stuff to and from the various places I lived as an undergraduate, helped me out financially and always put me on the right path. I would like to thank my Father, who has had far from an easy time this past few years, for all his enthusiasm and interest into what I do, and for arranging that meeting with Sir Patrick Moore all those years ago which originally set me upon this path, and which I have never forgotten. I would like to thank my Mother for all her unflinching support and financial advice, and for sacrificing several days of her life to fill in all those bloody forms you need to fill in for anything vaguely associated with university. It's only been since I came to university that I realised how lucky I am to have parents such as these.

Last of all but by no means least, I would thank most of all my girlfriend Nikki. I cannot believe how fortunate I am to have such a person to spend my time with and would like to thank her for living with all my ups and downs during my time here. As well as these ups and downs, I would also like to thank her for putting up with the following: toad impressions; bird impressions; angry toad impression; angry bird impressions; stealth attack toad impressions; impressions of the Cadbury's mini egg bird; actual toads; toad attacks; bird attacks; attacks from the Cadbury's mini egg bird; various traps, in particular the 'sticky mess trap'; the 'swinging pterodactyl of death trap'; the 'agitated cat trap' and the 'great big load of spiders trap'; for putting up with the gradual expansion of my armoury, including swords; staffs; nunchaku; sai; kama; kusari kama and the Cadbury's mini egg bird; for putting up with my constant attempts to expand her knowledge of classic films, including; Star Wars I, II and III (the good I, II and III...); Highlander; Blade Runner, Alien; Predator; Alien vs Predator, Alien II: Aliens, Predator II, Aliens vs Predator II, Aliens vs Predator Requiem; every single James Bond film including the new ones (she really hates those), oh and tv programs such as star trek, she really hates star trek. In particular I must thank her for putting up with the Cadbury's mini egg bird, which has been a constant source of terror for her over the past three years. Thank you Nikki.

And that's it I suppose. Goodbye all and thanks for all the fish :).

CONTENTS

1.	Introduction	1
1.1	Gamma Ray Bursts, a Brief History	1
1.1.2	BeppoSAX and the First Afterglow	3
1.1.3	GRB Progenitors	5
1.1.4	Blasts from the Past	8
1.2	Observational Cosmology	9
1.2.2	Cold Dark Matter	10
1.2.3	The Early Universe	11
1.2.4	The Beginning of Structure	13
1.3.5	Growth of Structure	13
1.3	Cosmological Probes	15
1.3.2	Quasars	16
1.3.3	Lyman-break Galaxies	16
1.3.4	Sub-millimeter Galaxies	17
1.3.5	Lyman-alpha Emitters	20
1.3.6	The Hubble Ultra Deep Field	22
1.3.7	Future Probes of the Cosmos	23
1.4	Gamma Ray Burst Cosmology	25
1.4.2	A Long Time Ago, in a Galaxy Far Far Away...	25
1.4.3	Stellar Mass Progenitors	27
1.4.4	In the Blink of an Eye	27

2.	Distance, Darkness and Dust	30
2.1	Dark Bursts	30
2.1.2	Causes of Dark Bursts	30
2.1.3	Dark Bursts at High Redshift and the Lyman- α Break	31
2.1.4	When is a Burst ‘Dark’?	34
2.1.5	Disentangling the Causes	39
2.2	The <i>Swift</i> Redshift Distribution	43
2.2.2	Constraining the <i>Swift</i> Sample	44
2.2.3	The Dark Burst Fraction	46
2.3	Defining the Sample	48
2.3.2	Extended Observability Criteria	52
2.3.3	The Sample	53
2.3.4	Redshift Distribution	56
2.3.5	Dark Burst Fraction	56
2.3.6	Distance and Dust, Dissecting the Dark Burst Fraction	59
3.	Conclusions	63
	Conclusions	63
	Appendix	70
	Table 1	71
	Table 2	77
	Bibliography	79
	Bibliography	79

Introduction

Gamma Ray Bursts are now undisputed as the most energetic and violent events the universe has to offer. Since their first detection in 1967 by the *Vela* satellites, the study of Gamma Ray Bursts (GRBs) has evolved into a flourishing area of modern astronomy. Their extreme energetics allow us to look into the heart of the most destructive phenomena known to man, and their massive luminosities light the way for us to look further back into the ancient universe than ever before.

1.1 Gamma Ray Bursts, a Brief History

The first GRB was detected in the late 60s by the U.S. *Vela* Satellites. Suspicious that the USSR would attempt to breach the nuclear test ban treaty of 1963, the U.S. military launched the *Vela* satellites to monitor any secret nuclear testing conducted in space. In July 1967 they detected a very strange burst of gamma radiation, inconsistent with the signature of any known nuclear weapon. By analyzing the arrival times of the burst at the different satellites, it was possible to determine that the bursts did not come from anywhere on or near earth. After ruling out similar scenarios it was concluded that these unidentified bursts of gamma radiation did not originate from anywhere within the solar system and were of some other extra-solar origin.

In 1973, after it was realized that these bursts of radiation were nothing to do with nuclear testing and were of no threat to national security, the phenomena was declassified and disclosed to the astronomical community. In this original article (Klebesadel et al.

1973), the straight forward term 'Gamma Ray Burst' was coined to describe the phenomena, and the name has been used ever since.

Little progress was made in explaining the phenomena however until the early nineties. Plenty of models were put forward (for a review see Nemiroff 1994 and the many references therein), but the lack of any detailed observational data prevented any from being proven or constrained further. A major problem was the inability to accurately determine where the bursts came from. This lack of any meaningful distance scale meant that large assumptions had to be made about the objects thought to be the progenitors of GRBs. Despite this, most models proposed a galactic origin, with GRBs thought to be produced by some mechanism within the Milky Way (e.g. Mitrofanov & Sagdeev 1990 consider a model of GRBs being produced in galactic neutron star/comet encounters).

This all changed however in 1991 when the *Compton Gamma-Ray Observatory's* *BATSE* instrument showed that the distribution of GRBs (Figure 1.1) on the sky was isotropic, not biased in any way to the galactic disk (Meegan et al. 1992). This provided strong evidence that GRBs originated from outside the Milky Way, although some models postulated that bursts originated from within the galactic halo.

The next confounding issue after the distance scale for astronomers was the lack of any counterpart object to the GRBs. Many progenitor objects were considered, but all searches for such objects were unsuccessful. The gamma ray detectors aboard *BATSE* only had a spatial resolution of 2.2° (Briggs et al. 1999), making accurate localization of a burst difficult. Error boxes were large enough to contain multiple objects potentially associated with a given burst, which provided no conclusive counterpart. Also, the few bursts with good localizations (thanks to their positions being triangulated from multiple space-craft) were shown to have no obvious bright counterparts associated with their error boxes (Schaefer 1999). This implied that bursts were associated with very dim stars or distant galaxies, but searches revealed that even very well localized bursts had many such dim objects associated with their position.

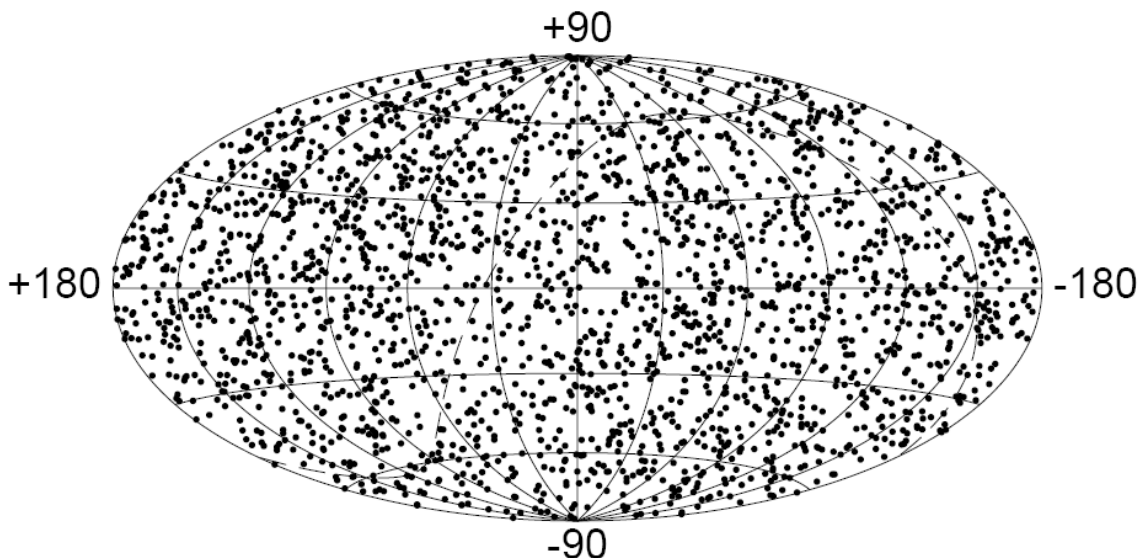


Figure 1.1: Sky map in galactic coordinates showing the distribution of 2704 Gamma Ray Bursts observed by *BATSE* over 9 years of operation. The bursts exhibit an isotropic distribution, except for a slight inhomogeneity along the celestial equator caused by the Earth's obscuration. Image credit: Fishman 1999.

It was clear that better instruments and faster communications were required to break the problem of discovering the burst progenitors. It was suggested by some models, most notably the fireball external shock model (for a review see Piran 1999 and references therein), that the initial burst of gamma rays would be followed by a more slowly fading emission at longer wavelengths, caused by the ejecta of a burst slamming into the local interstellar medium around its progenitor object. Early attempts to observe this 'afterglow' were unsuccessful, mainly due to their transient nature and the difficulties at the time in observing a burst position at long wavelengths immediately after the initial burst of gamma rays.

1.1.2 BeppoSAX and the First Afterglow

The breakthrough finally came in 1997 when the Italian-Dutch satellite *BeppoSAX* detected GRB 970228. Its X-ray camera detected a fading X-ray source coincident with the burst position (Costa et al. 1997) (*Figure 1.2*), and 20 hours after the burst the *William-Herschel Telescope* identified a fading optical counterpart (van Paradijs et al. 1997),

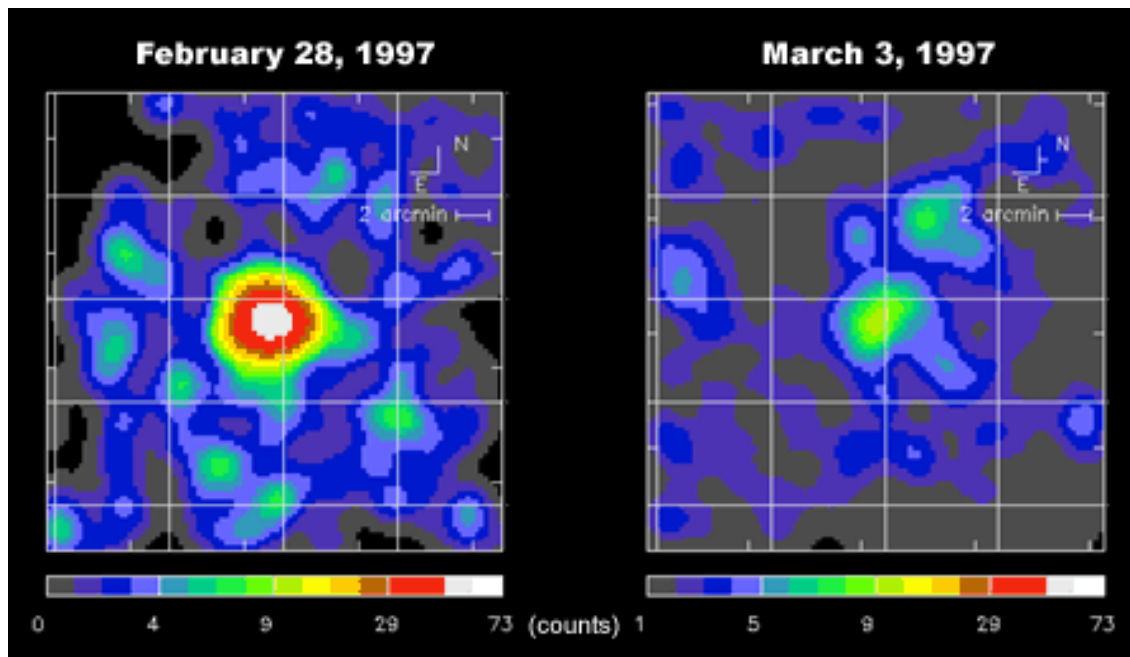


Figure 1.2: The X-ray afterglow of GRB 980228 as imaged by the Italian-Dutch satellite *BeppoSAX*. The left panel shows a fading X-ray source within the gamma ray detection error box 8hrs after the initial burst. The right panel shows the same source 3 days later exhibiting a significant amount of fading, and showing that this object was indeed the longer wavelength ‘afterglow’ emission associated with GRB 090228, and the first ever Gamma Ray Burst afterglow to be detected.

pinpointing the burst’s location. As the afterglow faded, deep imaging revealed a faint, distant galaxy at this position. Because of its very low luminosity, the distance to the galaxy was not actually measured for several years, but in the meantime *BeppoSAX* had detected and localized another GRB, GRB 970508. This was localized within 4 hours of discovery, allowing observations to begin much earlier than ever before. Spectroscopy revealed the afterglow had a redshift of $0.835 < z < 2.3$ (Metzger et al. 1997), the first ever accurate distance determination of a gamma ray burst, and proof that GRBs originated from extragalactic distances. This discovery that GRBs came from dim distant galaxies ended the controversy of the distance scale, and had massive implications about their nature.

These cosmological distances meant that the energetics of a GRB were phenomenal, with each GRB releasing to the order of $10^{52} - 10^{54.5}$ ergs of energy in the space of a few seconds (although this is now known to be slightly lower, $\sim 10^{51} - 10^{52}$ ergs, as the bursts are

actually 'beamed' rather than isotropic). This makes them the most violent event in the cosmos, beaten only by the Big Bang itself. This of course causes headaches when trying to work out how GRBs are created, what progenitor could possibly be capable of releasing such massive amounts of energy in such a short time? This is a question which is still far from answered at the moment, but the general consensus is, given there is evidence for some GRBs being associated with supernovae, and that their host galaxies tend to have regions of intense star formation, that GRBs are associated with the deaths of massive stars.

1.1.3 GRB Progenitors

The most popular GRB progenitor model is known as the 'collapsar' model (MacFadyen & Woosley 1999). In this model a massive, rapidly rotating, low to moderate metallicity star collapses down into a black hole formed at its centre. Material in the star's core accretes rapidly onto the newly created black hole in a high density accretion disk that powers two jets along the axis of rotation. These jets push through the star, punching a hole through the stellar envelope and emerging as an extreme velocity baryonic outflow, with gamma factors of several hundred. The burst of gamma radiation we then detect as a GRB here in the solar system is then created further out by intense internal shocks in part of what is known as the 'relativistic fireball model'. The afterglow at longer wavelengths is produced by a slightly different mechanism in this model, the extreme energetics of a GRB will mean that matter must be ejected from the progenitor at relativistic speeds, hammering into the interstellar medium and creating impressive shock fronts. Energetic electrons within the shock front are accelerated by strong local magnetic fields and radiate energy as synchrotron radiation across most of the electromagnetic spectrum which we then observe as an afterglow (see *Figure 1.3* for a schematic of the fireball model, and *Figure 1.4* for examples of optical GRB lightcurves, to demonstrate how the afterglow is seen by observers).

Although we believe the relativistic fireball model is the mechanism responsible for afterglow creation in all GRBs, there are other types of GRB thought to be created from different progenitors. There are broadly speaking two populations of GRBs, 'short bursts' which tend to last $< \sim 2s$ and are relatively spectrally harder, and 'long bursts', which tend

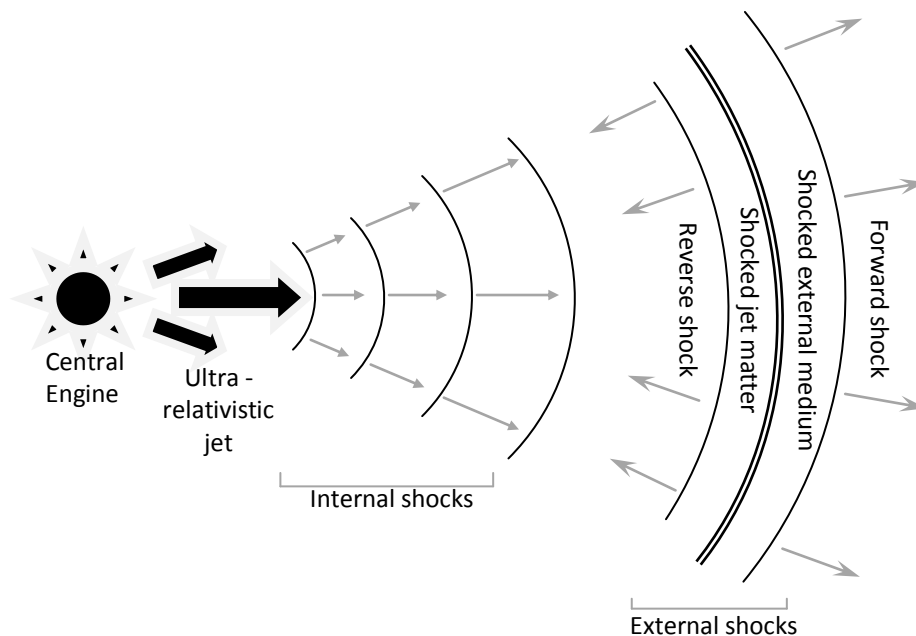


Figure 1.3: Diagram of the relativistic fireball model for GRB afterglows. The central engine powers the emission of an ultra-relativistic jet of collimated plasma. This baryonic matter can be envisaged as shells moving at different relativistic speeds which then interact with each other forming internal shock fronts. These internal shocks are thought to be responsible for the prompt gamma ray emission as well as the late time X-ray flares. As the blast wave impacts the external interstellar medium it creates an external forward shock. This superheats the ISM and is thought to cause the afterglow by subsequent synchrotron emission at longer wavelengths. A reverse shock accompanies the external shock, travelling back along the outgoing jet.

to last $> \sim 2s$ and are relatively spectrally softer. There is some overlap between these two populations, and they are far from distinct, but a plot of burst duration vs spectral hardness for a given sample of GRBs will reveal a broadly bimodal distribution.

These two populations are thought to be the result of different progenitor mechanisms. The collapsar model described above relates to the population of 'long' GRBs, rather than the population of 'short' GRBs, which are thought to be powered by a mechanism of two neutron stars in a binary system colliding and collapsing down into a black hole. Some of the earlier pre-*BATSE* GRB models also still go some way in explaining some phenomena that do release large amounts of gamma and X-rays, but we now know are not 'classical' GRBs. For example, Usov 1992 presents a model for GRB

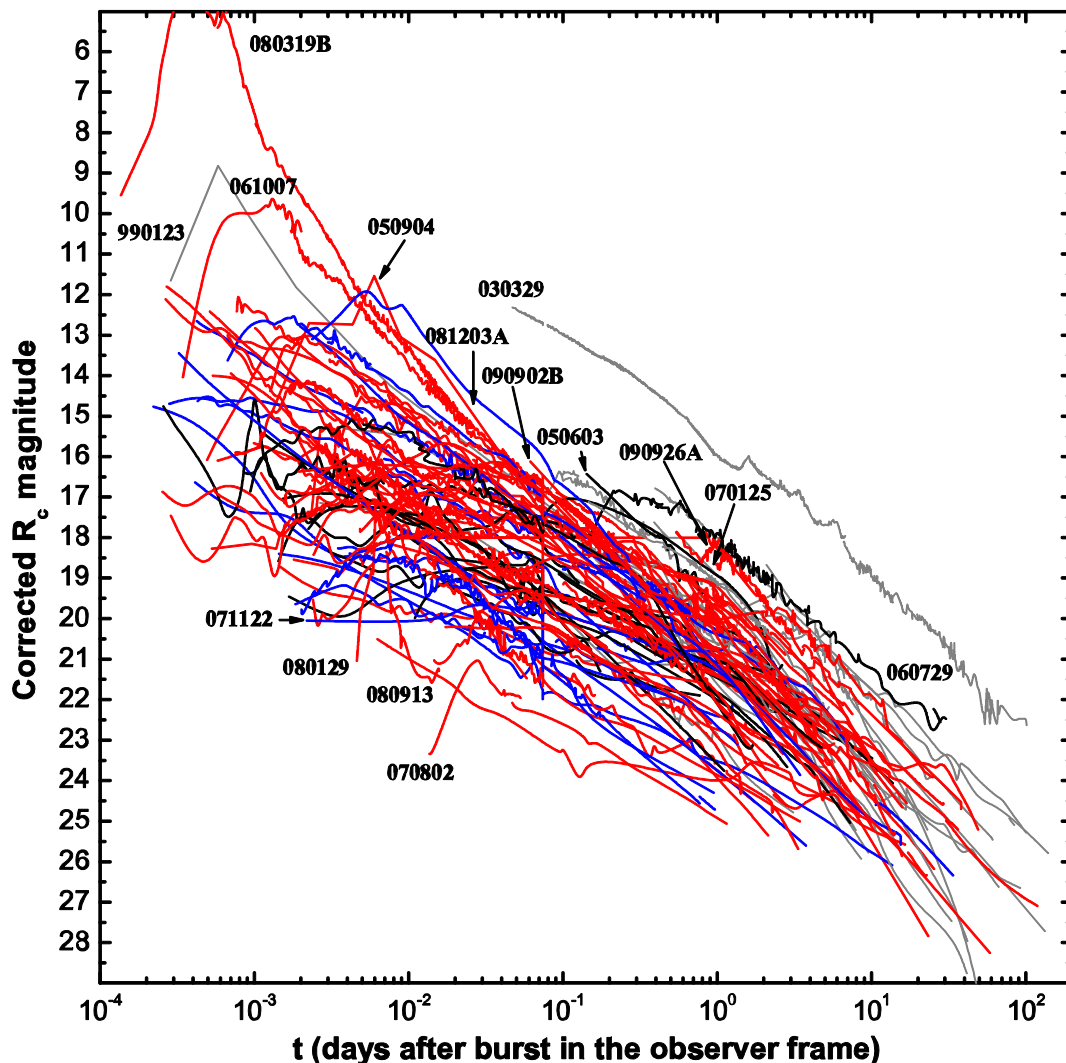


Figure 1.4: Taken from Kann et al. 2010, they present here the observers frame optical lightcurves of 76 *Swift* GRBs up to September 2009, with the differing colours representing their various subsets of the *Swift* sample (Red lines indicate the *Swift* Golden Sample, blue lines the Silver Sample and black lines the Bronze Sample, see Kann et al. 2010 for details on how these are defined). Bursts in light grey are pre-*Swift* bursts. The figure illustrates well how GRB lightcurves follow reasonably consistent decay behaviour, an initial rise followed by a fairly predictable power law decay, with observed decay indices typically well constrained in the range $\alpha = 0.5-1.3$. Some bursts do exhibit unpredictable flaring activity, as can be seen in several of the lightcurves above, but this usually only manifests at early times, and in most cases has died down after ~ 2 hours. It is also worth noting here the lightcurve of *GRB 080319B* (at a redshift of $z=0.937$), the so called ‘naked eye’ burst and brightest burst so far observed. As can be seen from its lightcurve, it is several orders of magnitude brighter than its next nearest rival during the initial rise, and, as its honorific suggests, at its peak brightness it was possible to observe the afterglow with the naked eye. The pre-*Swift* burst *GRB 030329* (at a redshift of $z=0.169$) can also be seen to exhibit an incredibly bright optical afterglow, and is still the burst with the brightest known afterglow at late times.

production that still has relevance in the field of magnetars, and Colgate and Petschek 1981 present a theory specifically explaining the March 5th 1979 event which we now understand to be a ‘Soft Gamma Repeater’ or SGR rather than a classical GRB. It is however the long GRBs that are of interest to cosmology.

1.1.4 Blasts from the Past

One of the great aims of cosmology is to build up a complete picture of how the universe has evolved since the Big Bang. This by definition involves observing very distant and thus very ancient objects. The major problem in doing this is that these objects tend to be very dim and increasingly harder to detect as cosmological redshift increases. However, due to their extreme luminosity, it is possible to detect GRBs at exceptionally large distances, and indeed with a redshift of $z = 8.3$, *GRB 090423* is currently the most distant object ever observed by mankind (although this has recently been beaten by a galaxy discovered by Lehnert et al. 2010 at $z = 8.55$, although there are many that dispute this result) (see *Figure 1.5* for the afterglow and spectra of *GRB 090423*). This makes them of fantastic interest to cosmology, by endeavoring to detect exceptionally distant GRBs, it is possible to detect ancient dim host galaxies that would have otherwise gone undetected in dedicated large area surveys. It is not however just dim galaxies that could be detected, it is in principle possible to detect GRBs at much greater redshifts than objects traditionally used for the task such as quasars, to the extent that it may be possible to obtain direct observations of an object from the era of reionization. There is even the possibility, given that long GRBs are thought to be generated by the deaths of low-metallicity massive stars, that high redshift GRBs could allow us to detect Population III stars, the first ever luminous objects in the universe.

The problem however, as with any study of GRBs, is their transient and random nature. It takes a formidable amount of effort and global co-ordination (with equal parts luck...) to detect these high redshift bursts, and unlike in the rest of astronomy where it is in principle possible to find similar interesting objects by essentially looking harder, in GRB astronomy it is necessary to wait for one to occur. Nonetheless, as *GRB 090423* has

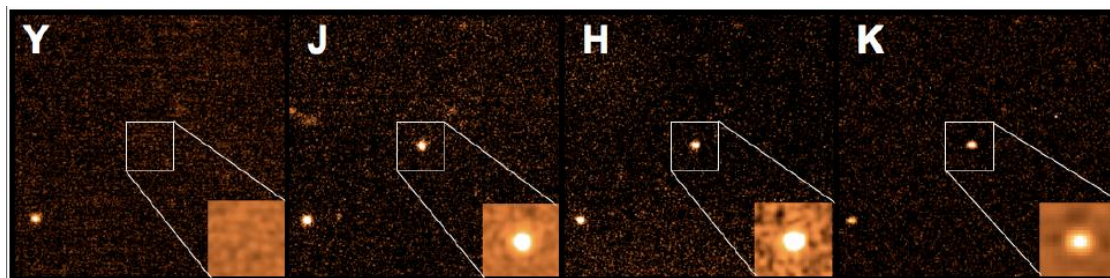
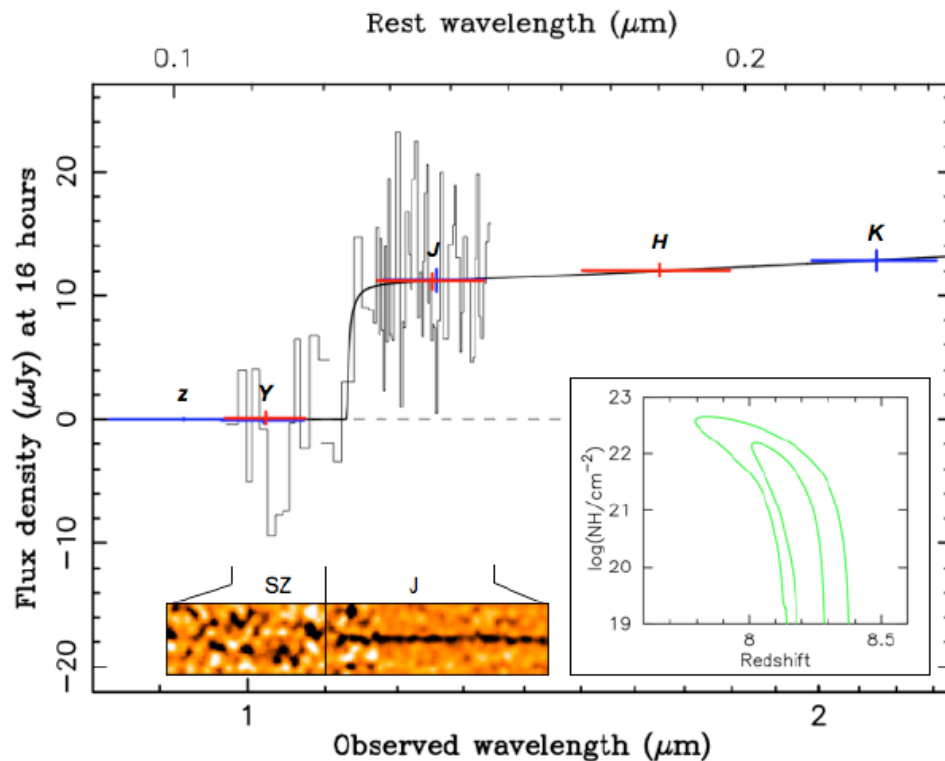


Figure 1.5: The spectra and afterglow of GRB 090423 taken from Tanvir et al. 2009. *Top panel:* Spectrum taken ~ 17.5 hours post burst with the European Southern Observatory (ESO). The main figure shows the spectrum and broadband observations over-plotted with a damping wing model. The bottom-left insert shows the spectra as taken by ESO, and no emission can be seen blueward of $\sim 1.14 \mu\text{m}$, confirming the spectral break to be caused by the leading edge of the Lyman- α forest at a redshift of $z \sim 8.3$. *Bottom Panel:* The afterglow of GRB 090423 imaged in the Y-band with Gemini-N (Tanvir et al. 2009) and JHK-bands with UKIRT (Tanvir et al. 2009). Note that the afterglow is clearly detected in the JHK bands but is invisible in the Y-band, the calculated spectral slope between the Y and J bands was found to be impossible to explain via dust extinction at any wavelength, and instead implied a spectral dropout via the Lyman- α forest being significantly redshifted to wavelengths of $1.1\text{-}1.2 \mu\text{m}$, which in turn implied a redshift of $z \sim 8$ as confirmed by the spectrum above.

proved, gamma ray bursts can push the boundary back by unprecedented amounts, and blast open avenues of research previously unavailable in the study of the cosmos.

1.2 Observational Cosmology

Cosmology is the study of the universe on its largest scales and at its earliest times, it was the object of debate for the very earliest of philosophers and is still very much an area of active research today. It was only really at the beginning of the last century we saw the beginning of what we tend to call 'modern' physical cosmology.

The development of the General Theory of Relativity by Albert Einstein allowed researchers to establish the Big Bang theory of the universe, and the redshift observations by Humason & Hubble in 1929 gave credence to this by suggesting the universe was expanding. Despite this, opinion was still divided over the subsequent decades as to whether the universe was reducing in density as it expanded, or if new material was being continuously created to keep it in an overall steady state. Momentum for the Big Bang theory however gathered pace with more and more observational evidence pointing to the universe having evolved from a hot dense state, and with the discovery of the cosmic microwave background in 1965, and its precise measurement by *COBE* in the early 90s, and later in 2003 by *WMAP* (Bennett et al. 2003, Spergel et al. 2003), few astronomers now believe in an alternative model for the origin of the cosmos.

1.2.2 Cold Dark Matter

The current standard cosmological model is the 'lambda cold dark matter' or *Λ CDM* model. This is the most currently accepted model as it provides the simplest explanation of the large scale structure of galaxies and galaxy clusters, the existence of structure in the cosmic microwave background, and the accelerating expansion of the universe. Like many modern cosmological models, *Λ CDM* assumes we do not occupy a special viewpoint in the universe and that the universe looks the same in all directions from any location (the cosmological principle). The model assumes a single originating event, The Big Bang, an abrupt appearance of an expanding space-time containing an incredible energy density.

This expansion proceeded in several stages to form the universe as we now know it today, with the expansion continuing to accelerate.

The constant Λ is the 'cosmological constant' associated with the vacuum or 'dark' energy which is responsible for the current accelerating expansion of the universe against the contracting pull of gravity. The model also calls into account 'cold dark matter', a form of matter required to explain the behavior of large scale structures in the universe and gravitational lensing by galaxy clusters, that cannot be explained by visible matter alone. Although we are yet to formally identify or detect dark matter, the Λ CDM model calls for it to be cold, almost certainly non-baryonic, and interacting only with other matter and photons gravitationally. Precisely constraining the fraction of dark matter and dark energy in the universe (amongst other parameters) is still very much an active area of research, but their relative abundances compared to our 'everyday' baryonic matter and electromagnetic energy can come as a surprise to those not familiar with it. We currently estimate that $\sim 73\%$ of the universes present mass-energy density is made up of dark energy, $\sim 23\%$ constitutes dark matter and only $\sim 5\%$ of the universes mass-energy contained within conventional matter and EM radiation. By tracing these parameters back, it is possible for us to gain an insight into the conditions present at the universe's inception, and use this information to describe how we got from these initial conditions to the universe full of complex structure we see around us today.

1.2.3 The Early Universe

The most up to date observations from the seven year *WMAP* data release put the universe to be 13.75 ± 0.11 Gyr old (Komatsu et al 2009), and its evolution is generally divided up into three stages. The first, the 'very early universe', existed in the split second after the universe was created and is still not completely understood. This is mainly because the energies that particles had in this era were much higher than those we can currently reproduce on earth, which gives us very little experimental precedence to describe any details. In most models, in the earliest stages of the Big Bang the universe was filled homogeneously with an incredibly high energy density and extreme temperatures, which was very rapidly expanding and cooling. At about 10^{-37} seconds after the Big Bang it is

thought that an unknown phase change caused a rapid exponential expansion of the universe, increasing its volume by a factor of at least 10^{78} . This phase lasted until 10^{-33} - 10^{-32} seconds after the Big Bang, and is referred to as 'inflation'. After inflation the universe continued to expand but at a much slower rate, and is believed to have consisted as a quark-gluon plasma and other elementary particles. The extreme temperature would have meant particles would have been moving at relativistic speeds, with particle-antiparticle pairs being continuously created and destroyed in collisions. At some point another unknown phase transition occurred which violated the conservation of baryon number and led to a small excess of particles over antiparticles, and resulted in the dominance of matter over antimatter in our universe.

The universe continued to expand and fall in temperature, corresponding to an overall decrease in particle energy. After about 10^{-12} seconds we have a much better idea of the physics taking place as we can replicate the energies involved here on earth, and things become less speculative. This phase of the universe is referred to as the predictably titled 'early universe'. At about 10^{-6} seconds, temperatures were low enough for quarks and gluons to combine and form baryons, and too low for the creation of proton-antiproton pairs. Mass annihilation immediately followed, leaving no antiparticles and the matter we now see today in the universe. A similar process occurred at ~ 1 second for electrons and positrons. After these annihilations temperatures were such that protons, neutrons and electrons were no longer moving relativistically and the energy density became dominated by photons. At a few minutes temperatures had dropped to about a gigakelvin and protons and neutrons could combine to form the universe's first helium and deuterium nuclei in a process called 'Big Bang nucleosynthesis', although most protons remained uncombined as hydrogen nuclei. At about 379,000 years after the Big Bang, electrons and nuclei combined into atoms. Photons scatter much more infrequently from neutral atoms, so when almost all of the electrons recombined, energy and matter decoupled, and the universe became transparent for the first time. With this, the cosmic microwave background was released, and the universe moved into its next stage of evolution, the era of structure formation.

1.2.4 The Beginning of Structure

With the building blocks of neutral hydrogen and helium in place, it was possible for processes to be set in motion that lead to the universe full of complex structures we see today. We know from the observed Cosmic Microwave background that the universe was remarkably homogenous for a time after the Big Bang, with little or no structure. The most commonly accepted theory of how the universe evolved from this very smooth state begins with 'primordial fluctuations', small density variations left over from inflation, whose growth gravitationally attracted clumps of dark matter. As these clumps grew, primordial gas condensed within, creating structures that would soon become the first star clusters and proto-galaxies.

Soon after these proto-galaxies formed, the hydrogen and helium within gravitationally collapsed to form the first stars. These were the first ever luminous objects in the universe, their creation marked the end of 'the dark ages' and heralded the next era of the evolution of the universe. The radiation they emitted acted to reionize the neutral intergalactic medium created in the era of recombination, in the so called 'era of reionization'. We know from the electron scattering optical depth measurements of *WMAP* that a substantial fraction of the intergalactic hydrogen was ionized at a redshift of $z \sim 11$, implying the first stars must have formed well before this (some argue that this may have occurred as early as $z = 30 - 60$). The ignition of the first stars also marks the formation of the first galaxies and the initiation of stellar nucleosynthesis.

1.2.5 Growth of Structure

We know from a variety of observations such as the *Hubble Deep Field* (Williams et al. 1996) that these early galaxies were much smaller than the massive spiral and elliptical structures common in the universe in the present epoch. This implies a 'bottom up' mode of structure growth, in which these small galaxies regularly merge and grow into larger structures in a process of 'hierarchical structure formation'. This is evident from the more recent *Hubble Ultra Deep Field* (Beckwith et al. 2006, *Figure 1.6*), which shows a number of small galaxies merging to form larger ones ~13 billion years ago, when the universe was ~ 5% of its current age.

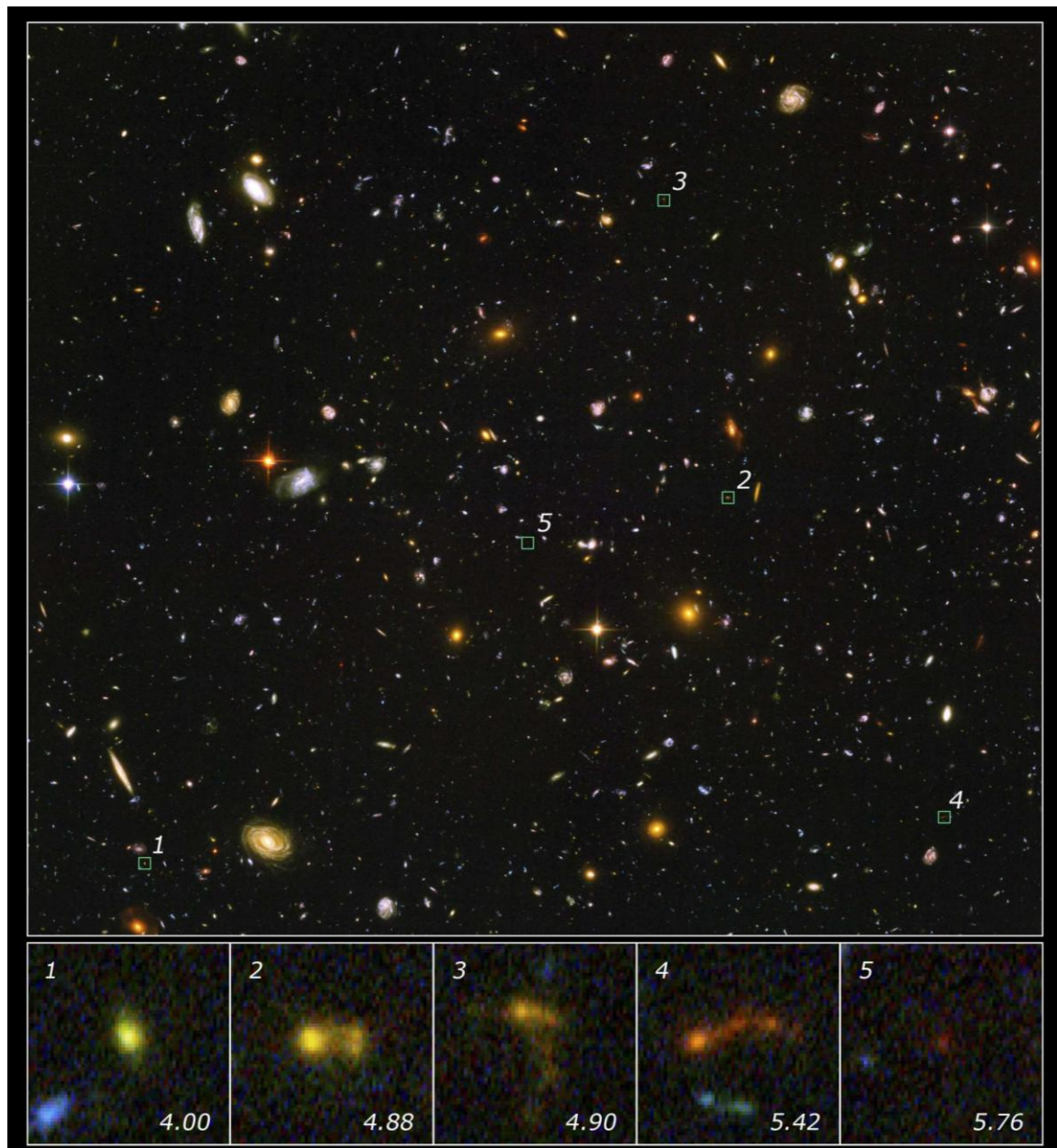


Figure 1.6: The *Hubble Ultra Deep Field* showing early galaxy mergers. *Top panel:* The *Hubble Ultra Deep Field*, the deepest image of the universe ever taken, comprising data gathered between September 2003 and January 2004 and estimated to contain $\sim 10,000$ galaxies. Like its predecessor, the famous *Hubble Deep Field*, it shows galaxies at high redshifts are much smaller than the grand design spirals seen in today's universe and a lack of large galaxies at early times, implying a 'bottom-up' mode of galaxy formation. *Bottom panels:* Early galaxy mergers in the *Hubble Ultra Deep Field*. There are a number of small early galaxies seen in the *HUDF* undergoing mergers, further supporting the idea these galaxies underwent frequent collisions and mergers in the early universe in a hierarchical growth of structure model of galaxy formation. The positions of these mergers in the *HUDF* are denoted by the green squares in the main image, and the number in the lower right of the bottom panels denotes the redshift. Image credit: NASA, ESA and N. Pirzkal (STScI-PRC07-31).

The formation of stars lead to another major change in the chemical makeup of the universe, in addition to re-ionization. In the cores of the stars, heavier elements were synthesized from the hydrogen and helium produced in the Big Bang, and cast out into the universe upon their deaths. This acted to chemically enrich the interstellar medium from which later generations of stars were formed. We know that in the present universe there are broadly two populations of stars, divided by relative age and chemical enrichment. The so called Population I stars are younger and relatively metal rich compared to the older Population II stars. The two distinct populations are the result of chemical enrichment from stellar nucleosynthesis, the Pop I stars being created from the interstellar medium chemically enriched by the deaths of Pop II stars.

It is believed that the first stars formed in the universe were Population III, which had essentially zero metallicity after being formed from the primordial hydrogen and helium created in the Big Bang. We do not at present have any direct observations of Pop III stars, mainly because searching for them in the ancient dwarf galaxies in which they are thought to have resided is intrinsically difficult. These galaxies were very small and thus very dim, making them extremely difficult to detect, with only a handful being observed past a redshift of $z = 6$, and none of these conclusively showing any traces of Pop III stars. Trenti et al 2009 suggest that Pop III stars should be observable at these redshifts due to the inhomogeneity of chemical enrichment as the universe evolved. Their simulations show that pockets of near zero-metallicity gas should exist at around $z \sim 6$, and that this is at present our best available window to find the Population III stars and represents our next observational boundary to break.

1.3 Cosmological Probes

Due to the hierarchical process of the growth of structures, objects such as galaxies and quasars in the early universe are intrinsically small and thus very dim, making them exceedingly difficult to detect. In order to look further and further back in time and unravel the secrets of the universe's formation it is thus necessary to utilize certain observational techniques or classes of object to peer back at the universes inception.

1.3.2 Quasars

Perhaps the most well known object used to push back the observational boundary are quasars. Their exceptional luminosities means they can be detected out to great distances, and their strong spectral lines provide reliable redshift measurements. They are good probes of the high redshift universe, reaching out as far as $z = 6.44$ (Willott et al. 2010), however they cannot be used to probe much past this as the number of bright quasars at redshifts of $z > 5$ drops off very sharply (Richards et al. 2006 and references therein). This can be explained in terms of how they are formed. Quasars are powered by a central supermassive black hole and fuelled by accretion. In the early universe quasars were still forming and growing, making them both dimmer and less numerous than at lower redshifts. This means that quasars cannot be used to probe the universe much past a redshift of $z \sim 7$, simply because there are very few bright enough to observe beyond this point in the universes history. There may yet be a few observable at redshifts of $z = 8$ or 9 , but their use as cosmological probes is definitely limited past $z \sim 7$. Another issue is the relative rarity of high redshift quasars, finding and detecting them requires observers to carry out very large scale sky surveys, which as well as being time intensive and technically challenging, also bias any detected sample in favour of brighter objects.

1.3.3 Lyman-break Galaxies

Another way of detecting high-redshift galaxies is to exploit an effect of the expansion of the universe. Lyman-break galaxies are high redshift star forming galaxies that exhibit a ‘break’ in their spectrum caused by the Lyman limit being redshifted through the observing bands. The Lyman limit itself is a spectroscopic phenomena corresponding to the shortest wavelength of the Lyman series at 912\AA , and thus the ionization wavelength of neutral hydrogen. Photons with shorter wavelengths than this, and thus higher energies, will ionize hydrogen and thus be readily absorbed. Given the abundance of hydrogen in the universe, the Lyman limit leads to a sharp cutoff in galaxy spectra below 912\AA . As cosmological redshift increases, this break will begin moving through spectra to longer wavelengths, and depending on the redshift will eventually move up through our observing bands. Thus by taking observations in several different filters, and looking for galaxies that appear at longer wavelengths but are invisible at shorter ones, it is possible to select high

redshift galaxies (this is illustrated in *Figure 1.7*). This has most extensively been done using optical and UV filters to detect objects with redshifts of $z = 3 - 4$ (Steidel et al 96, 99a, 99b, 03), but studies using optical and IR filters to search for objects with redshifts of $z \sim 6$ have met with success. Bouwens et al 2006 present a sample of ~ 506 *i*-band dropouts ($z \sim 6$) in a wide ranging series of observations including wide- area *HSTACS* fields, *HUDF*, *enhanced GOODS*, and *HUDF parallel ACS fields (HUDF-Ps)*.

The problem with this method is similar to that one of the drawbacks of using quasars. By simply directing telescopes skywards and looking for these objects, we will preferentially select only the brighter objects and thus only be looking at the brighter end of the luminosity function of this population of galaxies. The added difficulty that early galaxies are very small and dim does not aid us here, meaning we are likely to only be seeing the very brightest and most violently star forming galaxies of the epoch, and even then these galaxies are not easy to detect, requiring exceptionally deep observations even with the like of HST. This dimness also makes follow-up spectroscopy to confirm a redshift or investigate the object's metallicity highly challenging, with only the most powerful spectrographs being capable. Because of the size and shape of these early galaxies, it is also very easy to confuse $z > 6$ Lyman break galaxies morphologically with elliptical galaxies residing at lower redshifts, thus contaminating a galaxy sample. At redshifts of $z = 2 - 3$ these low redshift ellipticals are also more importantly spectrally similar to Lyman break galaxies, as the Balmer jump appears in more or less the same place as the Lyman limit would occur at higher redshifts. Foreground contamination with low redshift elliptical galaxies is in fact the major problem with studies of Lyman break galaxies, with the sample of Bouwens et al 06 discussed in the previous paragraph estimated to have contamination levels of $< \sim 8\%$.

1.3.4 Sub-millimeter Galaxies

Improvements in sub-millimeter observing technology have also offered an opportunity to detect high redshift galaxies over the past decade or so. These 'sub-millimeter galaxies' are distant star forming galaxies, whose bright sub-mm emission is detected from dust heated by star formation or an active galactic nucleus. Because we are

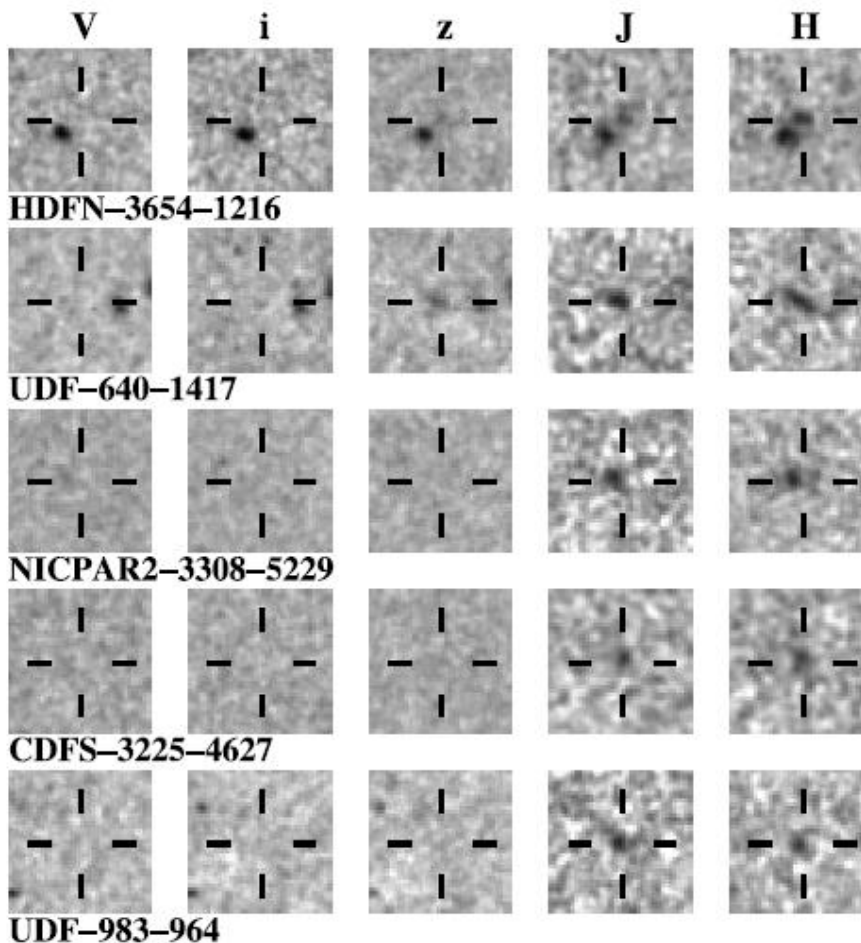


Figure 1.7: Selection of Lyman-break galaxies from the sample of $z \sim 7$ dropout candidates taken from Bouwens et al. 2008. Each row of images depicts a galaxy imaged across several different filters, as indicated by the labels above the top row. As can be seen in the images, all sources in the sample have fairly clear detections in the J and H bands, with only two having tenuous detections in the z -band and none having any form of detection in the i -band or shorter. This indicates that the Lyman limit from absorption by neutral hydrogen has been shifted through the optical bands and almost into the nIR, indicating in this case that the sources have redshifts of around $z \sim 7$, and demonstrates how Lyman-break galaxies are identified.

here essentially observing the dust's black body spectrum, the effects of cosmological redshift actually aid us. By looking at the galaxy in sub-mm wavelengths, we are actually observing the galaxy more towards the rest frame peak of its SED. This strong negative K-correction means that these high redshift galaxies are just as easy to detect at sub-mm wavelengths as their low redshift counterparts, and that their luminosity does not significantly decline with redshift but remains approximately constant at $z > 1$ (Blain et al. 2002). The field has seen success in detecting high redshift galaxies, with the redshift of

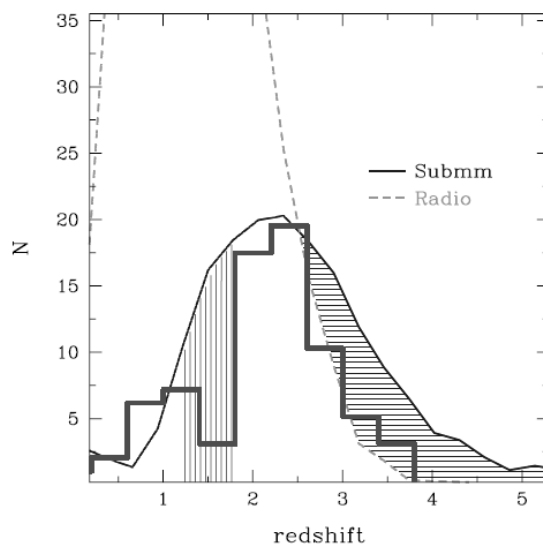


Figure 1.8: Redshift distribution of 73 radio-identified SCUBA submm sources taken from Chapman et al. 2005. The solid and dashed lines represent model distributions for SMGs (solid line) and radio sources (dashed line). The distribution has a median redshift of $z = 2.2$ and shows that the distribution does not extend much past $z = 4$, meaning SMGs cannot be used to effectively probe the early universe much past this redshift.

SCUBA localized sources from Chapman et al. 2005 having a median of $z \sim 2.2$ and not extending significantly past $z \sim 4$, the redshift distribution is shown in *Figure 1.8*. The method is however not without its drawbacks. Because this method essentially detects thermal emissions from dust, sub-mm galaxies tend to unsurprisingly be very dusty, and thus highly obscured at optical and near-IR wavelengths. This makes follow up observations very difficult, and the poor positional accuracy of current sub-mm arrays makes spectroscopic follow-up even more demanding. Sub-mm observations are also not without their selection effects. The detected sub-mm flux density of a dusty galaxy goes up by a factor of 10 if we double the dust temperature, firmly biasing us towards detecting the galaxies with the hottest dust. This population is however very important, as it contributes significantly to the star formation rate at these redshifts. At very high redshifts however these galaxies become less of interest. Dust takes time to form in galaxies from stellar nucleosynthesis, meaning early galaxies will not have much and will thus be poor submm emitters. So as we look further back, submm galaxies become much dimmer and consequently become of less interest.

1.3.5 Lyman-alpha Emitters

Another method of selecting high redshift galaxies that has met with success in the past decade is searching for 'Lyman-alpha Emitters', or LAEs. The Lyman- α line itself is caused by the electron in a hydrogen atom descending from the $n = 2$ excited state to the ground state. Thus, to create Lyman- α photons, we need incident photons with at least enough energy to get neutral hydrogen atoms into the $n = 2$ excited state or higher. This generally takes the form of hard UV radiation that often acts to completely ionize the hydrogen, with a Lyman- α photon being produced whenever the ionized hydrogen atom recaptures an electron and descends back down to its ground state. Thus, given that any excitation above the ground state will lead to the emission of a Lyman- α photon, and that both hydrogen and UV radiation are abundant in the universe (UV radiation is produced from a variety of sources, such as massive stars, AGN etc.), Lyman- α photons are exceptionally common. In rapidly star forming galaxies with large numbers of massive stars, such as those in the early universe, the Lyman- α line can be particularly intense. By using a narrow band filter focused on the Lyman- α emission line at a particular pre-decided redshift, and comparing this with simultaneous broad band observations with a similar central wavelength and looking for objects with a high narrow band to broad band flux ratio, we can pick out high redshift galaxies. These are the so called Lyman Alpha Emitters.

One of the most successful searches for LAEs has been the *Large Area Lyman Alpha* survey (*LALA*, Rhoads et al). Its first findings were presented by Rhoads et al in 2001, and reported the discovery of 156 objects at $z \sim 4.5$ and 13 sources at $z \sim 5.7$, 3 of which were confirmed spectroscopically by *Keck* observations in 2003 (Rhoads et al 03). In 2004, the survey was extended to a search at $z \sim 6.5$ and discovered its highest redshift LAE at $z = 6.535$ (Rhoads et al 04). The highest redshift LAE observed to date was discovered by Iye et al. 2006 at a redshift of $z = 6.96$, by developing the *NB973* narrowband filter for the *Subaru Suprime-Cam*. Kashikawa et al 2006 presented a comprehensive search for LAEs at $z = 6.5$ in the *Subaru Deep Field*, using both *Subaru* and *Keck* they have identified and spectroscopically confirmed 8 LAEs at $z \sim 6.5$, bringing the grand total up to 17, and complemented this with a photometric sample of 58 LAEs at $z \sim 6.5$.

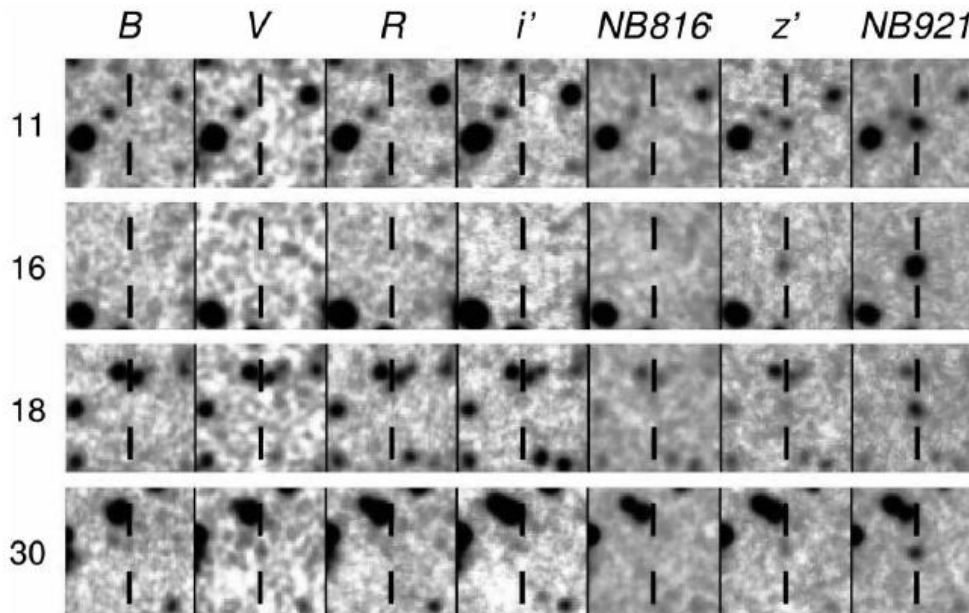


Figure 1.9: A selection of Lyman- α emitters from a search of the Subaru Deep Field at $z = 6.4$ by Kashikawa et al. 2006. Each row shows images of the same source taken across different filters as denoted by the headings above the top row, the *NB816* and *NB921* filters being narrowband filters at 8149\AA (FWHM = 119.5\AA) and 9196\AA (FWHM = 132\AA) respectively. It can be seen that the objects are very poorly detected (if detected at all) in the *BVRi'* broadband filters and in the *NB816* narrowband filter, but are clearly visible in the *NB921* narrowband filter. This implies the detection is from the intense Lyman- α emission line at a redshift of $z = 6.46\text{--}6.67$, and that the LAE is at a corresponding redshift.

Searching for LAEs is still however not without its own problems and difficulties. The first problem is that this method relies on Lyman- α emission, which although as previously stated is a relatively common atomic transition in the universe, can be significantly attenuated by dust. Lyman- α photons undergo frequent resonant scattering from other hydrogen atoms after their emission, giving them a very long path length which makes them much more likely to encounter a dust grain and be absorbed. Given that much Lyman- α emission comes from vigorously star forming galaxies with lots of massive stars emitting intense UV radiation, a large number of these galaxies are likely to be highly dusty. This means we may well be getting an incomplete picture of the overall population of LAEs at a given redshift, with the possibility of biasing us towards less dusty objects. The main problem with searching for LAEs is more one of practicality. To find LAEs at a given redshift, we have to perform a focused narrow band search for the Lyman- α line at that redshift. This differs from most of the other methods described in this section, whereby

we generally search for a class of galaxy likely to be at high redshift and then determine its actual redshift once it is detected. For LAEs, we have to pick a specific redshift band, typically with only a narrow range of $\Delta z \sim 0.05$, and see what we find. Thus to build up large samples of LAEs across a variety of redshifts takes a lot of dedicated telescope time, and the necessity to spectroscopically confirm the redshifts of these distant objects requires the attention of some of the world's most powerful telescopes. The efficiency of this method at finding $z > 5$ or 6 galaxies cannot however be denied, and the search for extreme redshift LAEs is far from over, for example the UltraVISTA public survey aims to perform a narrow band search for $z = 8.8$ LAEs using the *VISTA* telescope at ESO, and expects the find around ~ 30 LAEs at $z = 8.8$.

1.3.6 The Hubble Ultra Deep Field

Several groups (McLure et al. 2010, Bunker et al. 2010, Bouwens et al. 2009/10) have recently published work on finding high redshift galaxies by searching for spectral dropouts within the *Hubble Ultra Deep Field (HUDF)* (Beckwith et al 2006). The *HUDF* is a 1 million second exposure taken between 2003 and 2004, of an area of sky in the Fornax constellation using *Hubble's ACS*. The image was taken across 4 optical filters (*F435W (B435)*, *F606W (V606)*, *F775W (i775)*, and *F850LP (z850)*) to give limiting magnitudes of $m_{AB} \sim 29$ for point sources, and found 54 galaxies likely to have redshifts between $z = 6 \sim 7$ using the Lyman-break method to identify *i775* dropouts.

With the installation of *WFC3* in *Servicing Mission 4* in 2009, it was possible for several groups to use the early *WFC3/IR* observations taken over the *HUDF* area to search even deeper for $z > 8$ galaxy candidates. When searching for galaxies at these redshifts using a Lyman-break dropout method, the problem has traditionally been in obtaining very deep observations in the nIR where the redshifted UV emissions of $z > 7$ galaxies will be, and the *WFC3/IR* is an instrument that allows this boundary to be crossed. Bouwens et al. 2010 have thus far perhaps been the most successful in finding exceptionally high redshift galaxy candidates, using a two colour Lyman-break selection technique they have identified five *Y105* dropouts at $z \sim 8 - 8.5$. All candidates have very blue UV-continuum, suggesting that galaxies at these redshifts are incredibly young and free of dust. All groups working on

finding these high redshift dropouts in the *HUDF* (McLure et al., Bunker et al., Bouwens et al.) have shown that *Hubble's WFC3/IR* has crossed a threshold in detecting star forming galaxies at redshifts of $z = 8 - 8.5$, providing some fascinating groundwork for future missions such as *JWST* to build upon.

1.3.7 Future Probes of the Cosmos

The underlying problem with any direct search of the sky for ancient stars and galaxies is twofold, firstly the objects are incredibly dim and difficult to find with our current level of technology, and secondly, any large scale survey introduces a selection effect biasing it towards detecting the brightest objects, giving us an incomplete picture of the whole galaxy population. Looking for quasars allows us to get around the low luminosity problem to an extent, but only back to a certain redshift after which the number density of bright quasars falls off. Sub-mm galaxies also provide a novel way to detect reasonably high redshift galaxies, but also introduce a few awkward selection effects of their own that hinder direct follow-up observations. Also, given that the observed luminosity function does not extend much past $z \sim 4$ (Chapman et al 2005), we cannot at present use sub-mm galaxies to probe the high redshift universe at $z > 6$ we are currently trying to explore.

There are several future missions and instruments that are planned to unfurl over the next 5 years or so, that should improve our observing power of very distant objects dramatically. The *James Webb Space Telescope (JWST)* is a mission planned for 2014/15 as the successor to *Hubble*, and its primary scientific goal is specifically to observe the most distant objects in the universe beyond the reach of any current instrument. Due to the nature of this kind of work, *JWST* will not have the optical and UV capabilities of *Hubble*, but will instead be able to peer much further into the infra-red, and in its present design has a wavelength range of 0.6-28 microns. The two main aims of *JWST* is to detect the light from the first stars after the dark ages and to observe the formation of the first galaxies, answering some critical questions of modern observational cosmology that are out of reach of current telescopes. Researchers plan to use *JWST's* high resolution nIR spectroscopy capability to study reionization and answer questions such as when and how did

reionization occur and what astronomical sources were responsible for it, as well as ultra-deep nIR all-sky surveys to search for the universes first ever galaxies.

LOFAR (LOw Frequency ARray) is a highly sensitive interferometric radio array based primarily in the Netherlands but with stations across many European countries. It was developed to create a breakthrough in observational sensitivity below 250MHz in radio astronomy. Containing no actual moving parts, the array consists of a huge collection of double dipole antennas concentrated in stations throughout Europe with data integrated electronically by a Blue Gene supercomputer at the University of Groningen. Although planned construction of the antenna stations is only ~70% complete, science data has already started to be taken and processed. This is mainly thanks to how radio interferometry in this case is performed. The effective size of the array (i.e. the number of antenna) is not really limited by engineering or technological issues, as might be the case when building a large highly sensitive mirror for an optical telescope, but is instead only really limited by the processing power you have available to integrate the data. To this extent, more and more antenna stations can quite happily be built and added into the array (especially given an individual dipole antenna costs circa 3 euros each...). This is one of the many interesting innovative aspects of *LOFAR*, it is not often you have the power to increase the size of a telescope after it has been built!

This relatively simple engineering solution has of course only recently become possible with advances in computer processing power, the central core in the Netherlands has to be capable of dealing with a formidable terabyte or so of data per second. Because of the nature of this set up however, it allows several observers to observe the entire sky at once, or select a specific observing direction using the phase delays between antennas. This massive observing power, which is only limited by our computer processing ability, will allow us to attack some of the key issues of observational cosmology. The most exciting of which, and a key scientific goal of *LOFAR*, is to search for the signature of the reionization of neutral hydrogen. *LOFAR* is capable of observing the redshifted 21cm line emission from the Epoch of Reionization, redshifted into its observing band from 1420.40575 MHz.

LOFAR will thus allow us to obtain direct observations from this crucial phase change in the universes history, and give us insight into the sources responsible for reionization.

Another key scientific goal of *LOFAR* is to exploit its all sky capabilities to perform a series of sky surveys. This is intrinsically interesting as the sky has never been surveyed in this low frequency radio window and it will no doubt bring to our attention new classes of object and phenomena, but is also interesting due to what it can tell us about the high redshift universe and the process of galaxy formation. There are two primary scientific goals of these surveys of substantial interest to cosmology; the first is to use the radio emission from the AGN of high- z ($z > 6$) radio galaxies to probe their formation history over a large fraction of cosmic time, right from the epoch of reionization to the present day; and the second is to use *LOFARs* unprecedented radio sensitivity to view the population of star forming galaxies free from dust obscuration, allowing us to trace the star formation history of the universe through the radio emission of starburst galaxies.

1.4 Gamma Ray Burst Cosmology

The extreme luminosity and redshift of Gamma Ray Bursts make them ideal cosmological tools, and allow many of the problems associated with other high redshift sources to be bypassed. The brightness of their afterglows allow them to be detected in principle out as far as $z > 20$ (Lamb & Reichart 2000), much further than galaxies and quasars, and back as far as the formation of the earliest Pop II and III stars (although it is currently unclear whether the latter population created GRBs). This high-redshift detectability is the result of GRBs having stellar mass progenitors, which means that unlike traditional cosmological probes, the luminosity of a GRB and thus its detectability is independent of the properties of its host galaxy. This fundamental advantage allows GRBs to be detected out to greater distances and deeper limits than any other object, and opens up new avenues to explore the universe at its earliest of times.

1.4.2 A Long Time Ago, in a Galaxy Far Far Away...

The fact that the luminosity of a GRB is independent of the mass of its host galaxy means we can in principle detect the presence of very dim galaxies that would otherwise be

missed in dedicated sky surveys. We do not of course observe a host galaxy directly with a GRB, but rather the detection of a burst implies its presence and pinpoints its location for follow-up observations once the afterglow has faded. Also, because GRB afterglows are so much brighter than galaxies and quasars at these redshifts, GRBs can be seen out to greater distances than any other class of object, with the immense luminosities of the afterglows also allowing spectroscopic follow-up for robust distance determination that would be near impossible for objects at a similar redshift. This has been proven beyond doubt by the detection of *GRB 090423* at a colossal redshift of $z = 8.2$ (Salvaterra et al 2009, Tanvir et al. 2009), which at the time of its detection in 2008 held the title (by some way...) as most distant object ever observed by mankind.

Observing objects at redshifts such as this have the potential to give us the first direct observations of objects from deep within the era of re-ionization, particularly if we can push the boundary back even further to $z > 10$ when re-ionization is thought to be at its most vigorous, and give us insight into how the processes of reionization and chemical enrichment progressed after the formation of the first galaxies. Observations of high redshift GRB afterglows allow us to constrain the epoch of reionization by the presence or absence of flux shortward of the Lyman limit (in the GRBs restframe) (Barkana & Loeb 2004, McQuinn et al. 2008). An absence of flux implies absorption caused by neutral hydrogen along the line of sight, showing its presence in the IGM, and giving us a direct probe of the ionization state at these redshifts. Also, by measuring elemental abundances from absorption lines in GRB afterglow spectra, it is possible to obtain direct measurements of the chemical enrichment of the universe during this critical stage in its evolution. We are also aided here in studies of the early universe's ionization state by GRB host galaxies being very small. They do not significantly ionize the surrounding IGM as much as larger galaxies or quasars, allowing us to sample the IGM in a much more unperturbed state.

GRB afterglows also have very smooth spectra compared to the relatively complex ones of quasars, meaning there are very few complications involved in extracting detailed host galaxy information. Metal lines in the afterglow with sufficiently high signal to noise

can be used to directly measure host galaxy physical conditions such as temperature, chemical enrichment, ionization state and even kinematics, giving us a detailed insight into the properties of these early galaxies, and how these properties evolved with redshift. Information on re-ionization and chemical enrichment are of particular interest, as how they evolve describes how the character of star formation changed from a high mass dominated mode (Pop III) to the lower mass Pop II mode we are more familiar with today.

1.4.3 Stellar Mass Progenitors

Because GRBs have stellar mass progenitors, we can study more than just primordial galaxies, but primordial stars as well. Their association with the deaths of massive stars makes GRBs ideal probes of early star formation rates and the impact of stars upon the high redshift universe, as well as offering the tantalizing opportunity to detect Pop III stars one at a time. It is unclear as to whether Pop III stars would have produced GRBs (although Mészáros & Rees 2010 offer a model of what a Pop III GRB originating at redshifts to the order of $z \sim 20$ would look like to an observer), but if this is the case, there does exist the potential to actually detect a Pop III star in its very last moment. As well as potentially detecting Pop III stars, unraveling the early star formation history of the universe is of great interest to cosmology. If it is possible to obtain a complete redshift distribution, and if GRBs could be proven to be an unbiased tracer of star formation, we could obtain a complete picture of how early star formation progressed and be able to see directly how reionization and chemical enrichment progressed. It would be possible to learn how star formation moved from Pop III to Pop II and see the impact this had on the early universe. By unraveling the universal star formation history, we could also see how smooth this transition was, and how the evolution of these two stellar populations proceeded simultaneously for a time, with pockets of Pop II stars forming in more chemically enriched regions.

1.4.4 In the Blink of an Eye

Although GRBs have the potential to do some fascinating things for cosmology, just like the traditional cosmological probes of distant galaxies and quasars, GRBs have their own unique drawbacks. The first and most inescapable is their transience. GRBs are very

short lived transient events in the grand scheme of astronomy, and any observations that need to be made for them must be made before the afterglow fades. Often this is not possible, the burst may be at a poor position on the sky for follow-up observations, such as above one of the poles or too close to the sun or galactic disk, even if the burst does go off in a convenient patch of sky it may not necessarily be dark enough to carry out observations, or simply the observer in question does not have appropriate telescope time to observe a given burst. This presents the problem that if observations cannot be made at the time we will never be able to obtain those observations at a later point. This leads to many bursts, particularly in the earlier days of GRB follow-up, with highly incomplete datasets.

A particular problem here in the interests of cosmology is that not all bursts have measured redshifts. Some bursts may be ill placed, others just too dim for follow-up spectroscopy. This leads to us having a fairly incomplete and unconstrained redshift distribution of GRBs, which in itself is inappropriate for drawing any robust conclusions. Progress is however being made to obtain more complete sub-samples from the overall population, that give more reliable statistical information. In order to investigate the redshift distribution of *Swift* GRBs, Jakobsson et al 2006 defined a sub-set of GRBs 'well placed for follow-up observations'. Jakobsson's selection criteria act to remove bursts with observability conditions unfavourable for reliably determining a redshift, and give us a more complete picture of the true *Swift* redshift distribution. More recently, Perley et al 2009 also defined a sub-set of bursts followed up by the robotic *Palomar 60-inch* telescope. The bursts in this sample were selected purely on whether a GRB was rapidly followed up or not, and given the *Palomar 60-inch* automatically follows up all *Swift* GRB triggers, their sub-set constitutes an effectively uniform sample. Although this sample is relatively small (29 bursts) it can be used to place accurate constraints on the number of bursts originating at $z > 7$.

A final problem for GRB cosmology is that although it is possible to detect GRBs out to very high redshifts thanks to their luminosity, such events are still very rare. Whether we are managing to detect every high redshift GRB that comes our way or not, we have still only detected 6 GRBs with confirmed redshifts of $z > 5$. So although GRBs do

currently hold the crown of the highest redshift objects known to mankind and have the potential to do some amazing things for cosmology, they still come with their own unique set of problems and challenges.

Distance, Darkness and Dust

2.1 Dark Bursts

Long-duration Gamma Ray Bursts at their peak intensity are now acknowledged to be the most luminous objects known to mankind, and their optical afterglows frequently display similarly huge luminosities, outshining their host galaxies by several orders of magnitude. There are however cases where despite today's relatively efficient observational follow-up network, no afterglow has been detected even with very prompt or deep optical observations (Groot et al. 1998). This apparent lack of an optical afterglow has led to the so-called 'dark burst' problem. In this chapter we seek to shed light on the dark burst problem and its causes by investigating a new large and relatively redshift complete sample.

2.1.2 Causes of Dark Bursts

Many explanations for the phenomenon of dark bursts have been put forward and these generally fall into two categories. First are factors inherent to the burst itself:

- i. There may be an early break in the light curve leading to lower than expected afterglow flux at early times.
- ii. There may be a low density external medium surrounding the burst. GRB afterglow emission is thought to arise from shocks in the surrounding interstellar medium, around the immediate burst environment. A low density medium would mean this would not occur, or that the afterglow would be significantly dimmer than expected despite an energetic event. These are the so called 'naked bursts' (e.g. Godet et al 2006).

- iii. The burst may be an intrinsically weak event. It is known that the fluence of the initial GRB and the luminosity of the afterglow are well correlated, a powerful burst will lead to a bright afterglow. Thus a relatively underpowered GRB will produce an afterglow that may be dim enough to go unnoticed by follow-up observations not taken to deep enough limits.

Second are factors external to the burst:

- i. The GRB may originate in a dusty host galaxy which acts to extinguish optical afterglow emission. Given GRBs are thought to be associated with star formation it stands to reason that many bursts could originate from dusty host galaxies or localized dusty regions within them.
- ii. The GRB may be at a high enough redshift such that the Lyman break passes through the observing band and renders the afterglow invisible or severely diminished at these wavelengths. Indeed a non-detection in an optical filter combined with a detection at longer wavelengths where the Lyman break has not yet passed through is the primary indicator during follow-up observations that the burst is a high redshift candidate (e.g. Tanvir et al 2009, Jakobsson et al. 2006).

Any of these factors are of interest with the aim in mind of furthering our understanding of GRBs and their environments, but is of particular interest to cosmology to identify those dark bursts that occur at very high redshifts.

2.1.3 Dark Bursts at High Redshift and the Lyman- α Break

In *Section 1.3.3*, it was described how a break in a galaxy's spectra caused by the redshifted Lyman limit can be used to both select high redshift objects and accurately constrain their redshifts. In GRB astronomy, a very similar method is often used to determine whether or not a given burst is a high redshift candidate. Here, rather than looking for a break in the bursts spectrum caused by the Lyman limit redshifted through the observing bands (known commonly as the Lyman break), we instead generally look for what is called the 'Lyman- α break'. This is almost identical in principle to the Lyman break used to detect high redshift galaxies, but is physically distinct.

The Lyman- α break is produced by what is known as the ‘Lyman- α forest’, a spectral feature caused by Lyman- α absorption and the action of cosmological redshift. Given that both hydrogen and Lyman- α photons are abundant in the universe, Lyman- α absorption lines are an incredibly common spectral feature. As redshift increases, we will start to see additional Lyman- α absorption lines at different redshifts, caused by Lyman- α absorption in intervening clouds of hydrogen in the early universe at lower redshifts along the line of sight. Eventually these lines build up into an extensive ‘forest’ shortward of the Lyman- α wavelength of 1215\AA (in the emitting objects restframe), which we refer to as the ‘Lyman- α forest’.

As redshift increases, the ‘Lyman- α forest’ will start to move through the observing bands and we will see diminished flux at these wavelengths, much like in the case of the Lyman limit described in previous sections. At a redshift of around $z > \sim 4$ the forest starts to pass through the R -band (commonly the filter of choice used by telescopes carrying out optical follow up observations), meaning we will see diminished emission from a target source. As redshift increases beyond $z \approx 6$, neutral hydrogen in the early universe becomes so abundant that the lines of the Lyman- α forest become so dense that they effectively merge into what is called a Gunn-Peterson trough, which acts to damp all emission shortward of 1215\AA in the emitting objects rest frame. Emission at longer wavelengths will however be unaffected, and the object here may still be relatively bright. This break in the spectra is what we refer to as the ‘Lyman- α break’, and is often now how high redshift GRB candidates are initially identified, a non-detection of the afterglow at some optical wavelength, but a comparatively bright detection in longer optical or nIR filters.

As well as being a high redshift indicator, if enough observations are taken across several different filters the location of the Lyman- α break can be used to accurately constrain a GRBs redshift from its spectral energy distribution (as in the case of the Lyman break in high redshift galaxies), and are often referred to in these cases as ‘photometric redshifts’.

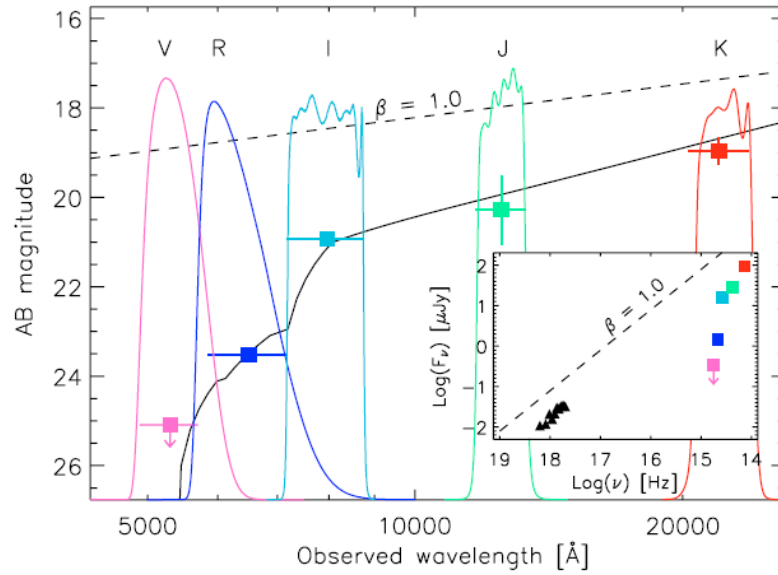


Figure 2.1: Spectral energy distribution of the afterglow of GRB 050814 at 14hrs post burst, taken from Jakobsson et al.'s 2006 paper. The spectral break blueward of the *I*-band is too steep to be explained by dust extinction alone, and the data is best fit with a Lyman- α break at a redshift of $z = 5.3$ (solid black line). The dashed line represents the spectral slope expected from synchrotron emission in the fireball model with a spectral index of $\beta = 1$. The inset figure shows the same optical/nIR observations alongside the X-ray spectrum, with the same dashed line representing the expected synchrotron emission as in the main figure.

This was first done in 2006 by Jakobsson et al. by modelling the spectral energy distribution of GRB 050814. This burst exhibited fairly blue *I-K* colours and much redder *R-I* colours, making it a high redshift candidate. Its SED is shown in *Figure 2.1* and clearly exhibits a strong break blueward of the *I*-band. This break is far too strong to be explained by any dust reddening alone, and is best fit with a Lyman- α break at $z = 5.3$ (although Curran et al. 2008 find in a more robust reanalysis of the data, the redshift to be $z = 5.77 \pm 0.12$). Jakobsson's fit is shown as the solid black line in the figure. If the break was due to dust reddening alone, we would expect a much smoother drop in flux as we move blueward through the optical bands, rather than the steep drop seen in this case. We can also note from Jakobsson's diagram that photometric redshifts obtained from GRB afterglows are more reliable than those obtained for galaxies due to their relatively simple underlying spectral energy distributions.

As hinted at previously, this useful effect for identifying high redshift GRBs can also be mimicked by interstellar dust. If a burst originates within an extremely dusty host, the dust will act to extinguish optical flux and we will similarly detect a diminished optical afterglow. Longer wavelengths are also less subject to dust extinction, meaning the afterglow's nIR emission will still be comparatively bright as in the case of high redshift. It is thus sometimes difficult to discern between the scenario of high redshift or a dusty host galaxy without detailed spectral fitting.

As discussed in the previous chapter, the extreme luminosity of GRBs makes their potential as cosmological probes of great interest, and with the recent detection of GRB 090423 as the most distant object ever observed to that date at $z = 8.3$ (Tanvir et al. 09) has certainly given more than a boost to this field. Dark bursts are thus arguably of great interest because of their potential to all be at very high redshifts. In reality however, the current sample of dark bursts is very likely a mixed bag, with a variety of factors leading to a diminished or undetected optical afterglow which prove difficult to distinguish.

2.1.4 When is a Burst ‘Dark’?

Complications also arise when actually trying to define whether or not a burst should be declared ‘dark’. It is not appropriate to decide a burst is dark if optical follow-up observations have been taken only to shallow limits, or at very late times after the burst trigger when the afterglow may have significantly faded. There is also a difference between a burst being optically ‘faint’ and optically ‘subluminous’. An afterglow might appear very optically faint, but if the afterglow is similarly faint across all other filters it cannot really be considered optically ‘dark’ or ‘subluminous’. If however an afterglow appears faint at optical wavelengths but is comparatively bright in the X-ray, then it could be considered ‘dark’. In this way it is also possible (somewhat counter-intuitively) for a burst with a clearly detected optical afterglow to be considered dark, as comparison with the afterglow at other wavelengths may reveal the optical component to be comparatively dim. This issue of deciding whether or not a burst should be classified as dark has been addressed by several authors (Jakobsson 2004, Rol 2005, Van der Horst 2009) who define somewhat

different criteria for establishing whether an afterglow is optically sub-luminous by comparing its optical luminosity with its X-ray luminosity.

Jakobsson et al. (2004) defined a burst to be dark based upon its optical to X-ray spectral index, β_{OX} ($F_\nu \propto \nu^{-\beta}$). In the blast wave model for afterglow emission (Piran 1999 and references therein), any energy not radiated away in the initial burst takes the form of the kinetic energy of baryonic ejecta that ploughs into the interstellar medium surrounding the GRB progenitor. This creates a relativistic shock wave that propagates outwards into space. Highly energetic electrons within this shockwave are accelerated by powerful local magnetic fields and radiate as synchrotron emission across much of the electromagnetic spectrum. It is this synchrotron emission that then forms the GRB afterglow. In the fireball model the photon spectral index, β , from synchrotron radiation is determined by the slope of the electron energy distribution, ρ , and the frequency of the cooling break, ν_C :

$$\beta = \begin{cases} (\rho - 1)/2, & \nu < \nu_C \\ \rho/2, & \nu > \nu_C \end{cases}$$

For an explanation of these parameters, see *Figure 2.2*. In the simplest form of the blast wave model ρ is expected to be greater than 2, with observations showing that this is almost always the case, resulting in a minimum value for β_{OX} of 0.5 (equivalent to a colour index of $B - V \approx 0.3$). Thus, Jakobsson et al. 04 state that any bursts with $\beta_{OX} < 0.5$ are optically subluminescent with reference to the blast wave model, and are classified as dark. As well as its physical motivation and simplicity, this method is advantageous in that by definition it immediately excludes those bursts that are intrinsically weak events. Such events would have weak X-ray fluxes as well as optical, and can be easily eliminated from a sample by Jakobsson's dark burst criteria.

The method does encounter problems however, in that in the original study all fluxes were evaluated at $t = 11$ hrs (in the observers frame) after the burst trigger to avoid calculating β_{OX} during early time flaring activity, which would lead to an erroneously high

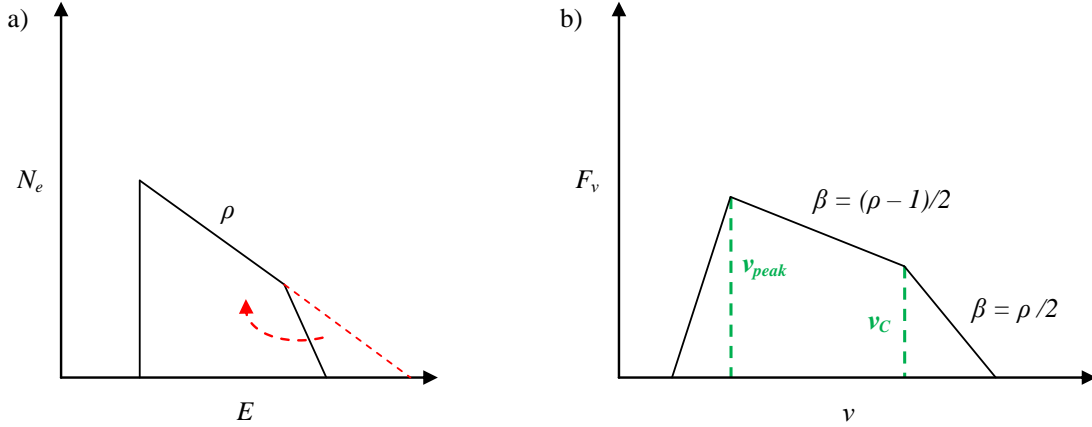


Figure 2.2: a) Electron energy distribution for a population of free electrons, as in the case of the GRB fireball model. The y-axis represents the number of electrons at a given energy, and the x-axis represents that electron energy. The population will have a base energy, represented by the vertical initial rise at lower energies, and a decreasing number of electrons at higher energies, represented by the steady slope of the electron energy distribution, ρ . The electrons at the highest energies will decay rapidly and move to lower energies, as represented by the red dashed lines. This leads to a ‘cooling break’ in the distribution. b) Corresponding synchrotron spectrum for the previous electron energy distribution. The y-axis represents the flux at a given frequency ν , and the x-axis represents that frequency. The decline at lower frequencies below the peak frequency ν_{peak} is caused by self absorption, i.e. below ν_{peak} the plasma is opaque and we see a decline in flux with frequency as these photons are absorbed. The cooling break in the electron energy distribution also gives rise to a cooling frequency, ν_C . The slope of the spectrum, β , at frequencies higher than ν_{peak} is directly related to the slope of the electron energy distribution, ρ . At $\nu_{peak} < \nu < \nu_C$, the slope of the synchrotron spectra is given by $\beta = (\rho - 1)/2$, and at $\nu > \nu_C$, $\beta = \rho/2$, as shown in the figure.

or low β_{OX} , depending on whether the flare was in the X-ray or optical. Melandri et al. 08, and Cenko et al. 08 however point out using their own dark burst samples that there is little temporal evolution of the spectral index, β_{OX} , after the initial rapid variability in the lightcurve has subsided. Although extrapolation of the optical and X-ray flux to the same times is obviously vital, their studies show that extrapolation to 11hrs post burst is not necessarily as important. Melandri et al. also caution that there is the potential of late time central engine activity leading to enhanced X-ray emission, which in fact *would* lead to temporal evolution of β_{OX} at late times and give the appearance of a burst being optically subluminal. These two arguments may sound fairly contradictory (i.e. there is little evolution of β_{OX} after the early flaring period, except when there is...), but the point here is

that it does not really matter to a degree at what time β_{OX} is evaluated, provided it is not evaluated during early times or periods of late flaring activity.

As well as this potential late time engine activity, there are issues of practicality that are more likely to manifest. Due to their transient nature and the limited availability of instruments and time to observe a given GRB, it is rather unlikely that a particular burst will have continuous multi-spectral coverage right from the burst alert to past $t=11$ hrs. It is thus often necessary to extrapolate data to 11 hrs (more likely for optical data as *Swift* usually provides ample continuous X-ray coverage until late times). Problems will thus arise if we extrapolate from early time optical observations which may have been affected by flaring, or simply extrapolating an observation to 11 hrs might not be very accurate as the temporal decay slope may not be well defined at these times. So in summary, extrapolation to 11 hrs does initially seem a good fiducial time to use as it avoids early time flaring activity, but may in practicality lead to inaccuracies and, as Melandri et al. 08 and Cenko et al. 08 point out, is not required due to very little evolution in β_{OX} with time after the aforementioned early activity.

Rol et al. (2005) used a more sophisticated approach involving extrapolating an afterglow's X-ray flux into optical wavelengths based on the physics of the fireball model. This is done by generating a range of values for the electron spectral index, ρ , using the values of the burst's X-ray spectral and temporal indices and considering eight different variations of the standard fireball model. Using these generated values of ρ , Rol et al. extrapolate the X-ray flux down into the epoch and frequency of the optical/nIR waveband in question and chose the most extreme values. By choosing the highest and lowest values of the extrapolated flux in this way, Rol et al. obtain the flux range within which we would expect to see an optical counterpart. Any burst with an observed flux below the lower limit of this range is thus subluminal with respect to the fireball model, and is classified as dark by Rol et al..

Despite producing largely congruent dark burst samples, these two methods of classifying dark bursts both have their respective drawbacks. Jakobsson et al point out

themselves that the problem with their method arises when deciding upon the value of the β_{OX} threshold used to decide whether a burst is subluminal. Although their value of $\beta_{OX} > 0.5$ is physically motivated, it has been shown that it is possible to obtain values of ρ of less than 2 by introducing a high energy cutoff in the electron energy distribution, meaning that values of $\beta_{OX} < 0.5$ would not strictly be subluminal. Both methods also make use of temporal decay indices in their extrapolation process, which, as mentioned previously, can lead to inaccuracies due to the complex behaviour of GRB lightcurves. Rol et al. also encounter potential problems from the errors associated with spectral extrapolations from X-ray wavelengths. Although they do only use the most extreme values for their dark burst classification, they still could be missing some bursts that would be classified as dark given more accurate data.

In an attempt to tackle these issues, Van der Horst et al 09 defined a third method of classifying dark GRBs, which attempts to free classification from assumptions about the electron energy distribution and reliance on temporal indices. Their only assumption is that both X-ray and optical emission result from synchrotron radiation, and that this emission comes from the same source. If this is the case, then the X-ray spectral index β_X should have the same value as the optical spectral index β_O , or $\beta_X - 0.5$ if there is a cooling break between the optical and X-ray observing bands (see *Figure 2.3*). The optical to X-ray spectral index, β_{OX} , should thus be somewhere between β_X and $\beta_X - 0.5$. Any burst which lies below $\beta_{OX} = \beta_X - 0.5$ is then subluminal in this classification scheme and categorized as dark.

Despite its relative lack of sophistication, Jakobsson et al's classification method is still more widely used than that of Van der Horst or Rol et al., and this is probably due to its simplicity. With the reliability of *Swift* X-ray data, the problems associated with flaring or late engine activity can usually be avoided, and simplicity is important when doing fast real time follow-up work. Jakobsson et al.'s method is also probably more widely used when we consider the context of why classifying a dark burst is important. As will be explained throughout the rest of this chapter, one is not so much interested in whether a burst is dark or how dark it is, but more why it is dark. As has been mentioned, if a burst is

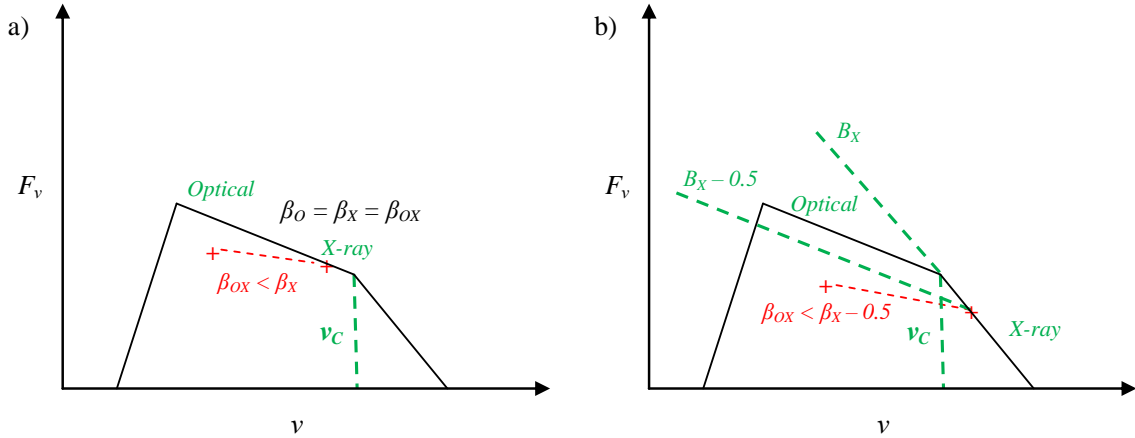


Figure 2.3: a) In the above synchrotron spectra the cooling break ν_c lies at higher frequencies than the X-ray emission. The optical and X-ray spectral indices should thus be the same, $\beta_o = \beta_x = \beta_{ox}$. If a burst is optically subluminal, as illustrated by the red data point in the figure, then $\beta_{ox} < \beta_x$ and the burst will be dark. b) Here the cooling break lies between optical and X-ray frequencies. The optical spectral index is here related to the X-ray spectral index by $\beta_o = \beta_x - 0.5$ (remembering that $F_\nu \propto \nu^\beta$). The red data point on the left represents a hypothetical X-ray flux, and the green dashed lines stemming from it represent lines with the gradients β_x and $\beta_x - 0.5$ as labelled. The optical to X-ray spectral index, β_{ox} , should thus be somewhere between β_x and $\beta_x - 0.5$. If the gradient is less than this (as indicated by the red dashed line between the hypothetical X-ray data point and a hypothetical subluminal optical data point on the right), i.e. $\beta_{ox} < \beta_x - 0.5$, then the burst is subluminal with respect to the fireball model and thus dark.

dark it is indicative of a potentially extreme redshift or high dust obscuration, and by seeking out the dark bursts, this is generally what researchers are after. We are thus generally only really interested to the first order to what degree a burst is dark so that we can answer more fundamental questions, meaning we don't necessarily need very exact criteria for darkness. Jakobsson et al.'s criteria is thus then almost always adequate for the needs of researchers where its simplicity is valued in the game of rapid follow-up (especially when deciding on whether or not to trigger a telescope to pursue a potentially high redshift event), and is robust enough to cope with sparse optical data, as is often the case in GRB research.

2.1.5 Disentangling the Causes

As well as the challenges associated with deciding when a burst should be declared dark, it is also difficult to disentangle the various causes of dark bursts, and also to explain

the apparently large fraction of dark bursts in the *Swift* era. Several authors, most notably Melandri et al. 08 and Fynbo et al. 09 have published large samples of data with the aim (or one of their aims) of constraining what fraction of bursts detected by *Swift* are actually dark. Melandri et al. 08 present the rapid follow-up of a sample of 63 bursts from their observation campaign at the Liverpool Telescope and the Faulkes Telescopes North/South.

Of these 63, they report that 39 are not detected to reasonable optical limits ($R < 22$ at early times), and of these 39 only 10 have published detections from other instruments resulting in a dark burst fraction of $\sim 50\%$ by the criteria of Jakobsson et al.. Fynbo et al. 09 publish a more robust sample of 146 bursts with data taken from a wide variety of instruments, and conclude a dark burst fraction of between 25% and 42% using Jakobsson's criteria (see *Figure 2.4* for dark burst distribution). These estimates are both larger than the $\sim 10\%$ dark burst fraction reported pre-*Swift* (Lamb et al. 2004), but as both authors (and Cenko et al. 08) point out, this may be due to pre-*Swift* selection effects.

Before *Swift*, follow-up observations often relied upon accurate optical or radio afterglow positions, intrinsically biasing the sample towards brighter optically detected bursts and higher values of β_{OX} . Also, because *Swift* is more sensitive, it detects afterglows at higher average redshifts than previous missions. At intermediate redshifts ($z \sim 2-3$), the observers R -band corresponds to a shorter GRB rest-frame wavelength that will be more suppressed by dust obscuration. Thus, given *Swift* bursts have a median redshift of $z \sim 2.2$, it is not surprising that detecting bursts with suppressed optical afterglows are more common than pre-*Swift*.

In their own study Cenko et al. 08 also present a burst sample exhibiting a large dark burst fraction. They report a sample of 29 bursts from their observing campaign at the *Palomar 60inch* robotic telescope. The sample is very uniform, with all bursts being *Swift* bursts observed within 1 hour and having multicolour ($g'Rci'z'$) observations. By applying the Jakobsson criteria they also find a dark burst fraction of $\sim 50\%$. As mentioned previously, they explain this large dark burst fraction in terms of biases in the pre *Swift* follow-up towards brighter more easily detectable events. More interestingly, they also

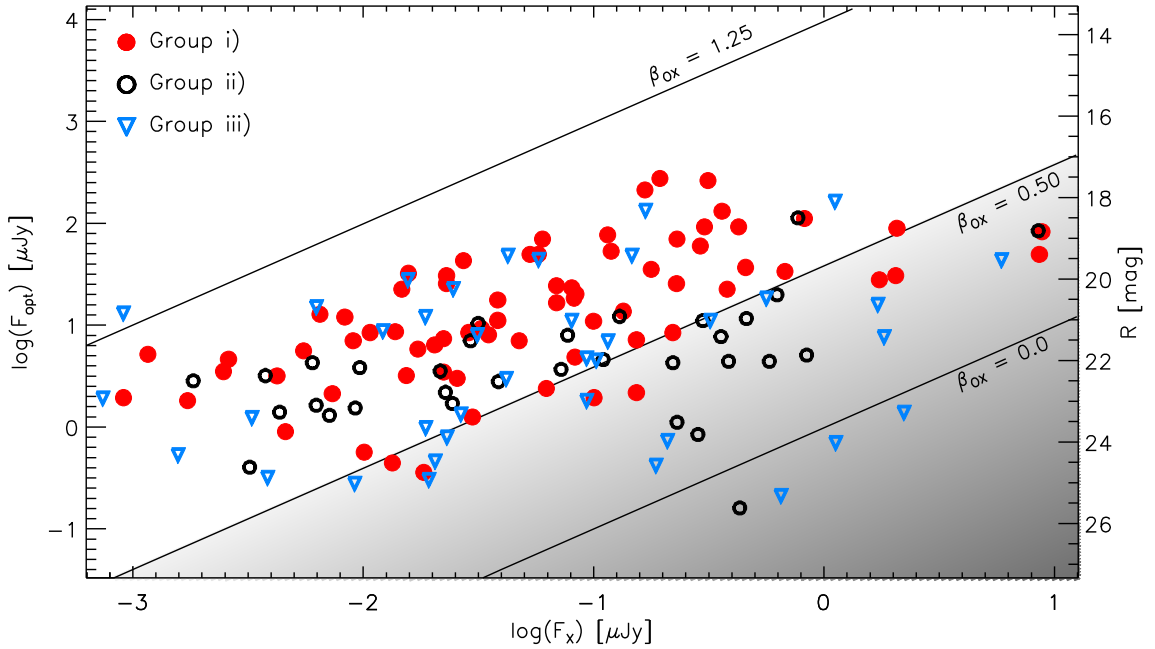


Figure 2.4: Taken from Fynbo et al’s 2009 paper, this plot shows a version of the dark burst diagram first presented by Jakobsson et al 2004, here presented for a more up to date sample of bursts by Fynbo et al. 2009. The diagram is a plot of F_{OPT} vs F_X for a sample of bursts and includes a line of constant $\beta_{OX} = 0.5$ running diagonally down the centre, with any burst lying below this line classified as ‘dark’ by the criteria of Jakobsson et al. 2004. This type of plot has been used in several studies since the original publication because of its simple way of illustrating the distribution of the dark burst population. This particular version by Fynbo et al. exhibits three subsets of bursts from a sample defined in their study, Group i) contains bursts from their sample with redshifts measured from optical afterglow spectroscopy, Group ii) contains bursts with a detected optical/nIR afterglow but no afterglow based redshift, and Group iii) contains bursts with no detection of the optical afterglow.

utilize their multi-colour observations to help disentangle those dark bursts caused by dust obscuration. Of the 7 cases where it was possible for Cenko et al. to measure the optical spectral index β_O , 6 were too steep to be explained by standard afterglow synchrotron emission. Also, by fixing β_O to an average value of 0.6, fitting an SMC extinction curve with the host galaxy reddening as a free parameter, and then correcting the optical fluxes for this extinction, they find that in all cases where this was possible a previously dark GRB is no longer subluminal by Jakobsson’s criteria.

This implies that dust obscuration accounts for a large number of dark bursts, and is backed up by the argument that the apparently large *Swift* dark burst fraction could be caused by the large proportion of *Swift* bursts at intermediate redshift where the observers *R*-band corresponds to a shorter more dust-attenuated wavelength. This has other implications in itself; many dark bursts with host galaxy observations have only modest extinction levels, implying that the dust is not homogeneously spread in the host galaxy and is instead confined to the region around the GRB or other concentrated star forming environments. This further implies that such regions may be missed in galaxy observations undertaken at rest-frame optical/UV wavelengths.

There have been several examples showing that when we find a dark burst with a host galaxy detection, we generally find that the galaxy itself is not very dusty, but there is still strong evidence for dust obscuration being the cause of the GRBs optical faintness. Tanvir et al. 2008 reporting on the optically dark burst GRB 060923A, and more recently Holland et al. 2010 reporting on GRB 090417B, both detect host galaxies that do not exhibit massive dust content. However, dust extinction is implicated in both cases over redshift as the reason for the optical dimness, implying these bursts (and potentially many other dark bursts) reside in localized dusty regions within their host galaxies.

Zheng et al. 2009 find a rather lower dark burst fraction based on a sample of 229 *Swift* bursts (including 19 short bursts). They select their sample from bursts detected by *Swift* up until the end of 2007, collecting the redshift, *BAT* fluences between 15-150 KeV, *R*-band flux densities and X-ray integral fluxes of 0.2-10 KeV at 11hr after the *BAT* trigger, and intrinsic hydrogen column density, N_H . They extract X-ray flux densities at 3KeV and calculate β_{OX} values at 11hrs for the sample. As well as a subset of dark bursts that they define via Jakobssons criteria of $\beta_{OX} < 0.5$, they define a set of 'gray' bursts between $0.5 < \beta_{OX} < 0.6$ that lay on the threshold of being dark to take into account potential sources of error. Of the long bursts they find $\sim 12\%$ are dark, and $\sim 18\%$ if all the 'gray' bursts are considered as potential dark bursts. However, given that many of their bursts only have upper limit estimates to β_{OX} , the true dark burst fraction could be as high as $\sim 50\%$, which

encompasses the determinations of Cenko et al., Melandri et al. and Fynbo et al. discussed above.

Zheng et al. also examine the high redshift ($z > \sim 4$) bursts in their sample. They find that although the high redshift bursts do tend to be 'darker' than those at low redshift, only two bursts out of the ten with $z > 4$ make it into their dark burst category and a further 3 fall into their 'gray' burst category at $0.5 < \beta_{OX} < 0.6$. Although in general a large fraction of high redshift bursts appear 'dark', as would be expected, Zheng et al. point out that these bursts make up a very small fraction of the overall dark burst population. They do however caution that very few ($\sim 8/36$ in their dark/gray sample subset) have measured redshifts, so the actual fraction of high redshift dark GRBs in their sample may be much higher. They also speculate on the fraction of dark bursts being caused by dust extinction using N_H hydrogen column densities as an approximate proxy for host galaxy extinctions, and the fact that high redshift bursts are thought to have low N_H , as the photons we observe in these cases started at higher energies are therefore absorbed less by a given column of gas. They find that on average dark bursts have higher N_H values than normal ones, and that it is very unlikely that the two populations can be drawn from the same N_H distribution, reinforcing the idea that the majority of dark bursts are caused by dust obscuration in the GRB host galaxy or immediate environment.

This is not to say that all dark bursts are caused by dust rather than redshift, the highest redshift bursts (GRB 080913A at $z = 6.7$, GRB 090423 at $z = 8.2$) are very definitely dark! It is in unraveling the various causes of dark bursts that are of interest to us, and particularly in extracting any extremely high redshift bursts from the dark GRB sample.

2.2 The *Swift* Redshift Distribution

The high sensitivity of *Swift* allows it to detect very faint bursts at large luminosity distances, meaning that *Swift* bursts have a much higher mean and median redshift than any found for previous instruments. The *Swift* redshift distribution is however drawn from a

highly incomplete sample, as only ~25% have robust spectroscopically or photometrically determined redshifts. This incompleteness has the potential to easily bias the sample due to the tendency to obtain redshifts for bright or otherwise interesting GRBs where follow up observations are more comprehensive, and/or biasing it towards GRBs at redshifts where common absorption lines appear in optical spectra. Thus when attempting to constrain the true *Swift* redshift distribution in order to estimate the fraction of bursts which lie at high redshift, a number of difficulties arise.

2.2.2 Constraining the *Swift* Sample

Many *Swift* bursts are actually poorly placed for optical follow-up observations. They may lie within the galactic plane or close to the sun, and thus have little observability from ground based instruments. It is therefore impossible to obtain a redshift measurement for many bursts that have otherwise been detected by *Swift*. In order to study the true *Swift* redshift distribution it is thus necessary to reduce the sample size in order to improve its completeness. By excluding all bursts with poor conditions for optical follow-up observation, we can obtain a sample that more accurately describes the real form of the *Swift* redshift distribution. *Figure 2.5* shows the redshift distribution of GRBs from a sample defined by the criterion of Jakobsson et al 2006 for bursts which have observing conditions 'favourable for redshift determination'. These conditions are;

- i. The burst must be well localized by the *Swift XRT*.
- ii. The *XRT* error circle should be distributed within 12 hours for a relatively rapid follow-up.
- iii. The foreground Galactic dust extinction in the direction of the burst must be sufficiently small ($A_V < 0.5$).
- iv. The burst must be well placed on the sky for follow-up observations (declination between $+70^\circ$ and -70°).
- v. The Sun-to-field distance must be large enough to not interfere with follow-up observations ($\theta_{Sun} > 55^\circ$).
- vi. There must be no bright star near the burst position that would act to contaminate any photometric or spectroscopic redshift measurements.

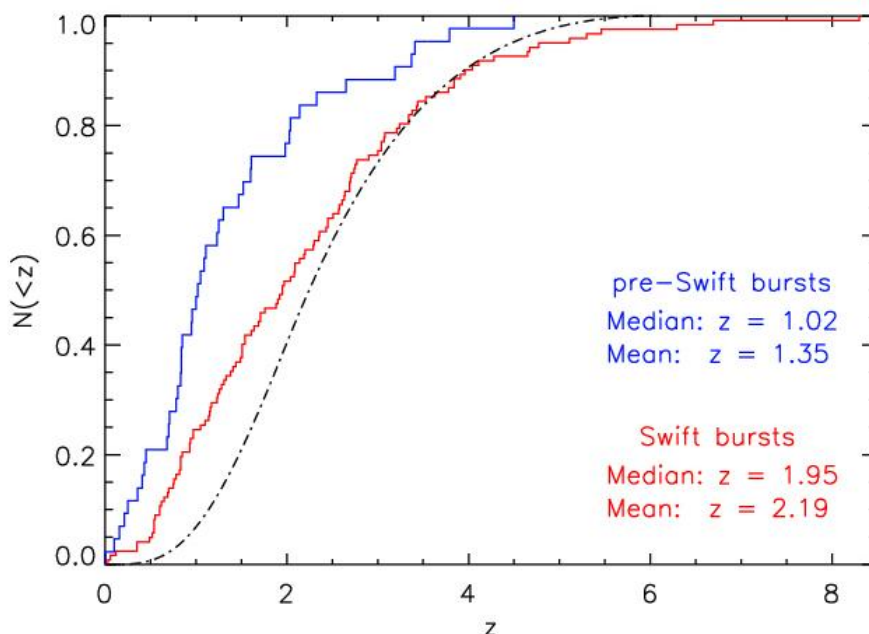


Figure 2.5: Taken from his website (www.raunvis.hi.is/~pja/GRBsample.html), this plot shows Jakobsson’s GRB redshift distribution (last updated 2nd August 2010). The plot shows the cumulative fraction of GRBs as a function of redshift. The blue line represents a sample of 44 pre-*Swift* GRBs and the red line a sample of 122 *Swift* bursts with well constrained redshifts from the overall sample of *Swift* bursts that meet Jakobsson’s criteria for being well placed for redshift determination. The black dotted line represents a simple model for the expected redshift distribution of GRBs (Jakobsson et al. 2006).

This sample contains 227 bursts, between March 15th 2005 and August 2nd 2010, of which 122 have well constrained spectroscopic or photometric redshifts. These 122 bursts are represented by the red line in *Figure 2.5*, and from this it could be concluded that at approximately ~5% (6/122 bursts) of all GRBs have redshifts of $z > 5$, but this does ignore the 105 bursts with no redshift measurement. A more robust view of the *Swift* redshift distribution can be obtained by including redshift upper limits in the sample. Many bursts do not have precisely measured redshifts but do have optical/IR afterglow detections. These can in themselves be used to place an upper limit on a bursts redshift. If, for example, a burst was detected in the *B*-band, it would place a constraint that the burst must have originated from $z < 3$, as at $z > 3$ the Lyman- α forest would have passed through $\sim 4500\text{\AA}$ and hydrogen absorption would make the afterglow faint or invisible in this band. If upper limits are included in this way then the maximum number of GRBs originating from $z > 5$

can be constrained to $\sim 14.5\%$ (33/227 bursts). This method is not necessarily the most accurate way to measure the fraction of GRBs originating at high redshift, but does set a reasonably constraining upper limit.

2.2.3 The Dark Burst Fraction

Fynbo et al. 09 also compiled a large sample of *Swift* bursts based on the selection criteria of Jakobsson with the aim in mind of creating a highly complete sample with little dependence on afterglow properties in order to analyze the true *Swift* redshift distribution. With the criteria applied the sample contains 146 bursts between March 2005 and September 2008, 108 of which (74%) have optical or nIR afterglow detections, 72 have redshift determinations. A further 12 have their redshift determined from a likely host galaxy and a further 25 have the upper limit to their redshift constrained from the longest wavelength filter they were detected in, as explained in the previous section. For the remaining 37 bursts Fynbo et al. apply the method of Grupe et al. 2007, whereby the probability of a burst being at low redshift is inferred from its excess hydrogen column density as derived from X-ray absorption. This is based on the principle that as redshift increases, X-ray absorption from hydrogen becomes harder to detect in the *Swift/XRT*, thus meaning bursts with high excess hydrogen absorption are likely to be at lower redshifts. Grupe et al. 2007 assign a redshift upper limit of $z < 2$ to bursts with excess X-ray absorbing column density above an equivalent *HI* column density of $2 \times 10^{21} \text{ cm}^{-2}$. Fynbo et al. however use a more conservative upper limit of $z = 3.5$ for their sample, rather than the $z = 2$ used by Grupe et al.. Their redshift distribution can be seen in *Figure 2.6*. They constrain the fraction of $z > 6$ bursts to be in the range 1 - 23%, and the fraction of $z > 7$ bursts to be less than $\sim 18\%$.

Perley et al. 09 constrain the fraction of high redshift *Swift* GRBs with an imaging campaign at the *Keck* observatory aimed at identifying the host galaxies of dark gamma ray bursts. The principle here is broadly the same as described above, it is possible to constrain a bursts redshift if we have an afterglow or host detection in any optical/nIR waveband. By searching for a dark burst's associated host galaxy at optical wavelengths, it is thus possible

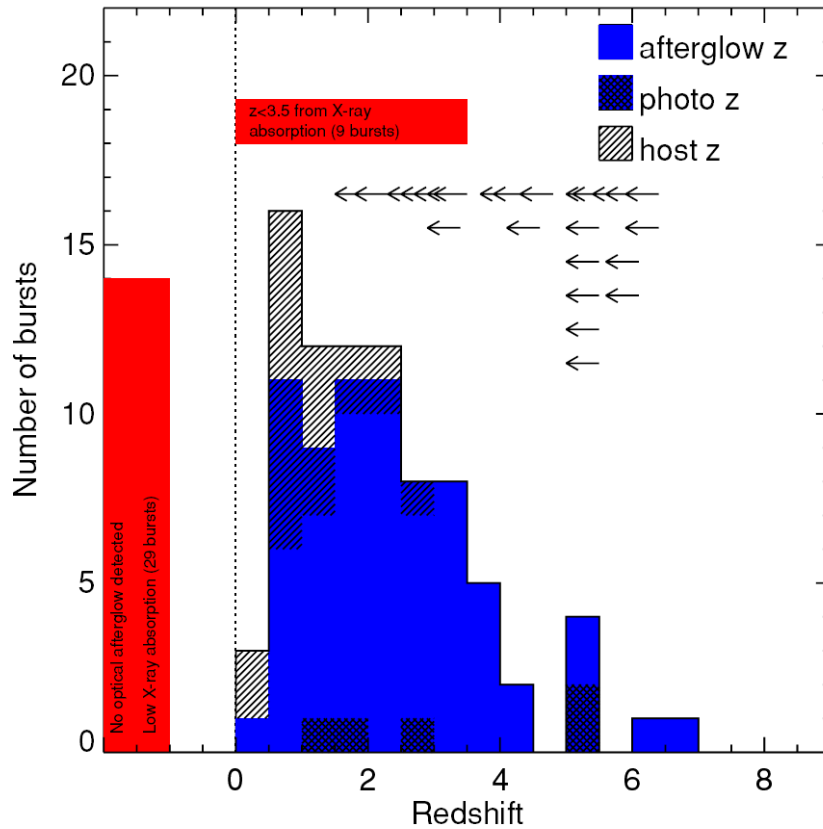


Figure 2.6: Taken from their 2009 paper, this plot shows the redshift distribution for the Fynbo et al. 2009 burst sample. Whether the redshift was obtained from afterglow spectroscopy, afterglow photometry or host galaxy spectroscopy is indicated by colour and the diagonal shading as shown in the figure. The arrows denote bursts where upper limits to their redshifts could be obtained from afterglow photometry. The red bar on the left represents 28 bursts with no optical afterglow detection and no redshift measurement from a host galaxy detection, and the red bar above the main histogram represents the 10 bursts with no optical afterglow detection but where upper limits of $z = 3.5$ could be placed based on excess X-ray absorption.

to constrain the burst's redshift in a similar manner. They find that out of a uniform sample of 29 *Swift* GRBs, of which they classify 14 as dark, all bursts in their sample have an optical detection, a candidate host galaxy detection, or both. Given that the optical detection of an afterglow or host galaxy rules out a high redshift scenario, they conclude that all events in their sample have a redshift of $z < 7$. Using a sophisticated Monte Carlo analysis they also generalize their sample to the whole *Swift* burst population. Taking into account

the probability of occurrence of host galaxy chance alignments, they conclude that at most 14% of all *Swift* GRBs are at $z > 5$, and at most 7% are at $z > 7$ at a 90% confidence level.

Another interesting conclusion that Perley et al. come to, in agreement with arguments in previous sections, is that the dominant cause of dark bursts is dust extinction. By identifying a host galaxy and measuring its redshift, it becomes possible to directly determine how much dust extinction is required to generate the dark burst's level of optical suppression. Six bursts out of the 22 in their sample (where this constraint could be derived) have rest frame $A_V > 0.8$, and three have $A_V > 2.5$. They also note that the host galaxies themselves are fairly mundane, not having huge dust extinctions and sometimes even being quite blue. This, combined with the evidence from other studies, may imply that the dust could be intrinsically linked with the GRB site itself, or that the dust is sufficiently patchy across the host galaxy that its effects are concealed. However, a subsequent followup survey with the *Spitzer* telescope has revealed that a substantial proportion of the dark burst hosts are found to be bright at 3-5 microns, even if they appear blue at optical wavelengths, suggesting that a relatively highly obscured stellar component does exist in many of them (Perley et al. private communication), implying both the presence of dust and explaining the blue colours.

In the rest of this chapter we endeavor to define as complete a sample of GRBs as possible by extending the observability criteria of Jakobsson et al., in order to place as stringent constraints as possible on the *Swift* redshift distribution and the dark burst fraction, and also to provide constraints on the breakdown of causes of dark bursts.

2.3 Defining the Sample

Due to the nature of Gamma Ray Bursts, the *Swift* sample (and all other samples of bursts detected by different instruments) tends to be highly incomplete in terms of redshifts. Because they are random transient events, there are no two GRBs with a consistent set of identical follow-up observations. GRBs are observed on a target of opportunity basis, with observers triggering observing programs when and wherever a GRB occurs, with the

window of observation only open for a few days or maybe even only a few hours depending on how rapidly the burst fades. This presents two major problems when attempting to derive meaningful statistics from a sample of GRBs that are not common in other branches of astronomy. Firstly, in any normal astronomical study involving a reasonably substantial sample of objects, an observer would submit their observing proposal in order to obtain telescope time, if their proposal is successful, wait until those observations have been carried out and then analyze the data in their own good time. When their observations are carried out is generally not very important, since galaxies are not going to move anywhere or vanish on the timescales that observations are taken and papers are submitted. This would then provide a sample of objects for analysis that have been observed in a uniform manner, that meaningful statistics and conclusions can be easily drawn from.

GRB astronomers do not have such luxuries, and are generally faced with a more tricky problem. As soon as a GRB is detected by *Swift* or a similar instrument, there is a limited time from that point onwards that follow-up observations can be made by other ground based telescopes, and if observations are not made of the GRB afterglow there and then, then they never will be. Also, neither does the opportunity exist to go back at a later date and re-observe them. This means that whatever observations are taken before the afterglow significantly fades are the only observations of that burst you will ever have to work with. Of course it is possible in some instances to obtain redshift measurements from a host galaxy (assuming they are correctly identified) once the afterglow has faded, but in many cases the hosts are very faint, thus requiring large amounts of telescope time with no guarantee of success. This is not however the full extent of the problem.

As well as rapidly fading and never-to-return-again, GRBs are highly inconsiderate with their timing and positioning on the sky. It could be envisaged that a highly coordinated and efficient system could obtain comprehensive and homogenous follow-up observations of every GRB to occur, but even if you have the most well-drilled system imaginable, it is of little use if your GRB goes off in the sky above your observatory during the day and has faded beyond observability limits come the night. It is also of little use if

your GRB goes off above the North Pole, a few degrees away from the sun/moon or behind an extensive cloud system.

Another problem along a similar theme is that GRB astronomers do not have completely free reign to command the world's telescopes as they see fit. A GRB astronomer does not know when a GRB will occur, so their granted telescope time works on a basis of telescope triggers for targets of opportunity. Thus there are circumstances where a GRB astronomer may wish to save their triggers until there is a particularly interesting burst, meaning that even if a GRB is well placed for observations it will go unobserved by some instruments. Conversely if a GRB astronomer has expended all of their trigger time, they may not be able to carry out observations if an interesting burst does occur. Furthermore, there is no factor restricting more than one GRB going off inside a day. Indeed infamously, the 19th of March 2008 played host to GRB 080319A, GRB 080319B, GRB 080319C and GRB 080319D, with GRB 080320 going off in the early hours of March 20th, and with the added factor that GRB 080319B was one of the most interesting bursts of all time, being the brightest burst ever and having an afterglow visible with the naked eye (Racusin et al. 2008). This meant that observatories (and observers....) were more than stretched that day, and further meaning that several of these bursts were not as well observed as they would have been if they had been detected on a different day.

So in summary, a given GRB is likely to have a mixed bag of observations from a variety of different instruments across a variety of filters for different amounts of time, with the possibility of having very sparse coverage if the burst was poorly placed or timed for follow-up observations. This makes any sample of GRBs incomplete with respect to consistent observations being taken, but there is always the possibility of going back after an afterglow has faded to search for a host galaxy.

The sample of Swift bursts with redshifts is also very likely to be a biased subset of the population. Clearly, it will generally be easier to measure redshifts for brighter afterglows, and indeed observers may target those since they believe they will get the most useful data-sets. Working contrary to this is the fact that some teams have specifically

targeted "dark" bursts, believing they are likely to be high-redshift events. Apart from these issues of prior selection of targets, it is also the case that certain ranges in redshift are likely to produce rather few absorption lines in the optical spectra (which are usually acquired). For example, around redshifts of $z = 1.5 - 2$, Lyman- α will still be in the UV, but common interstellar lines such as MgII (2799Å) will be redshifted to the red end of the optical window where sky subtraction is hard. Similarly very low redshifts, e.g. $z < 0.7$, the common UV absorption lines will still be in the blue, and may be missed by a spectrum which covers a restricted (and redder) spectral range. These effects may produce "redshift deserts", regions of redshift where it is harder to find spectral features, and so they become under-represented in the final samples. Indeed, a recent survey of GRB redshifts obtained from emission-line spectra of the host galaxies of GRBs found a lower median redshift than had been found from afterglows, illustrating that many afterglows for which redshifts were not measured were actually at relatively modest redshifts (Jakobsson priv. comm.).

As described earlier in this chapter, Jakobsson et al. 2006 go some way towards dealing with this by defining a subset of bursts 'well placed for redshift determination' in order to derive a more accurate redshift distribution for *Swift* GRBs. The set of criteria previously described act to significantly reduce the size of the sample, but also to increase its completeness, allowing the derivation of more meaningful statistics. Jakobsson et al.'s criteria are effective in doing this, with ~80% (at the time of writing) of their sample having spectroscopically or photometrically constrained redshifts (including upper limits to redshifts derived from the bluest band the afterglow was observed in), as opposed to ~25% of the *Swift* burst sample as a whole, however they do not take into account some practical observing considerations that could be used to increase completeness further.

Jakobsson's criteria do take into account factors governing whether a burst is observable on the sky or not, such as angle from the sun, depth into the galactic disk and high/low extreme polar latitudes, but do not take into account practical observing considerations such as how many hours of darkness is a burst above the horizon at a given observatory. A burst may be perfectly placed on the sky, but could still be considered poorly placed for observations if the Mauna Kea Observatory could not see it for any hours

of darkness, or if it were at such latitudes that the observatory at Cerro Paranal could not see it at all. Similarly if a burst was well placed on the sky and had sufficient hours of darkness to observe at a given observatory, it could still be considered poorly placed for observations at that observatory if weather conditions there prevented observations being taken, despite all other factors being favourable.

We thus propose an extension to the criteria of Jakobsson et al. 2006 in order to further increase the completeness of the statistical sample and better define a sample of GRBs ‘well placed for follow-up observation’.

2.3.2 Extended Observability Criteria

Afterglow observations can only be reliably made if an object is favourably positioned on the sky as in Jakobsson et al.’s criteria, but also only if that position on the sky is observable for a reasonable amount of time from a reasonable number of ground based observatories. We thus extend the criteria of Jakobsson et al. to include;

“A GRB should be visible above the horizon ($\text{airmass} < 2$) for at least 3.0 hours of darkness and in good weather on the first night of the GRB after the burst trigger, for at least one of the major observatories that ‘generally carry out GRB follow-up observations’.”

We choose 3.0 hours as the cut-off for good observations based on the precedent of GRB 081127, where no major observatory could see the afterglow for more than 3.0 hours and consequently it was recorded that no ground based observations were carried out.

The difficulty arises when trying to define the observatories that ‘generally carry out GRB follow-up observations’. For the purposes of this study, we define these observatories to be; *Roque de los Muchachos* at *La Palma*, Spain, *Mauna Kea* in *Hawaii*, USA and *ESO* at both *La Silla* and *Cerro Paranal* in Chile, on the grounds that the majority of all afterglow redshifts are obtained from these sites.

2.3.3 The Sample

We began by taking the sample of *Swift* bursts defined by Jakobsson et al.’s criteria between March 15th 2005 and August 12th 2009. Of the 442 GRBs detected by *Swift* during this period, 190 fulfill these criteria, with 112 having photometrically or spectroscopically constrained redshifts, and a further 51 having upper limits to their redshifts based upon the bluest filter their afterglow/host was detected in. The remaining 27 bursts have no constraints to their redshifts. Of the bursts with well constrained redshifts, 22 have redshifts derived from host galaxy observations, and 6 out of the 51 bursts with upper limits have upper limits based on host galaxy observations. These host galaxy observations are not only important in increasing the redshift completeness of the sample, but also go some way towards addressing the intrinsic redshift biases introduced by ‘redshift desert’ regions, where afterglow redshifts are more challenging to obtain and thus more likely to be under-represented in a given redshift sample.

It is of course possible that some of these redshifts derived from host galaxy observations could be erroneous due to the misidentification of a GRB host via chance alignment. This should not be a common occurrence as bursts typically lie directly on top of their hosts (Fruchter et al. 2006), and the density on the sky of dim galaxies typical of GRB hosts is not very high (Bloom, Kulkarni and Djorgovski 2002, Cobb and Bailyn 2008). However, as one goes to deeper and deeper magnitudes in search of a host, the chance of a random galaxy being mistaken for the true host goes up, simply because there are more small faint galaxies in the universe than bright ones, but it is unlikely we would be able to obtain a redshift for galaxies this faint anyway.

In order to examine the dark burst fraction of our sample it was necessary to calculate the X-ray to optical spectral index, β_{OX} , which, given several authors previously discussed have shown is relatively independent of the time post burst it is evaluated. We chose to evaluate at 2 hours after the burst trigger (in the observers frame) when most early time flaring activity should have died down. Extrapolating to 2hrs in the observers frame does of course correspond to even earlier times in the emission frames of high redshift bursts due to cosmological time dilation, meaning we are in principle looking further

towards the early flaring activity. Despite this, in the observers frame we still rarely see bursts that exhibit flaring past 2hrs, making it an acceptable time to use, and any bursts that do experience flaring activity at 2hrs or beyond are treated as special cases, as described below.

X-ray fluxes were interpolated at 2hrs from the *Swift* XRT lightcurves (Evans et al. 2009, 2007). Three bursts underwent flaring activity at $t \sim 2$ hrs (GRB 050904, GRB 070110 and GRB 071021). For GRBs 050904 and 070110, the GRB lightcurve decay fits of Willingale et al. 2008 were used, thus excluding the effects of flaring. For GRB 071021, such fits were unavailable, so only flux values either side of the flare event were used in the interpolation, resulting in suitably large errors. *R*-band magnitudes were gathered for each burst from existing literature and GCN reports, and extrapolated/interpolated to 2hrs post burst depending on the data available. For those bursts where data was too sparse to perform a reliable power law fit, but where some observations were still carried out, we selected the deepest *R*-band measurement closest to 2hrs and extrapolated assuming typical upper limits to decay indices of $\alpha = 0.5-1.3$ observed for GRBs, thus providing robust upper and lower limits to the *R*-band flux for these bursts. In some cases this did lead to exceptionally large errors when an observation had to be extrapolated back across several hours. For 3 bursts, no *R*-band data was taken at all, but sufficient *I*-band data was available to perform a spectral extrapolation into the *R*-band. For these bursts we assumed a spectral index of $\beta = 1.0$, typical for GRB afterglows. For 26 bursts, no suitable X-ray or optical data was available and thus we were unable to calculate values of β_{OX} for these bursts.

We then applied our additional observability criteria in order to investigate its effect on the sample. We gathered observability and weather information for each of the four observatories mentioned in *Section 1.3.2*. The UT times between which a burst was above the horizon below $airmass = 2$ during hours of darkness (on the night of the burst after the burst trigger) were gathered using the *Staralt*¹ tool (Sorensen & Azzaro 2002). The number of hours between these two UT times during which a burst was unobservable due to adverse weather conditions was gathered for each burst from several sources. Weather

¹ catserver.ing.iac.es/staralt/

information for *La Palma* was gathered from the *WHT*² and *NOT*³ observation log archives which both list when and for how long these telescopes were closed due to cloudy weather or wind. Weather information for *Mauna Kea* was gathered using the *CFHT Sky Probe* archive⁴ and the *UKIRT* observation log archives⁵ in a similar fashion, and weather information was available for the *ESO* observatories from the online *ESO Ambient Conditions Database*⁶. The number of hours a burst was unobservable due to weather conditions was then subtracted from the number of hours of darkness it was above *airmass* = 2, to effectively give the number of hours a burst was observable for. If, for any burst, *all* 4 observatories could not see a burst for at least 3 hours of darkness above *airmass* = 2 during good weather conditions, it was rejected from our sample. Applying this criteria to the sample of 190 bursts defined by Jakobsson et. al.'s criteria reduced the sample to 139 bursts. These are detailed in the appendix in *Table 1*, and the 51 bursts rejected by our additional observability criteria are detailed in *Table 2*.

This reduced sample of 139 bursts now contains 87 (~62.5%) bursts with photometrically or spectroscopically constrained redshifts (16 from host galaxy observations), 37 (~26.5%) bursts with upper limits to their redshifts derived from the bluest filter they were observed in (3 from host galaxy observations) and 15 (~11%) bursts with no redshift measurement at all. The sample also contains 9 (~6.5%) bursts where insufficient X-ray or *R*-band data was available to calculate a value of β_{OX} .

The 51 bursts excluded from the sample contain 25 (~49%) bursts with photometrically or spectroscopically constrained redshifts, 14 (~27.5%) bursts with upper limits to their redshift and 12 (~23.5%) with no redshift measurement at all. The rejected sample also contains 15 (~29%) bursts where insufficient X-ray or *R*-band data was available to calculate a value of β_{OX} . It can be seen by comparing the relative percentages of these two subsets that the rejected sample is much more incomplete, having proportionally over twice as many bursts with unconstrained redshifts, 13.5% less bursts overall with any

² www.ing.iac.es/Astronomy/observing/inglogs.php

³ www.not.ias.es/weather/index.php

⁴ www.cfht.hawaii.edu/cgi-bin/uncgi/elixir/skyprobe.pl?list

⁵ www.jach.hawaii.edu/UKIRT/telescope/engineering/seeing/

⁶ Archive.eso.org/asm/ambient-server

secure redshift measurement, and proportionally almost five times as many bursts with insufficient X-ray or *R*-band data. This shows that our additional observability criteria are fulfilling their role of excluding bursts that were poorly placed for follow-up observations, and ensuring that our GRB subset represents as complete a sample as possible.

2.3.4 Redshift Distribution

As well as accurately constraining the abundance of dark GRBs in the *Swift* sample and the relative significance of their causes, it is also of interest to use a sample as complete as this to investigate the overall redshift distribution of GRBs, and to constrain the fraction of *Swift* GRBs that occur at high redshift.

We derived the redshift distribution for our entire sample of GRBs, as shown in *Figure 2.7*. The sample reduced by our additional observability criteria has a median redshift of $\langle z \rangle = 2.20$, calculated from the 87 bursts with photometrically or spectroscopically constrained redshifts. We also derived the median redshift for our unreduced sample, $\langle z \rangle = 2.04$ (calculated from the 112 bursts within this with photometrically or spectroscopically constrained redshifts), and for our sample of rejected bursts, with a median redshift of $\langle z \rangle = 1.38$ (calculated from 25 bursts with photometrically or spectroscopically constrained redshifts). Using our reduced sample, we constrain the fraction of *Swift* bursts occurring at $z > 6$ to be $2.2 \pm 1.2\% - 23.0 \pm 3.6\%$ ($3 - 25 / 139$ bursts), and the number of bursts at $z > 5$ to be in the range $5.0 \pm 1.8\% - 27.3 \pm 3.8\%$ ($7 - 31 / 139$ bursts). Note that the upper limit is maximally conservative in allowing all the bursts with no redshift constraint to have the possibility of being at $z > 6$. In practice, it is very likely that some of these simply had inadequate observations made for other reasons, such as technical downtime.

2.3.5 Dark Burst Fraction

In order to constrain the dark burst fraction we derive the optical to X-ray spectral index, β_{OX} , for all bursts in our reduced sample. In keeping with other studies utilizing a large sample of bursts to constrain the overall population of *Swift* bursts, we adopt the criteria of Jakobsson et al. 2004 and define a burst to be dark if $\beta_{OX} < 0.5$.

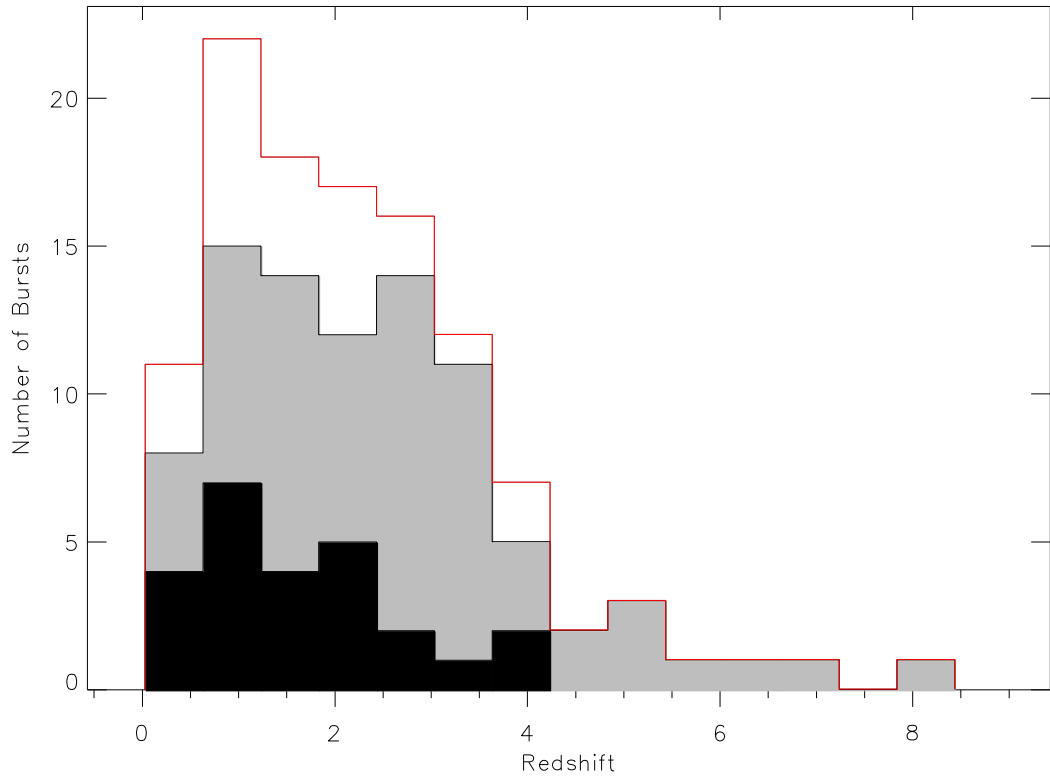


Figure 2.7: The overall redshift distribution of our sample. The grey-shaded region represents the 87/139 bursts with photometrically or spectroscopically constrained redshifts from our reduced sample of GRBs. The black shaded region represents the redshift distribution of the 25/51 rejected bursts with similarly constrained redshifts. The solid red line represents the redshift distribution of the 112/190 bursts between March 2005 and August 2009 defined by the criteria of Jakobsson et al. 2004 with photometrically or spectroscopically constrained redshifts, before our additional observability criteria were applied.

For 9/139 (~6.5%) bursts in the reduced sample it was not possible to calculate β_{OX} due to insufficient data, and for a further 41/139 (~29.5%) only upper limits were available, leaving 89/139 (~64%) bursts with robust measurements of β_{OX} . By excluding all upper limits and unconstrained values, and considering strict limits of only bursts whose upper value of β_{OX} (within a $1\text{-}\sigma$ error range) falls below $\beta_{OX} = 0.5$, we derive a conservative lower limit to the dark burst fraction of our reduced sample of $\sim 16 \pm 3\%$ (22/139 bursts). This limit thus represents the fraction of bursts in our sample that are dark beyond any doubt. By similarly considering more liberal limits of bursts whose lower limit of β_{OX} (again, within a $1\text{-}\sigma$ error range) falls below $\beta_{OX} = 0.5$, and including all upper limits and

unconstrained values of β_{OX} , which cannot be ruled out as having $\beta_{OX} < 0.5$, we derive a maximum possible upper limit to the dark fraction of $\sim 58 \pm 4\%$ (81/139 bursts). Given we believe our reduced sample is a representative, unbiased subset of the overall *Swift* population, we thus constrain the fraction of dark GRBs detected by *Swift* to be in the range $16 \pm 3\% - 58 \pm 4\%$ (22 – 81 / 139 bursts), but caution that our upper value here represents a highly conservative limit, and given it contains all unconstrained values and upper limits of β_{OX} , should be seen as the maximum conceivable dark burst fraction.

Indeed this maximum upper limit to the dark burst fraction, as well as fractions derived by the similar studies already described, contains many bursts that are not very dark at all, many having clear optical detections. This is illustrated in *Figure 2.8*. Although a relatively small fraction of bursts lie below the line representing $\beta_{OX} = 0.5$, a large number of bursts lie within $1\text{-}\sigma$ and cannot be ruled out as being dark by the criteria of Jakobsson et al.. This is not necessarily a flaw in their criterion, it is physically motivated in terms of the fireball model, and they themselves caution that $\beta_{OX} > 0.5$ is a conservative limit. This means that although our upper limit of 58% contains all bursts that could possibly be dark, it is likely that the actual fraction is much lower. Conversely, our lower fraction of 14% contains all bursts that are dark beyond any reasonable doubt and provides a solid lower limit to the dark burst fraction.

As well as calculating the number of optically ‘dark’ bursts, we also calculate the number of optically ‘faint’ bursts, which we define as having magnitudes of $R > 22.5$. This is of interest if for example we have a burst with no X-ray coverage to calculate a value of β_{OX} , and should follow the dark burst population. Of the original sample of 190 bursts we find $10 \pm 2\% - 45 \pm 4\%$ (19 – 85 / 190) to be optically faint, with the upper value here again containing all upper limits and bursts without *R*-band data. Of the reduced sample we find $11 \pm 3\% - 41 \pm 4\%$ (15 – 57 / 139) to be faint. This very closely follows the number of dark bursts in our sample and is only very slightly lower than our derived dark burst fraction. This slight difference can be understood in that some bursts that are not optically ‘faint’ can still be optically ‘dark’ when their *R*-band flux is compared to their X-ray flux.

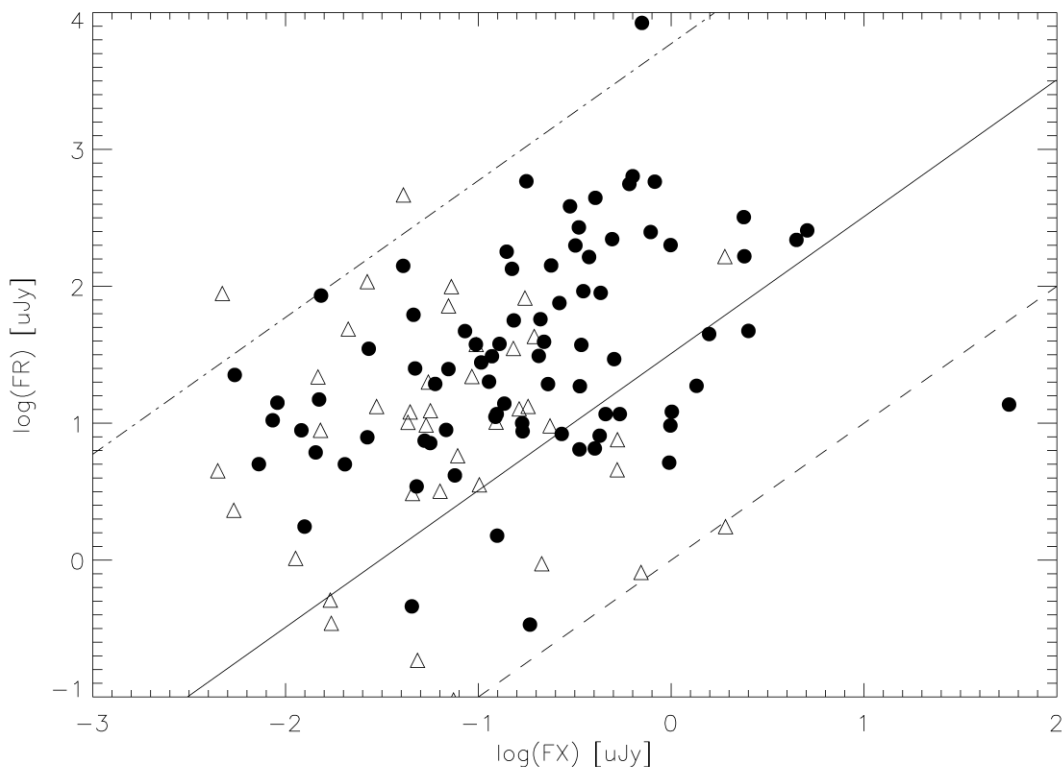


Figure 2.8: The ever-popular ‘dark burst plot’ first pioneered by Jakobsson et al. 2006 to visually represent the distribution of dark bursts in a given sample. The x-axis indicates the X-ray flux density at 3KeV of each burst in log space in units of micro-Janskys (and also in this case at 2hrs post burst), and the y-axis represents the R -band flux density also in micro Janskys. The plot contains the 130/139 bursts in our reduced sample with well-constrained values or upper-limits of β_{OX} . The solid black line represents $\beta_{OX} = 0.5$, with any burst below it thus being dark, the dashed line represents $\beta_{OX} = 0.0$ and the dot-dashed line represents $\beta_{OX} = 1.25$. The open triangles represent upper limits of R -band flux, with these bursts only having upper limits to their R -magnitudes available.

2.3.6 Distance and Dust, Dissecting the Dark Burst Fraction

In order to place constraints on the causes of dark bursts it is necessary to analyze their own redshift distribution, independent from that of the main *Swift* population. Having already gathered redshift information for our reduced sample as described in previous sections, we derive the median redshift for our subset of dark bursts to be in the range $1.92 - 2.45$, by considering only those bursts with spectroscopically or photometrically constrained redshifts as before.

Number of bursts obeying Jakobsson et al's criteria:	190
<i>(between March 15th 2005 and August 12th 2009)</i>	
Number at $z > 5$:	7 – 51 / 190 (4 – 27%)
Number at $z > 6$:	3 – 40 / 190 (2 – 21%)
Number of bursts obeying extended observability criteria:	139
Number at $z > 5$:	7 – 31 / 139 (5.0 – 27.3%)
Number at $z > 6$:	3 – 25 / 139 (2.2 – 23.0%)
Number of dark bursts ($\beta_{OX} < 0.5$) in reduced sample:	22 – 81 / 139 (16 – 58%)
Fraction of dark bursts known to be at less than $z = 5$:	(61.7%)
Fraction of dark bursts known to be at less than $z = 6$:	(71.6%)

Table 2.1: Compilation of various statistical values, including high redshift burst fractions and dark burst fractions, see main body of text for full description.

By again considering our most conservative and liberal constraints to β_{OX} , we find a lower limit to the number of dark bursts occurring at $z > 6$ of $4.5 \pm 4.4\%$, and an upper limit of $28.4 \pm 5.0\%$. We again caution that the upper limit here is an extreme one, and includes all bursts with upper limits to redshift based on the bluest filter in which they were observed that cannot constrain it to having a redshift of $z < 6$, and bursts with unconstrained values of z that cannot be ruled out as having $z > 6$. We thus find that the fraction of dark bursts occurring at extreme redshifts of $z > 6$ in our reduced sample of GRBs, and thus the *Swift* sample as a whole, to be in the range $4.5 \pm 4.4\% - 28.4 \pm 5.0\%$ ($1/22 - 23/81$ bursts). Similarly, we find the fraction of dark GRBs at $z > 5$ to be $4.5 \pm 4.4\% - 38.3 \pm 5.4\%$ ($1/22 - 31/81$ bursts). We can thus state that the fraction of dark GRBs *known* to occur at redshifts less than $z = 6$ is at bare minimum $72 \pm 5\%$, and at redshifts of less than $z = 5$, $62 \pm 5.4\%$. The full redshift distribution of our dark burst sample can be seen in *Figure 2.9*, which shows that the largest fraction of dark bursts can be found at redshifts of $z \sim 1 - 3$ rather than at more extreme redshifts.

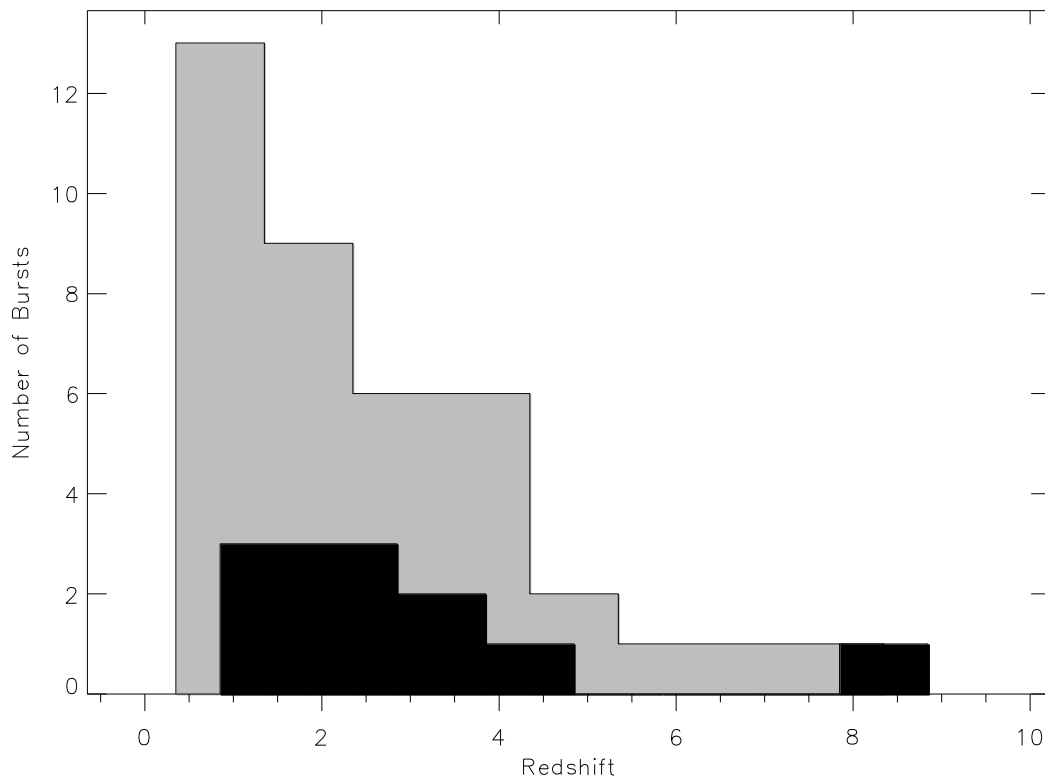


Figure 2.9: Redshift distribution of the dark burst subset. The grey shaded region represents the population of dark burst as defined by our liberal limits, and thus includes all bursts with unconstrained values of β_{OX} that cannot be ruled out as being dark, and all upper limits of β_{OX} which also do not rule out a burst as being dark. The black shaded region represents the population of dark bursts defined by our strict limits, and contains only bursts that are dark beyond any doubt. It is important to note that the two populations are congruous, in that the liberal subset also contains all bursts of the conservative subset.

This demonstrates that only a relatively small fraction of dark bursts are caused by optical suppression due to an extreme redshift. Thus, given that by defining a dark burst using $\beta_{OX} < 0.5$ intrinsically removes any weak or under-energetic events from the dark burst sample, the dominant cause of dark gamma ray bursts is likely to be dust extinction in the immediate burst environment, with a mixed bag of special cases making up a smaller percentage. This is the same conclusion reached by several other authors (Perley et al. 2009, Fynbo et al. 2009, Greiner et al. 2011), in particular the recent work of Greiner et al. Greiner et al. constrain the fraction of dark bursts from their observations with the *GROND* (Gamma Ray Optical and Near-infrared Detector) instrument, which uses a 7 channel

g'r'i'z'JHK camera to capture SEDs. They then combine these with *Swift/XRT* data to produce broad-band spectral energy distributions and derive rest frame extinctions for their sample. They compare these host A_V extinctions with that of the sample of Kann et al. 2010, made up of all optically bright bursts with available photometry. Greiner et al. find significantly larger extinction values in their sample, in particular approximately twice as many bursts with $A_V \sim 0.5$, and a substantial fraction ($\sim 10\%$) with extinctions of $A_V > 1$. They also demonstrate that it only takes moderate levels of dust at moderate redshifts ($A_V = 0.5 - 2.0$, $z = 1 - 3$) to produce significant dimming ($1 - 3$ mags) in the *R*-band, which combined with their extinction information, implies that moderate host extinction at moderate redshifts is a major cause of optical non-detections for GRB afterglows. This, with similar evidence from other authors, and our evidence that at the very highest possible extreme only $\sim 28\%$ of dark bursts are the result of high redshift, allows us to conclude that the majority of dark bursts are caused by dust extinction.

Although most GRBs are not found to originate in dusty environments, consistent with a preference for low metallicities, we can show from the small percentage of dark GRBs occurring at extreme redshifts that a significant fraction of GRBs do occur in dusty environments, and further suggesting that this preference for low metallicities is not a strict one.

Conclusions

We derive absolute limits to the dark burst fraction of *Swift* GRBs of 16 – 58% by the criteria of Jakobsson et al. 2004, with the caveats that the upper limit represents a highly conservative one, containing all bursts that cannot be discounted as being dark, and that the lower limit contains only those bursts that can be considered dark by the criteria of Jakobsson et al. 2004 beyond any doubt. We believe that the true dark burst fraction most probably lies at 25 – 40%, in agreement the work of Fynbo et al. 2009 and Greiner et al. 2011, as although these studies were based on much smaller samples than in this study, their samples are likely more complete. We also caution that many of these bursts (particularly in our optimistic estimate) are not ‘very dark’, with many having quite clear optical detections. Just because a burst is optically dark does not necessarily mean it is optically faint.

We find that the fraction of dark bursts occurring at redshifts of $z > 6$ to be $\sim 4.5 - 28\%$, and the fraction of dark bursts occurring at redshifts of $z > 5$ to be $\sim 4.5 - 38\%$. Given that Jakobsson et al.’s criteria intrinsically excludes any weak or under-energetic events from a dark burst sample, we thus conclude that at bare minimum $\sim 62 - 72\%$ of all dark bursts are caused by dust extinction, with a few other special cases such as ‘naked bursts’ making up a small percentage of this. This is in agreement with the conclusions of other recent authors (Perley et al. 2009, Fynbo et al. 2009, Greiner et al. 2011). It shows that although most GRBs originate in small low dust-content galaxies, which tend to have low metallicities and imply GRBs have a preference for low metallicity environments, a significant portion in fact do not, suggesting this preference is not strict. Although dusty

galaxies do indeed have variable metallicities, with some having significantly higher metallicities than others, the highly star forming galaxies where we might expect to see GRBs have both high dust and probably quite high metallicities. This conclusion that GRBs do not necessarily have a strict preference for low metallicities is also supported by some direct measurements of host metallicity from afterglow spectroscopy, these show that it is possible for GRB host metallicities to range up to about solar levels, and in the case of *GRB 020819*, much higher than this (Levesque et al. 2010).

The redshift distribution of our dark bursts (*Figure 2.9*) is similar to that of the general population of our sample (*Figure 2.7*), and similar redshift distributions derived by other authors (e.g. Fynbo et al. 2009, presented in *Figure 2.6*). The largest fraction of our dark burst population appears to reside in the redshift range $z \sim 1.5 - 3$. It is not possible for a burst to be dark at these redshifts via the Lyman-break being shifted into the *R*-band, as would be the case at or beyond redshifts of $5 - 6$, meaning that the cause of darkness for this fraction of bursts is most likely due to dust extinction. This is supported by many cases now where a full spectral energy distribution for a dark gamma ray burst has been determined through spectroscopic or photometric follow up, and revealed that the darkness is indeed explained by a dust law (e.g. Cenko et al. 08, Eliasdottir et al. 2009). Given that most star formation is thought to have occurred in this redshift range of $z \sim 1.5 - 3$, much of it in dusty environments (Hopkins & Beacom 2006), our finding that many of the dusty bursts also occur in this range, is consistent with the notion that long-GRBs are produced by the deaths of massive stars in regions of intense star formation.

Greiner et al. 2011 also show that it only takes moderate dust extinction ($A_V = 0.5 - 2.0$) at moderate redshifts ($z = 1.5 - 3$) to cause suppression in the *R*-band to the order of $1 - 3$ magnitudes. Given that from the various derived GRB redshift distributions, a substantial portion of GRBs (dark or otherwise) lie at redshifts of $z = 1.5 - 3$, where the majority of star formation is thought to take place in dusty regions, it follows that there should be a large fraction of dark gamma ray bursts whose cause is primarily dust extinction.

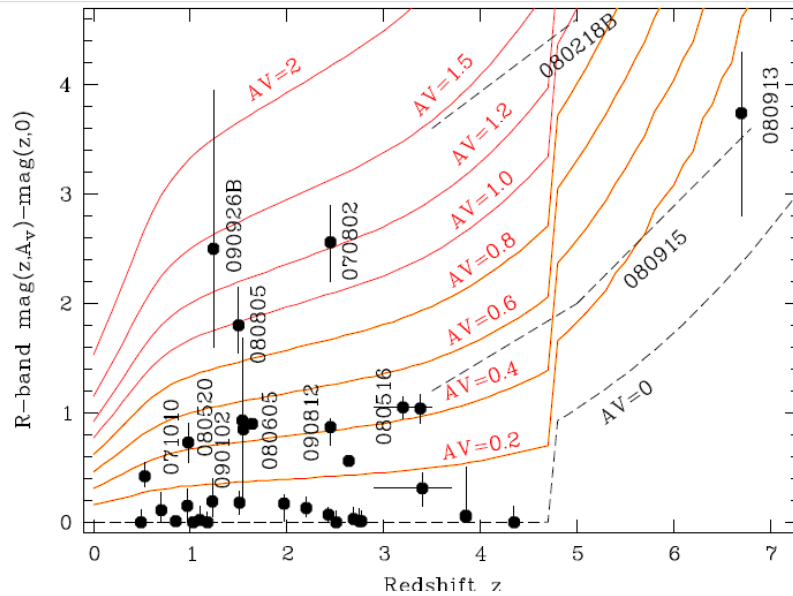


Figure 3.1: Taken from Greiner et al. 2011, this plot gives the effective dimming in the R -band (y-axis) as a function of both redshift and rest frame A_V , and shows that only moderate levels of dust at moderate redshifts can give rise to significant optical suppression, resulting in a dark burst.

There is evidence for at least some dark GRBs originating in dusty host galaxies. The host galaxy of the dark burst *GRB 030115* was found to be an extremely red object ($R - K = 5$) at a redshift of $z \sim 2.5$, indicative of a galaxy undergoing obscured star formation (Levan et al. 2006). The over-density of surrounding galaxies suggests this burst occurred in a high redshift forming cluster, with some nearby galaxies also showing very red colours, but most being much bluer, indicative of ongoing unobscured star formation. Perley et al. 2009 also suggest that many dark bursts may occur in localized dusty regions within an otherwise non-dusty host galaxy. They compare the host-frame V -band extinction along the line of sight inferred from the afterglow with the V -band extinction inferred from host galaxy observations, where they were available. In several cases they find large extinctions based on afterglow measurements ($A_V > 0.8 \text{ mag}$ in 6/22 cases where constraints could be derived, and $A_V > 2.5 \text{ mag}$ in a further 3), but find no such evidence for large amounts of reddening when analyzing the host galaxy observations. They interpreted this as dust in the host galaxy being sufficiently patchy that bluer emission dominates its SED and the dusty regions go unnoticed, or that these bursts reside in very

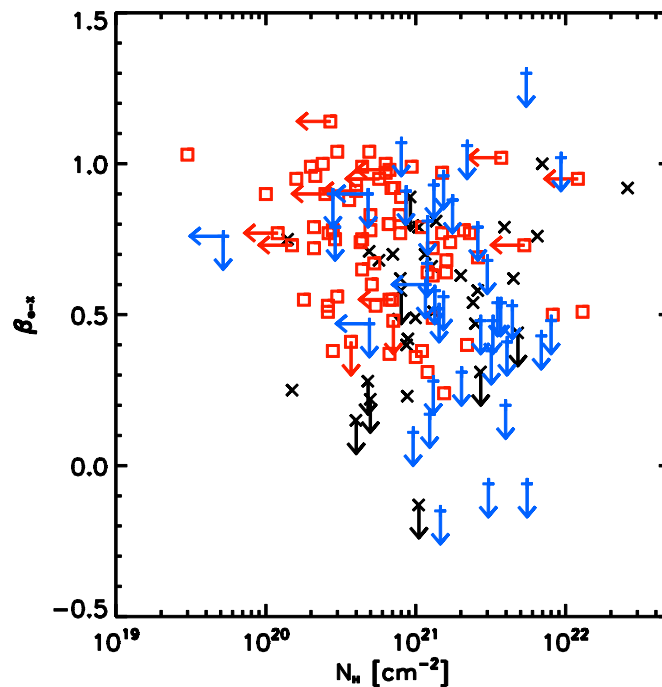


Figure 3.2: Taken from Fynbo et al. 2009, this plot shows hydrogen column density from excess X-ray absorption, N_H , against β_{OX} for their sample of bursts. Bursts with higher values of N_H tend to have lower values of β_{OX} , and thus tend to be darker. The differing colours represent the various subsets of their overall sample, red squares represent bursts in their sample with redshifts measured from OA spectroscopy; black crosses represent bursts with detected optical and/or near-IR afterglow but no afterglow-based redshift; and blue plus symbols represent bursts in their sample with no detection of the OA.

localized dust regions within an otherwise unremarkable galaxy. However, a subsequent followup survey with the *Spitzer* telescope has revealed that a substantial proportion of the dark burst hosts are found to be bright at 3-5 microns, suggesting that a relatively highly obscured stellar component does exist in many of them (Perley et al. private communication).

Fynbo et al. 09 also present evidence for dark bursts being the result of dust extinction by showing that dark bursts have higher excess X-ray absorption (*Figure 3.2*). X-ray absorption (in excess of foreground absorption from gas in our own galaxy) is used to measure gas column densities in GRB hosts, these are then used to infer levels of dust in the host using an assumed gas-to-dust ratio, usually based on values from the Magellanic

clouds. They find that darker bursts (i.e. bursts with lower β_{OX}) have higher excess X-ray absorption, thus implying higher levels of dust. Watson et al. 2006 however present the case of *GRB 050401*, where the estimated A_V extinction from X-ray column densities is almost an order of magnitude higher than more direct measurements from optical observations of the GRB host galaxy. Looking at the same principle, Schady et al. 09 examine a larger sample of bursts. They find that the measured gas/dust ratios for their sample of GRB hosts was up to two orders of magnitudes larger than the Milky Way or Magellanic Clouds, further implying that typical assumptions about gas/dust ratios overestimate the amount of dust inferred from excess X-ray absorption. These relatively small gas-to-dust ratios may however be explained by the GRB itself, or the intense radiation fields in their star forming locations, depleting dust in the vicinity of the GRB (Waxman & Draine 2007). However, despite this evidence that a high X-ray column density may not necessarily imply anything more than modest levels of dust, Fynbo et al. 09 still do show that on average X-ray column densities are higher for dark GRBs.

So, in summary we conclude that at very most 16 – 58% of bursts are dark, and that these values represent absolute upper and lower limits from a relatively statistically complete sample, and that the true fraction of dark GRBs most likely lies in the range 25 – 40% in line with the work of Fynbo et al. 2009, and Greiner et al. 2011. We conclude that at minimum, ~ 62 – 72% of dark gamma ray bursts are not the result of a high redshift origin, and that these are most likely the result of dust extinction. This, combined with all the other evidence presented here from other authors, leads us to conclude that most dark gamma ray bursts are caused by moderate levels of dust at intermediate redshifts, and that despite GRBs having a preference for low metallicities, a significant portion do in fact originate in dusty environments.

This does not however mean for a moment that GRBs are not of interest to cosmology. Even though rapid spectroscopic follow-up may well be the best way of detecting high redshift bursts rather than chasing dark GRBs, it still remains that once detected, every dark gamma ray burst has the potential to be at phenomenally high redshift. There is indeed at least one near-future term project working towards this goal in the form

of the large *VLT/Xshooter* program currently underway to obtain deep medium-high resolution spectroscopy for all *Swift* GRBs that can be seen by *VLT* with very little time delay. *XShooter* is a multi wavelength (300-2500nm) high resolution spectrograph mounted on the *VLT*, and since it covers both the IR and the visible, once the program has achieved its time-granted goal of building up a sample of 100 afterglows over ~3 years, it should greatly clarify the question of how many dark bursts are dusty or at high redshift.

As well as the current work with *XShooter*, there are several current missions proposed or in the pipeline that have the potential to answer many of our questions about dark bursts, and potentially crack the field of GRB cosmology wide open. *SVOM* is a currently funded Chinese-French mission due to launch around ~2014. Similar to *Swift*, it will have a gamma-ray telescope to detect GRBs and an X-ray camera based on the X-ray instrument used on Bepi-Colombo. This will ultimately give it similar capabilities to that of *Swift*, but more importantly in terms of studying dark gamma ray bursts, *SVOM* will have a much larger and more efficient optical telescope than the *Swift/UVOT* which goes down as far as 950nm (as opposed to the 650nm of *UVOT*). This will allow for rapid early identification of optically faint bursts, and thus rapid early identification of high redshift candidates.

Another mission concept currently being proposed is *JANUS*. This would be a gamma ray burst detector featuring a 0.7 – 1.7 micron nIR camera, giving *JANUS* the ability to locate and provide approximate redshifts for high redshift GRBs on board. This would allow ground observers to greatly increase their follow up efficiency by putting all their resources into rapid IR spectroscopic follow up when candidates are found, and greatly focusing our abilities in studying high redshift bursts.

It is most likely with current and future missions such as these that the world of GRB cosmology at extreme redshifts will really start to come alive and give us the ability to realistically pinpoint and observe the first ever stars and galaxies so that we might understand the evolution of the universe during its earliest epochs, and to unravel the star

formation history of the universe so that we can further our understanding of how the cosmos came to be as it is today.

As well as these specific GRB focused missions there are also many new facilities due to come online at the same time that will present us with many new opportunities to study GRB host galaxies, as well as providing many new opportunities for astronomy as a whole. Most notable of these is perhaps the *James Webb Space Telescope (JWST)*, due to be launched in 2014/15. Designed as the successor to the *Hubble Space Telescope*, the primary science goal of *JWST* is specifically to observe the most distant objects in the universe beyond the reach of any current instrument. *JWST* will not have the optical capabilities of *HST* but will have much greater infra-red coverage and depth, allowing us to not only use its sheer collecting power to image characteristically faint GRB host galaxies, but also to potentially observe the host galaxies of extremely high redshift bursts such as *GRB 090423* for the first time.

As well as this, two new huge radio arrays will soon come online, the *Atacama Large Millimeter Array (ALMA)* and *LOFAR (LOW Frequency Array)*, both of which are believed will cause huge breakthroughs in radio astronomy, but may also allow advances in GRB astronomy. Their unprecedented observing power at submm wavelengths will allow us to observe dusty GRB host galaxies bright at these wavelengths, and perhaps thus help to solve to some extent the dark burst problem.

Lastly but by no means least, targeted for completion around 2018, is the *European Extremely Large Telescope (E-ELT)*. *E-ELT* will be the largest of the new generation of ground based extremely large telescopes, and will boast a huge 42m diameter mirror capable of gathering 15 times more light than the largest operational telescopes today, and with advanced adaptive optics systems will be able to provide images of exceptional detail. The sheer power of *E-ELT* will allow us to study GRB afterglows and host galaxies in never before seen detail, more than likely greatly forwarding our understanding of GRB afterglows and thus their mechanisms, and also the environments within which these phenomenal events originate.

APPENDIX

Table 1

139 Bursts between March 15th 2005 and August 12th 2009 obeying the observability criteria of Jakobsson et al. 2006 and accepted by our extended observability criteria, the ‘reduced sample’.

Burst	RA	Dec	Z	β_{OX}	R (μJy)¹	Reference for R-band data³
090812	23:32:48.55	-10:36:17.0	2.45	0.38 ± 0.08	9.17 ± 1.08	Updike et al. 09 (GCN 9773)
090809	21:54:43.19	-00:05:01.83	2.74	0.71 ± 0.11	67.76 ± 25.15	Xu et al. 09 (GCN 9755)
090728	01:58:36.69	+41:37:59.5	<6.40			
090715B	16:45:21.52	+44:50:20.3	3.00	0.70 ± 0.11	6.54 ± 1.71	Malesani et al. 09 (GCN 9671)
090709A	19:19:42.64	+60:43:39.3	<6.10	< -0.08	<1.26	Cenko et al. 2010
090607	12:44:40.59	+44:06:18.10			<4.49	Guidorzi et al. 2009 (GCN 9492)
090530	11:57:40.50	+26:35:38.6	<2.00	0.90 ± 0.22	27.77 ± 7.51	Im & Urata 09 (GCN 9459)
090529	14:09:52.56	+24:27:32.2	2.63	0.95 ± 0.13	34.98 ± 18.49	Kann et al. 09 (GCN 9436)
090516A	09:13:02.62	-11:51:15.4	4.11	0.63 ± 0.15	72.03 ± 45.57	Gorosabel et al. 09 (GCN 9379)
090429B	14:02:40.05	+32:10:14.32	<9.4	<0.24	<0.19	D'Avanzo et al. 09 (GCN 9284)
090424	12:38:05.11	+16:50:15.1	0.54	0.50 ± 0.07	120.00 ± 16.63	Gorosabel et al. 09 (GCN 9236), Guidorzi et al. 09 (GCN 9238), Olivares et al. 09 (GCN 9245), Im et al. 09a (GCN 9248), 09b (GCN 9275), Rumyantsev et al. 09 (GCN 9320)
090423	09:55:33.29	+18:08:57.8	8.23	<0.45	<1.26	Tanvir et al. 2010
090418A	17:57:15.21	+33:24:21.8	1.61	0.50 ± 0.15	35.61 ± 24.17	Pavlenko et al. 09 (GCN 9179)
090417B	13:58:46.59	+47:01:05.0	0.35	<0.67	<164.80	Xin et al. 2009 (GCN 9142)
090404	15:56:57.52	+35:30:57.5	<3.40	<0.54	<9.55	Afonso et al. 09 (GCN 9069)
090313	13:13:36.21	+08:05:49.8	3.38		305.65 ± 42.07	Melandri et al. 2010
090308A	12:14:00.28	-48:49:01.6		0.88 ± 0.12	5.02 ± 2.45	Cenko et al. 09 (GCN 8965)
090205	14:43:38.65	-27:51:10.7	4.65	0.77 ± 0.17	19.35 ± 9.05	D'Avanzo et al. 09 (GCN 8887)
090113	02:08:13.63	+33:25:42.85		0.34 ± 0.06	<1.51	de Ugarte et al. 09 (GCN 8810)
090102	08:32:58.54	+33:06:51.10	1.55	0.53 ± 0.04	29.37 ± 2.83	Gendre et al. 2010
081230	02:29:19.51	-25:08:49.95	<3.30	0.75 ± 0.09	30.83 ± 9.09	Afonso et al. 08 (GCN 8760)
081222	01:30:57.56	-34:05:41.50	2.77	1.28 ± 0.10	8390.00 ± 2347.86	Kuroda et al. 08 (GCN 8724)
081221	01:03:10.20	-24:32:53.16	<3.40	<0.27	<3.83	Malesani et al. 08 (GCN 8688)
081210	04:41:56.20	-11:15:26.68	<3.30	<0.85	37.55 ± 1.40	Rumyantsev et al. 08 (GCN 8667)

Burst	RA	Dec	Z	β_{ox}	R (μJy)¹	Reference for R-band data³
081128	01:23:13.03	+38:07:37.70		0.67 ± 0.06	5.86 ± 0.81	Rumyantsev et al. 08 (GCN 8630)
081127	22:08:15.41	+06:51:01.80				
081121	05:57:06.15	-60:36:10.00	2.51	0.67 ± 0.12	342.87 ± 137.91	Cobb 08 (GCN 8547)
081118	05:30:22.18	-43:18:05.30	2.58	0.98 ± 0.12	14.11 ± 7.16	D'Avanzo et al. 08 (GCN 8528)
081109	22:03:09.72	-54:42:39.50	<5.00	<0.77	<42.99	Guidorzi et al. 08 (GCN 8508)
081104	06:41:57.26	-54:43:11.64	<3.40	<0.79	<9.68	Melandri et al. 08 (GCN 8475)
081029	23:07:05.35	-68:09:19.80	3.85	0.98 ± 0.07	384.00 ± 7.07	Cobb 08 (GCN 8452)
081016B	00:58:15.44	-43:31:48.54		<0.87	<13.24 ⁴	Cobb 09 (GCN 8534)
081012	02:00:48.22	-17:38:17.88		<1.00	<47.58	de Ugarte et al. 08 (GCN 8366)
081008	18:39:49.88	-57:25:52.87	1.97		269.37 ± 70.29	Cobb 08 (GCN 8356)
081007	22:39:50.40	-40:08:48.80	0.53			
080928	06:20:16.85	-55:11:59.30	1.69	0.92 ± 0.12	163.59 ± 106.70	Rossi et al. 08 (GCN 8296)
080916A	22:25:06.19	-57:01:22.80	0.69	0.77 ± 0.17	56.33 ± 37.69	Rossi et al. 08 (GCN 8266)
080913	04:22:54.74	-25:07:46.20	6.70	<0.56	<0.51	Greiner et al. 2009
080905B	20:06:57.89	-62:33:47.00	2.37	0.32 ± 0.11	12.12 ± 6.26	Vreeswijk et al. 08 (GCN 8191)
080810	23:47:10.51	+00:19:11.30	3.35	0.96 ± 0.07	559.20 ± 65.35	Page et al. 2009
080805	20:56:53.44	-62:26:39.80	1.51			
080804	21:54:40.20	-53:11:04.60	2.20	0.73 ± 0.16	39.32 ± 0.73	Kruehler et al. 08 (GCN 8075)
080727A	13:53:33.72	-18:32:41.24		<0.90	<2.31	Malesani et al. 08 (GCN 8039)
080721	14:57:55.86	-11:43:24.54	2.59	0.48 ± 0.05	218.12 ± 25.50	Starling et al. 2009
080710	00:33:05.67	+19:30:04.68	0.85	0.40 ± 0.05	6.44 ± 0.06	Li et al. 08 (GCN 7959)
080607	12:59:47.24	+15:55:08.74	3.04	0.56 ± 0.13	18.62 ± 1.80	Perley et al. 2011
080605	17:28:30.01	+04:00:56.40	1.64	0.36 ± 0.05	14.90 ± 2.07	Jakobsson et al. 08 ((GCN 7832), Rumyantsev et al. 08 (GCN 7857), Kann et al. 08 (GCN 7845)
080604	15:47:51.70	+20:33:28.10	1.42	1.25 ± 0.16	86.38 ± 46.51	Rol et al. 08 (GCN 7801)
080603B	11:46:07.66	+68:03:39.99	2.69	0.83 ± 0.05	221.00 ± 20.38	Klotz et al. 08a (7795), 08b (GCN 7799), Xin et al. 08 (GCN 7814), Ibrahimov et al. 08 (GCN 7975)
080520	18:40:46.41	-54:59:31.10	1.55	0.80 ± 0.17	5.01 ± 7.98	Jakobsson et al. 08 (GCN 7757)
080430	11:01:14.76	+51:41:08.30	0.77	0.77 ± 0.10	57.50 ± 10.65	Kocka et al. 08 (GCN 7651)
080330	11:17:04.50	+30:37:23.53	1.51	1.04 ± 0.04	83.12 ± 3.12	Guidorzi et al. 2009
080325	18:31:34.13	+36:31:19.80	<3.00	<0.87	<39.23	Munz et al. 08 (GCN 7563)
080320	11:50:56.47	+57:09:26.64	<6.40	0.08 ± 0.10	0.34 ± 0.16	Tanvir et al. 08 (GCN 7488)

Burst	RA	Dec	Z	β_{OX}	R (μJy)¹	Reference for R-band data³
080319C	17:15:55.51	+55:23:30.80	1.95		5.15 ± 0.24	Cenko et al. 2009
080319B	14:31:40.98	+36:18:08.80	0.94	0.67 ± 0.04	595.15 ± 14.74	Li et al. 08 (GCN 7438)
080319A	13:45:20.01	+44:04:48.60	$<4.20^{\text{H}}$		6.12 ± 1.58	Cenko et al. 2009
080310	14:40:13.80	-00:10:29.60	2.43	0.79 ± 0.12	198.71 ± 19.17	Cenko et al. 2009
080307	09:06:30.72	+35:08:20.26	<6.10	0.58 ± 0.07	3.45 ± 0.97	Xin et al. 08 (GCN 7371)
080212	15:24:35.49	-22:44:29.00	<3.50	0.78 ± 0.14	98.84 ± 59.44	D'Avanzo et al. 08 (GCN 7311)
080207	13:50:03.01	+07:30:08.82	<3.40	<0.42	<4.57	Cucchiara & Fox 08 (GCN 7276)
080205	06:33:00.62	+62:47:31.98	<5.50	0.64 ± 0.19	7.16 ± 4.08	Burenin et al. 08 (GCN 7275)
071117	22:20:10.42	-63:26:35.50	1.33^{H}	0.54 ± 0.16	10.00 ± 5.38	Fynbo et al. 2009
071112C	02:36:50.93	+28:22:16.68	0.82	0.75 ± 0.11	32.80 ± 9.18	Klotz et al. 07 (GCN 7065), Updike et al. 07(GCN 7084), Minezaki et al. 07 (GCN 7135)
071031	00:25:37.27	-58:03:34.20	2.69		57.54 ± 5.55	Krühler et al. 2009
071025	23:40:17.08	+31:46:42.87	<6.10	0.64 ± 0.08	37.30 ± 6.91	Milne et al. 07 (GCN 7011)
071021	22:42:34.31	+23:43:06.50	<5.60	-0.19 ± 0.60	<13.68	Xin et al. 07 (GCN 6962)
071020	07:58:39.78	+32:51:40.40	2.15	0.57 ± 0.09	23.96 ± 0.04	Jakobsson et al. 07 (GCN 6952)
070808	00:27:03.36	+01:10:34.86	$0.68^{2,\text{H}}$	<0.80	<12.06	Stefanescu et al. 07 (GCN 6723)
070802	02:27:35.88	-55:31:39.30	2.45	0.55 ± 0.07	4.15 ± 0.68	Eliasdottir et al. 2009
070721B	02:12:32.97	-02:11:40.40	3.63	0.35 ± 0.16	8.10 ± 5.96	Malesani et al. 07 (GCN 6651)
070621	21:35:10.14	-24:49:03.07	<3.40	<0.55	$<4.69^5$	Malesani et al. 07 (GCN 6565)
070611	00:07:58.00	-30:18:39.40	2.04	0.99 ± 0.14	53.12 ± 26.15	Fynbo et al. 2009
070521	16:10:38.59	+30:15:21.96	1.35^{H}	<0.06	<0.81	Rau et al. 07 (GCN 6436)
070518	16:56:47.50	+55:17:50.64	<2.00	0.94 ± 0.06	14.90 ± 2.76	Xin et al. 07 (GCN 6416), Covino et al. 07 (GCN 6426)
070419A	12:10:58.83	+39:55:34.06	0.97	0.98 ± 0.09	6.11 ± 0.91	Melandri et al. 2008
070412	12:06:10.59	+40:08:24.83		<0.43	<1.49	Malesani et al. 07 (GCN 6281)
070330	17:58:09.98	-63:47:34.80	<5.50	<1.33	464.42 ± 41.35	Klotz et al. 07 (GCN 6235)
070306	09:52:23.38	+10:28:55.20	1.50^{H}			
070224	11:56:06.65	-13:19:48.80	<6.10	0.90 ± 0.12	8.87 ± 1.64	Thoene et al. 07a (GCN 6142), 07b (GCN 6154)
070223	10:13:48.39	+43:08:00.70	<6.10	0.31 ± 0.12	0.46 ± 0.19	Mirabal et al. 07 (GCN 6162)
070208	13:11:32.61	+61:57:54.37	1.17	0.66 ± 0.11	11.66 ± 1.12	Melandri et al. 2008
070129	02:28:00.94	+11:41:04.00	$2.35^{2,\text{H}}$	0.61 ± 0.08	11.13 ± 0.32	Malesani et al. 07 (GCN 6055)
061222A	23:53:03.42	+46:31:58.60	$<20.0^{\text{H}}$	<0.48	<1.75	Melandri et al. 2008
061110B	21:03:45.40	+06:52:34.10	3.44	0.78 ± 0.07	7.89 ± 1.23	Thoene et al. 06 (GCN 5807)

Burst	RA	Dec	Z	β_{ox}	R (μJy)¹	Reference for R-band data³
061110A	22:25:09.90	-02:15:30.70	0.76	0.97 ± 0.06	10.50 ± 0.97	Thoene et al. 06a (GCN 5799), 06b (GCN 5812), Fynbo 06 (GCN 5818)
061007	03:05:19.51	-50:30:02.50	1.26	0.65 ± 0.20	11.66 ± 1.12	Mundell et al. 2007
061004	06:31:10.71	-45:54:28.70		<0.59	<3.19	Jakobsson et al. 06
060927	21:58:12.20	+05:21:52.20	5.47	0.68 ± 0.09	7.45 ± 2.08	Ruiz-Velasco et al. 2007, Sarugaku et al. 06 (GCN 5634))
060923C	23:04:28.49	+03:55:26.60	$0.86^{2\text{H}}$	<1.15	<19.96	Melandri et al. 06 (GCN 5594)
060919	18:27:42.21	-51:00:50.40	<3.40	<1.27	<89.47	Melandri et al. 06 (GCN 5579)
060912A	00:21:08.16	+20:58:17.80	0.94^{H}	0.81 ± 0.09	37.66 ± 8.57	Hafizov et al. 06 (GCN 5567)
060908	02:07:18.36	+00:20:31.20	1.88	0.95 ± 0.17	47.07 ± 12.19	Covino et al. 2010
060807	16:50:02.60	+31:35:30.70	<3.40	0.42 ± 0.12	11.65 ± 6.45	Fynbo et al. 2009
060719	01:13:43.57	-48:22:55.00	$<2.00^{2\text{H}}$	<0.09	<0.10	Fugazza et al. 06 (GCN 5347)
060714	15:11:26.45	-06:33:58.30	2.71	0.84 ± 0.07	116.63 ± 10.26	Asfandyarov et al. 06 (GCN 5434)
060708	00:31:13.85	-33:45:32.40	1.92	0.70 ± 0.21	69.36 ± 58.33	Jakobsson et al. 06 (GCN 5319)
060707	23:48:19.00	-17:54:17.00	3.43	<0.75	<82.04	de Ugarte et al. 06 (GCN 5288)
060614	21:23:32.14	-53:01:36.12	0.13^{H}	0.76 ± 0.06	75.47 ± 10.66	Schmidt et al. 06 (GCN 5258)
060607A	21:58:50.40	-22:29:46.68	3.08	<0.42	165.66 ± 15.98	Nysewander et al. 2009
060605	21:28:37.32	-06:03:31.30	3.78	0.87 ± 0.07	142.00 ± 26.31	Malesani et al. 06 (GCN 5225), Karska et al 06 (GCN 5260), Sharapov et al. 06 (GCN 5263)
060604	22:28:55.01	-10:54:55.80	<2.80	0.80 ± 0.16	20.09 ± 5.20	Tanvir et al. 06 (GCN 5216), Garnavich & Karska 06 (GCN 5253)
060526	15:31:18.36	+00:17:04.92	3.21	0.98 ± 0.04	179.00 ± 4.95	Covino et al. 06 (GCN 5167), Baliyan et al 06 (GCN 5185)
060522	21:31:44.80	+02:53:10.35	5.11	0.86 ± 0.05	25.11 ± 2.55	D'Avanzo et al. 06 (GCN 5151)
060512	13:03:05.81	+41:11:27.24	2.10	0.99 ± 0.10	61.89 ± 5.97	Melandri et al. 2008
060502A	16:03:42.48	+66:36:02.50	1.51	0.19 ± 0.07	19.30 ± 2.86	Cenko et al.2009
060428B	15:41:25.63	+62:01:30.30	<5.50	<0.88	<21.72	Abe et al. 06 (GCN 5021)
060427	08:17:04.40	+62:40:18.30		<0.78	<10.14	Lopez-Sanchez et al. 06 (GCN 5013)
060323	11:37:45.40	+49:59:05.50	<4.40	0.65 ± 0.16	8.93 ± 4.76	Covino et al. 06 (GCN 4911)
060319	11:45:33.80	+60:00:39.00	1.15^{H}	<0.53	<3.55	D'Avanzo et al. 06 (GCN 4890)
060219	16:07:21.10	+32:18:56.30	<3.40	<0.62	<3.06	Sharapov et al. 06 (GCN 4902)
060210	03:50:57.37	+27:01:34.40	3.91	0.55 ± 0.07	9.62 ± 2.49	Melandri et al.2008
060206	13:31:43.42	+35:03:03.60	4.05^{H}	0.90 ± 0.08	581.00 ± 80.52	Monfardini et al. 2006, Wozniak et al. 06 (GCN

Burst	RA	Dec	Z	β_{OX}	R (μJy) ¹	Reference for R-band data ³
						4687, Homewood et al. 06 (GCN 4688), Ofek et al. 06 (GCN 4691), Lin et al. 06 (GCN 4696), Milne et al. 06 (GCN 4699), Malesani et al. 06 (GCN 4706)
060204B	14:07:14.80	+27:40:34.00	<4.80	0.56 ± 0.14	8.34 ± 2.86	Melandri et al. 2008
060202	02:23:22.88	+38:23:04.30	0.78	<0.62	13.24 ± 0.85	Yang et al. 06 (GCN 4631)
060115	03:36:08.40	+17:20:43.00	3.53	0.79 ± 0.15	24.84 ± 11.52	Yanagisawa et al. 06 (GCN 5417)
060108	09:48:01.98	+31:55:08.60	<3.20		5.46 ± 1.74	Oates et al. 2006
051117B	05:40:43.00	-19:16:26.50	$0.48^{2,\text{H}}$	<1.43	<88.55	Sharapov et al. 05 (GCN 4308)
051001	23:23:48.80	-31:31:17.00	< $2.30^{2,\text{H}}$			
050922C	21:09:33.30	-08:45:27.50	2.20	0.68 ± 0.04	31.00 ± 1.43	Jakobsson et al. 05 GCN 4015), Henyck et al. 05 (GCN 4026), Piranomonte et al. 05 (GCN 4032)
050922B	00:23:13.20	-05:36:16.40				
050915A	05:26:44.80	-28:00:59.27	$0.44^{2,\text{H}}$		<5.78	Cenko et al. 2009
050908	01:21:50.75	-12:57:17.20	3.34	0.88 ± 0.08	16.60 ± 4.65	Durig et al. 05 (GCN 3950), Piranomonte et al. 05 (GCN 3953)
050904	00:54:50.79	+14:05:09.42	6.30	0.62 ± 0.12	17.40 ± 4.87	Fox et al. 05 (GCN 3912), Rumyantsev et al. 05 (GCN 3939)
050824	00:48:56.05	+22:36:28.50	0.83	<0.98	71.79 ± 53.55	Sharapov et al. 05 (GCN 3897)
050822	03:24:26.70	-46:02:01.70	$1.43^{2,\text{H}}$			
050820A	22:29:38.11	+19:33:37.10	2.61	0.80 ± 0.05	320.00 ± 12.01	Cenko et al. 2009
050819	23:55:01.20	+24:51:36.50		<0.93	<8.87	Bikmaev et al. 05 (GCN3831)
050814	17:36:45.39	+46:20:21.60	5.30	0.59 ± 0.16	13.49 ± 8.74	Jensen et al. 05 (GCN 3809)
050803	23:22:38.00	+05:47:02.30				Pavlenko et al. 05 (GCN 3783)
050726	13:20:12.30	-32:03:50.80	<5.50	<0.73	48.97 ± 35.46	Haislip et al. 05 (GCN 3719)
050716	22:34:20.40	+38:40:56.70	<11.0	<0.64	<10.166	Lin et al. 05 (GCN 3628)
050525A	18:32:32.57	+26:20:22.50	0.61	0.88 ± 0.05	347.00 ± 32.01	Malesani et al. 05 (GCN 3469), Mirabal et al. 05 (GCN 3488), Yanagisawa et al. 05 (GCN 3489), Homewood et al. 05 (GCN 3491), Cobb & Bailyn 05 (GCN 3506)
050505	09:27:03.20	+30:16:21.50	4.28	0.52 ± 0.13	25.97 ± 15.00	Hurkett et al. 05
050502B	09:30:10.10	+16:59:44.30	5.20	<0.80	<12.32	Sanchawala et al. 05 (GCN 3334)
050416A	12:33:54.60	+21:03:24.00	0.65	0.63 ± 0.11	13.90 ± 1.93	Kahharov et al. 05 (GCN 3274)

Burst	RA	Dec	Z	β_{OX}	R (μJy)¹	Reference for R-band data³
050412	12:04:25.06	-01:12:03.60		<0.61	<1.03	Kosugi et al. 05 (GCN 3263)
050401	16:31:28.82	+02:11:14.83	2.90	1.02 ± 0.09	44.79 ± 9.06	Watson et al. 2006, D'Avanzo et al. 05 (GCN 3171), Kahharov et al. 05 (GCN 3174), Misra et al. 05 (GCN 3175)
050319	10:16:50.76	+43:32:59.90	3.24	0.73 ± 0.04	89.50 ± 8.25	Yoshioka et al. 05 (GCN 3120), Sharapov et al. 05 (GCN 3124), Misra et al 05 (GCN 3130)

¹ R-band fluxes all evaluated at 2-hours post burst.

² Redshift from Jakobsson et al. (in prep).

³ Given that in the case of GCN reports, observers may have published tens or maybe even over 100 during a given year, we provide the GCN report number with each citation where data from a GCN report has been used for easy reference.

⁴ I-band extrapolation.

⁵ No object confirmed as afterglow, limit derived by assuming afterglow dimmer than dimmest object observed in XRT error circle.

^H Host galaxy redshift.

Table 2

51 Bursts between March 15th 2005 and August 12th 2009 obeying the criteria of Jakobsson et al. 2006 but rejected by our extended observability criteria, the ‘rejected sample’.

Burst	RA	DEC	z	β_{ox}	R (μJy)¹	R Reference
090519	09:29:07.0	+00:10:49.1	3.85	0.68 ± 0.05	1.76 ± 0.07	Levan et al. 09
090518	07:59:49.03	+00:45:33.1	<3.40	<0.78	<21.91	Rossi et al. 09
090429A	06:02:13.86	-52:23:14.2		<0.8	<35.13	Olivares et al. 09
090407	04:35:55.14	-12:40:45.2	<3.40	<0.65	<12.71	Malesani & Fynbo 09
090201	06:08:12.48	-46:35:24.2	<3.40	0.34 ± 0.13	18.74 ± 9.08	D'Avanzo et al. 09
090123	00:27:08.74	-23:30:03.89	<2.00	0.73 ± 0.21	37.96 ± 26.86	Rossi & Greiner 09
081211A	21:52:27.97	-33:50:08.34				
081203A	15:32:07.58	+63:31:14.80	2.10	0.94 ± 0.04	637.00 ± 11.74	Andreev et al. 09, Liu et al. 08, Rummyantsev et al. 08
081028A	08:07:34.73	+02:18:29.10	3.04	1.06 ± 0.10	197.20 ± 76.72	Olofsson et al. 08
080916B	10:54:39.78	+69:03:57.90				
080707	02:10:28.40	+33:06:34.20	1.23			
080703	06:47:12.65	-63:13:09.12	<5.50	0.61 ± 0.09	14.36 ± 3.53	Malesani et al. 08
080613B	11:35:11.46	-07:06:18.04		<1.13	<48.63	Christina et al. 08
080602	01:16:42.18	-09:13:55.45			<8.16	Malesani et al. 08
080523	01:23:11.51	-64:01:50.92	<3.00	0.76 ± 0.10	5.90 ± 2.23	Fynbo et al. 09
080413B	21:44:34.65	-19:58:52.40	1.10	0.91 ± 0.15	442.57 ± 259.61	Krimm et al. 08
080210	16:45:04.01	+13:49:36.12	2.64	0.58 ± 0.11	17.17 ± 6.19	Updike et al. 08
071122	18:26:25.31	+47:04:30.14	1.14			
070520B	08:07:31.11	+57:36:32.26		<1.05	<21.76	Shakhovskoy et al. 07,
070506	23:08:52.39	+10:43:20.30	2.31			
070419B	21:02:49.82	-31:15:49.30	<2.20 ^{2,H}	0.33 ± 0.05	36.90 ± 1.09	Tristram et al. 07
070328	04:20:27.60	-34:04:00.48	0.37 ^{2,H}			
070318	03:13:56.83	-42:56:46.30	0.84	1.04 ± 0.23	585.30 ± 449.52	Cobb 07
070219	17:20:45.99	+69:22:10.60	<3.40	<0.46	<0.35	D'Avanzo et al. 07
070110	00:03:39.27	-52:58:26.90	2.35	0.88 ± 0.16	134.09 ± 93.63	Melesani et al. 07
070103	23:30:13.90	+26:52:34.17	<3.40			
061121	09:48:54.58	-13:11:42.72	1.31	0.69 ± 0.06	340.00 ± 9.40	Halpern et al. 06a, 06b, Cenko 06,

Burst	RA	DEC	z	β_{OX}	R (μJy)¹	R Reference
<i>061102</i>	09:53:37.64	-17:01:26.50				
<i>061021</i>	09:40:36.12	-21:57:05.40	0.35	0.69 ± 0.18	199.98 ± 137.49	Thoene et al. 06
<i>061002</i>	14:41:23.29	+48:44:30.50				
<i>060929</i>	17:32:29.00	+29:50:08.90				
<i>060923B</i>	15:52:46.83	-30:54:11.90				
<i>060923A</i>	16:58:28.15	+12:21:38.90	$<2.80^{\text{H}}$	<0.25	<0.94	Fox et al. 06
<i>060904A</i>	15:50:54.90	+44:59:07.80		<0.65	<13.01	Cenko & Rau et al. 06
<i>060814</i>	14:45:21.48	+20:35:11.80	0.84^{H}	<0.02	<0.60	Malesani & Patat 06
<i>060805A</i>	14:43:43.59	+12:35:13.20	$<2.50^{2,\text{H}}$	<1.18	<107.99	Muehleger et al. 06
<i>060729</i>	06:21:31.29	-62:22:13.40	0.54			
<i>060712</i>	12:16:16.30	+35:32:17.80		<0.77	<13.53	Cenko & Ofek 06
<i>060306</i>	02:44:23.00	-02:08:52.80	$<2.50^{2,\text{H}}$	0.53 ± 0.08	8.72 ± 2.95	Price et al. 06
<i>060218</i>	03:21:39.68	+16:52:01.82	0.03^{H}	1.05 ± 0.17	1039.89 ± 536.59	Zheng et al. 06
<i>060124</i>	05:08:25.50	+69:44:26.00	2.30	0.40 ± 0.09	47.21 ± 8.12	Rumyantsev et al. 06
<i>060111A</i>	18:24:49.00	+37:36:16.10	<5.50	<1.04	99.37 ± 53.31	Cenko et al. 06
<i>051016B</i>	08:48:27.60	+13:39:25.50	0.94^{H}	0.71 ± 0.13	29.81 ± 14.40	Sharapov et al. 05
<i>051006</i>	07:23:13.52	+09:30:24.48	$1.06^{2,\text{H}}$	1.11 ± 0.20	85.57 ± 67.96	Rumyantsev et al. 05
<i>050802</i>	14:37:05.69	+27:47:12.20	1.71	0.79 ± 0.08	249.00 ± 22.97	Pavlenko et al. 05
<i>050801</i>	13:36:35.00	-21:55:41.00	1.38	1.11 ± 0.05	141.00 ± 6.50	Fynbo et al. 05
<i>050730</i>	14:08:17.13	-03:46:16.70	3.97	0.54 ± 0.05	256.00 ± 23.61	Holman et al. 05, Burenin et al. 05, Klotz et al. 05, Damerdji et al. 05, D'Elia et al. 05, Bhatt & Sahu et al. 05
<i>050714B</i>	11:18:48.00	-15:32:49.90	<3.40			
<i>050406</i>	02:17:52.30	-50:11:15.00	2.70	1.12 ± 0.15	22.51 ± 11.16	Berger et al. 05
<i>050318</i>	03:18:51.15	-46:23:43.70	1.44			
<i>050315</i>	20:25:54.10	-42:36:02.20	1.95	0.73 ± 0.17	92.16 ± 55.84	Cobb & Bailyn 05

¹ R-band fluxes all evaluated at 2-hours post burst.

² Jakobsson et al. (in prep)

^H Host galaxy redshift

Bibliography

- Abe, M., Sarugaku, Y., Mito, H. et al. 2006, GCN 5021
Afonso, P., Clemens, C., Klose, S. et al. 2008, GCN 8760
Afonso, P., Kruehler, T., Greiner, J. et al. 2009, GCN 9096
Andreev, M., Babina, J, Petkov, V. et al. 2008, GCN 8094
Andreev, M., Sergeev, A., Babina, J et al. 2008, GCN 7655
Andreev, M., Sergeev, A., Babina, J. and Pozanenko, A. 2008, GCN 8615
Antoniuk, K., Rumyantsev, V. and Pozanenko, A. 2006, GCN 5647
Asfandyarov, I., Pozanenko, A. and Ibrahimov, M. 2006, GCN 5434
Baliyan, K. S., Ganesh, S., Vats, H. O. et al. 2006, GCN 5185
Barkana, R. & Loeb, A. 2004, ApJ, 601, 64
Beckwith, S. V. W., Stiavelli, M., Koekemoer, A. M. et al. 2006, ApJ, 132, 1729
Bennett, C. L., Hill, R. S., Hinshaw G. et al. 2003, ApJ, 148, 97
Bennett, C. L., Halpern, M., Hinshaw G. et al. 2003, ApJ, 148, 1
Bennett, C. L., Bay, M., Halpern, M. et al. 2003, ApJ, 583, 1
Berger, E., Oemler, G. and Gladders, M. 2005, GCN 3185
Bersier, D., Gomboc, A., Melandri, A. et al. 2006, GCN 5655
Bikmaev, I., Galeev, A., Sakhbullin, N. et al. 2005, GCN 3831
Blain, A. W., Small, I., Ivison, R. J. et al. 2002, PhR, 369, 111
Bloom, J. S., Kulkarni, S. R., and Djorgovski, S. G. 2002, ApJ, 123, 1111
Bouwens, R. J., Illingworth, G. D., Blakeslee, J. P. and Franx, M. 2006, ApJ, 653, 53
Bouwens, R. J., Illingworth, G. D., J. P. and Franx, M. and Ford, H. 2008, ApJ, 686, 230
Bouwens, R. J., Illingworth, G. D., Bradley, L. D. et al. 2009, ApJ, 690, 1764
Bouwens, R. J., Illingworth, G. D., Oesch, P. A. et al 2010, ApJ, 709, L133
Briggs, M. S., Pendleton, G. N., Kippen, R. M. et al. 1999, ApJ, 122, 503
Bunker, A. J., Wilkins, S., Ellis, R. S. et al. 2010, MNRAS, 409, 855
Burenin, R., Tkachenko, A., Pavlinsky, M. et al. 2005, GCN 3718
Burenin, R., Tkachenko, A., Pavlinsky, M. et al. 2008, GCN 7275
Cenko, S. B. 2006, GCN 5844
Cenko, S. B., Butler, N. R., Ofek, E. O. et al. 2009, ApJ, 140, 224
Cenko, S. B., and Ofek, E. O. 2006, GCN 5309
Cenko, S. B., and Rau, A. 2006, GCN 5512
Cenko, S. B., Soderberg, A. M., Ofek, E. and Fox, D. B. 2006, GCN 4490
Cenko, S. B., Kelemen, J., Harrison, F. A. et al. 2009, ApJ, 693, 1493
Cenko, S. B., Morgan, A. N., Perley, D. A. et al. 2009, GCN 8965
Chapman, S. C., Blain, A. W., Smail, I. and Ivison, R. J. 2005, ApJ, 622, 772
Chapman, R., Tanvir, N., Rol, E. et al. 2005, GCN 3375
Chen, I. C., Huang, K. Y. and Urata, Y. 2007a, GCN 7067
Chen, I. C., Huang, K. Y. and Urata, Y. 2007b, GCN 7083
Cobb, B. E. 2007, GCN 6296

Cobb, B. E. 2008, GCN 8356
Cobb, B. E. 2008, GCN 8452
Cobb, B. E. 2008, GCN 8547
Cobb, B. E. 2009, GCN 8534
Cobb, B. E. and Bailyn, C. D. 2005, GCN 3104
Cobb, B. E. and Bailyn, C. D. 2005, GCN 3506
Cobb, B. E. and Bailyn, C. D. 2008, ApJ, 677, 1157
Colgate, S. A. and Petschek, A. G. 1981, ApJ, 248, 771
Costa, E., Frontera, F., Heise, J. et al. 1997, Nature, 387, 783
Covino, S., Campana, S., Conciatore, M. L. et al. 2010, A&A, 521, A53
Covino, S., Israel, G. L., Ghinassi, F., and Pinilla, N. 2006, GCN 5167
Covino, S., Malesani, D., Antonelli, L. A. and Fugazza, D. 2006, GCN 4911
Covino, S., Tagliaferri, G., Chincarini, G. et al. 2007, GCN 6426
Cucchiara, A. and Fox, D. B. 2008, GCN 7276
Curran, P. A., Wijers, R. A. M. J., Heemskerk, M. H. M. et al. 2008, A&A, 490, 1047
D'Avanzo, P., D'Elia, V., Covino, S. et al. 2008, GCN 8528
D'Avanzo, F., Fugazza, D., Antonelli, L. A. et al. 2008, GCN 7311
D'Avanzo, P., Fugazza, D., Masetti, N. et al. 2005, GCN 3171
D'Avanzo, P., Israel, G. L. and Cosentino, R. 2006, GCN 4890
D'Avanzo, P., Levan, A. J., Malesani, D. et al. 2009, GCN 9284
D'Avanzo, P., Magazzu, A., de Gurtubai, A. G. and Antonelli, L. A. 2007, GCN 6108
D'Avanzo, P., Piranomonte, S., Magazzu, A. and Mainella, G. 2006, GCN 5151
D'Avanzo, P., Thoene, C. C., Fugazza, D. et al. 2009a, GCN 8873
D'Avanzo, P., Thoene, C. C., Fugazza, D. et al. 2009b, GCN 8887
D'Elia, V., Melandri, A., Fiore, F. et al. 2005, GCN 3746
D'Elia, V., Melandri, A., Fiore, F. et al. 2005, GCN 3775
D'Elia, V., Piranomonte, S., Fiore, F. et al. 2005, GCN 4044
Damerdjji, Y., Klotz, A., Boer, M. and Atteia, J. L. 2005, GCN 3741
de Ugarte Postigo, A., Gorosabel, J. and Castro-Tirado, A. J. 2006, GCN 5288
de Ugarte Postigo, A., Gorosabel, J., Knapen, J. H. et al. 2009, GCN 8810
de Ugarte Postigo, A. and Kubanek, P. 2006, GCN 5656
de Ugarte Postigo, A. and Malesani, D. 2008, GCN 8366
Durig, D. T., McLarty, N. P. and Manning, J. R. 2005, GCN 3950
Eliasdottir, A., Fynbo, J. P. U., Hjorth, J. et al. 2009, ApJ, 697, 1725
Evans, P. A., Beardmore, A. P., Page, K. L. et al. 2007, A&A, 469, 379
Evans, P. A., Beardmore, A. P., Page, K. L. et al. 2009, MNRAS, 397, 1177
Fishman, G. J. & Meegan, C. A. 1995, ARA&A, 33, 415
Fox, D. B. and Cenko, S. B. 2005, GCN 3912
Fox, D. B., Rau, A. and Ofek, E. O. 2006, GCN 5597
Fruchter, A. S., Levan, A. J., Strolger, L. et al. 2006, Nature, 461, 463
Fu, K. J., Lee, Y. H., Huang, K. Y. et al. 2007, GCN 6311

Fugazza, D., Malesani, D., and Covino, S. 2006, GCN 5347
 Furlanetto, S. R. & Loeb, A. 2003, ApJ, 588, 18
 Fynbo, J. P. U. 2006, GCN 5818
 Fynbo, J. P. U., Gorosabel, J., Jensen, B. L. and Naeraenen, J. 2006, GCN 4677
 Fynbo, J. P. U., Jakobsson, P., Prochaska, J. X. et al. 2009, ApJ, 185, 526
 Fynbo, J. P. U., Jensen, B. L., Hjorth, J. et al. 2005, GCN 3736
 Fynbo, J. P. U., Jensen, B. L., Hjorth, J. et al. 2005, GCN 3756
 Garnavich, P. & Karska, A. 2006, GCN 5253
 Gendre, B., Klotz, A., Palazzi, E. et al. 2010, MNRAS, 405, 2372
 Godet, O., Page, K. L., Osborne, J. P. et al. 2006, A&A, 452, 819
 Gorosabel, J., Kubanek, P., Jelinek, M. et al. 2009, GCN 9236
 Gorosabel, J., de Ugarte Postigo, A., Montes, D. et al 2009, GCN 9379
 Greiner, J., Krühler, T., Fynbo, J. P. U. et al. 2009, ApJ, 693, 1610
 Greiner, J., Krühler, T., Klose, S. et al 2011, A&A, 526, A30
 Groot, P. J., Galama, T. J., van Paradijs, J. et al. 1998, ApJ, 493, L27
 Grupe, D., Nousek, J. A., vanden Berk, D. E. et al. 2007, ApJ, 133, 2216
 Guidorzi, C., Bersier, D., Burgdorf, M. 2008, GCN 8508
 Guidorzi, C., Bersier, D. and Tanvir, N. 2009, GCN 9238
 Guidorzi, C., Clemens, C., Kobayashi, S. et al. 2009, A&A, 499, 439
 Guidorzi, C., Melandri, A., O'Brien, P. T. et al. 2009 GCN 9492
 Hafizov, B., Ibrahimov, M. and Pozanenko, A. 2006, GCN 5567
 Haislip, J. and Reichart, D. 2005, GCN 3719
 Halpern, J. P., Mirabal, N. and Armstrong, E. 2006a, GCN 5840
 Halpern, J. P., Mirabal, N. and Armstrong, E. 2006b, GCN 5847
 Henych, T., Kocka, M., Hroch, F. et al. 2005, GCN 4026
 Hicken, M. and Garnavich, P. 2007, GCN 5070
 Hopkins, A., and Beacom, J. F. 2006, ApJ, 651, 142
 Holland, S. T., Sbarufatti, B., Shen, R. et al. 2010, ApJ, 717, 223
 Holman, M., Garnavich, P. and Stanek, K. Z. 2005, GCN 3716
 Homewood, A. L., Garimella, K. V., Hartmann, D. H. et al. 2006, GCN 4688
 Homewood, A., Hartmann, D. H., Garimella, K. et al. 2005, GCN 3491
 Hurkett, C. P., Osborne, J. P., Page, K. L. et al. 2005, MNRAS, 368, 1101
 Ibrahimov, M., Karimov, R., Rumyantsev, V. and Pozanenko, A. 2008, GCN 7975
 Iizuka, R., Matsuda, K., Naito, H. et al. 2007, GCN 6316
 Im, M., Park, W., Jeon, Y. et al. 2009a, GCN 9248
 Im, M., Jeon, Y., Park, W. et al. 2009b, GCN 9275
 Iye, M., Ota, K., Kashikawa, N. et al. 2006, Nature, 443, 186
 Jakobsson, P., Fynbo, J. P. U., Jensen, B. L. et al. 2006, GCN 5782
 Jakobsson, P., Fynbo, J. P. U., Malesani, D. et al. 2008, GCN 7757
 Jakobsson, P., Hjorth, J., Fynbo, J. P. U. et al. 2004, ApJ, 617, L21
 Jakobsson, P., Hjorth, J., Malesani, R. et al. in prep.

Jakobsson, P., Levan, A., Fynbo, J. P. U. et al. 2006, *A&A*, 447, 897
 Jakobsson, P., Paraficz, D., Telting, J. et al. 2005, GCN 4015
 Jakobsson, P., Vreeswijk, P., Ellison, S. et al. 2006, GCN 5319
 Jakobsson, P., Vreeswijk, P. M., Hjorth, J. et al. GCN 6952
 Jakobsson, P., Vreeswijk, P. M., Xu, D., and Thoene, C. C. 2008, GCN 7832
 Jelinek, M., Castro-Tirado, A. J., Casanova, V. et al. 2007, GCN 6418
 Jelinek, M., de Ugarte Postigo, A., Casanova, V. et al. 2005, GCN 3255
 Jensen, B. L., Fynbo, J. P. U., Hjorth, J. et al. 2005, GCN 3809
 Kahharov, B., Ibrahimov, M., Sharapov, D. et al. 2005, GCN 3174
 Kahharov, B., Ibrahimov, M., Sharapov, D. et al. 2005, GCN 3274
 Kann, D. A., Klose, S., Zhang, B. et al. 2010, *ApJ*, 720, 1513
 Kann, D. A., Laux, U., and Ertel, S. 2008, GCN 7845
 Kann, D. A., Laux, U. and Stecklum, B. 2009, GCN 9436
 Karska, A. and Garnavich, P. 2006, GCN 5260
 Kashikawa, N., Shimasaku, K., Malkan, M. A. Et al. 2006, *ApJ*, 648, 7
 Khamitov, I., Bikmaev, I., Sakhibullin, N. et al. 2006, GCN 5173
 Khamitov, I., Saygac, A. T., Aslan, Z. et al. 2006, GCN 5235
 Kistler, M. D., Yüksel, H., Beacom, J. F. et al. 2009, 705, L104
 Klebesadel, R. W., Strong, I. B. and Olson, R. A. 1973, *ApJ*, 182, L85
 Klotz, A., Boer, M. and Atteia, J. L. 2005, GCN 3720
 Klotz, A., Boer, M. and Atteia, J. L. 2007a, GCN 6235
 Klotz, A., Boer, M. and Atteia, J. L. 2007b, GCN 7065
 Klotz, A., Boer, M. and Atteia, J. L. 2008a, GCN 7795
 Klotz, A., Boer, M. and Atteia, J. L. 2008b, GCN 7799
 Kocka, M., Nekola, M., Strobl, J. et al 2008, GCN 7651
 Komatsu, E., Dunkley, J., Nolta, M. R. et al. 2009, *ApJ*, 180, 330
 Komatsu, E., Smith, K. M., Dunkley, J. et al. 2011, *ApJS*, 192, 18
 Kosugi, G., Kawai, N., Aoki, K. et al. 2005, GCN 3263
 Krimm, H., Barthelmy, S. D., Baumgartner, W. et al. 2008, GCN 7926
 Krühler, T., Greiner, J., McBreen, S. et al. 2009, *ApJ*, 697, 758
 Kruehler, T., Schrey, F., Greiner, J. et al. 2008, GCN 8075
 Kuroda, D., Yoshida, M., Yanagisawa, K. et al. 2008, GCN 8724
 Lamb, D. Q. & Reichart, D. E. 2000, *ApJ*, 536, 1
 Lamb, D. Q., Donaghy, T. Q. and Graziani, C. 2004, *NewAR*, 48, 423
 Lapez-Sanchez, A. R., Garcea-Rojas, J., Jelaneck, M. et al. 2006, GCN 5013
 Lehnert, M. D., Nesvadba, N. P. H., Cuby, J. G. et al. 2010, *Nature*, 467, 940
 Levan, A., Fruchter, A., Rhoads, J. et al. 2006, *ApJ*, 647, 471
 Levan, A. J., Jakobsson, P., Thoene, C. C. et al. 2009, GCN 9409
 Levesque, E. M., Kewley, L. J., Graham, J. F. and Fruchter, A. S. 2010, *ApJ*, 712, L26
 Li, W., Chornock, R., Perley, D. A. et al. 2008a, GCN 7438
 Li, W., Chornock, R., Perley, D. A. et al. 2008b, GCN 7959

Lin, Z. Y., Huang, K. Y., Ip, W. H. et al. 2005, GCN 3628
 Lin, C. S., Huang, K. Y., and Ip, W. H. 2006, GCN 5169
 Lin, C. S., Lin H. C., Chen, C. W. et al. 2006, GCN 4696
 Liu, H., Wang, J., Xin, L. P. et al. 2008, GCN 8618
 MacFadyen, A. I., & Woosley, S. E. 1999, ApJ, 524, 262
 Malesani, D., Augustteijn, T., Mackay, C. et al 2009, GCN 9671
 Malesani, D., Fiore, F., Masetti, N. et al. 2006, GCN 5225
 Malesani, D. and Fynbo, J. P. U. 2009, GCN 9108
 Malesani, D., Fynbo, J. P. U., Leloudas, G. et al. 2008, GCN 8639
 Malesani, D., Fynbo, J. P. U., Stempels, E., and Pursimo, T. 2008, GCN 8688
 Malesani, D., Fynbo, J. P. U., Vreeswijk, P. M. et al. 2008, GCN 7436
 Malesani, D. and Uthas, H. 2007, GCN 6281
 Malesani, D., Jakobsson, P., Fynbo, J. P. U. et al. 2007, 6651
 Malesani, D., Jakobsson, P., Levan, A. J. et al. 2008, GCN 8039
 Malesani, D., Jakobsson, P., Vreeswijk, P. M. et al. 2007, GCN 6055
 Malesani, D., Jaunsen, A. O. and Vreeswijk, P. M. 2007, GCN 6015
 Malesani, D., Navasardyan, H., Piranomonte, S. et al. 2006, GCN 4706
 Malesani, D. and Patat, F. 2006, GCN 5450
 Malesani, D., Quirion, P. O., Fynbo, J. P. U. and Jakobsson, P. 2008, GCN 7783
 Malesani, D., Piranomonte, S., Fiore, F. et al. 2005, GCN 3469
 Malesani, D., Thoene, C. C., Fynbo, J. P. U. et al. 2007, GCN 6565
 Malesani, D., Vreeswijk, P. M., Fynbo, J. P. U. et al. 2008, GCN 7940
 Malhotra, S. & Rhoads, J. E. 2006, ApJ, 647, L95
 Mao, J., Cha, G. and Bai, J. 2009, GCN 9305
 McLure, R. J., Dunlop, J. S., Cirasuolo, M. et al. 2010, MNRAS, 403, 960
 McNaught, R. and Price, P. A. 2005, GCN 3163
 McQuinn, M., Lidz, A., Zaldarriaga, M. et al. 2008, MNRAS, 388, 1101
 Meegan, C. A., Fishman, G. J., Wilson, R. B. et al. 1992, Nature, 355, 143
 Melandri, A., Bersier, D. F., Burgdorf, M. et al. 2008, GCN 8475
 Melandri, A., Gomboc, A., Smith, R. J. and Tanvir, N. 2006, GCN 5579
 Melandri, A., Guidorzi, C., Gomboc, A. et al. 2006, GCN 5594
 Melandri, A., Kobayashi, S., Mundell, C. G. et al 2010, ApJ, 723, 1331
 Melandri, A., Mundell, C. G., Kobayashi, S. et al 2008, ApJ, 686, 1209
 Mészáros, P. & Rees, M. J. 2010, ApJ, 715, 967
 Metzger, M. R., Djorgovski, S. G., Kulkarni, S. R. et al 1997, 387, 878
 Milne, P. A. and Williams, G. G. 2006, GCN 4699
 Milne, P. A. and Williams, G. G. 2007, GCN 7011
 Minezaki, T., Price, P. A., Yoshii, Y. et al. 2007, GCN 7018
 Minezaki, T., Price, P. A., Yoshii, Y. and Cowie, L. L. 2007, GCN 7135
 Mirabal, N., Bonfield, D., and Schawinski, K. 2005, GCN 3488
 Mirabal, N., Melandri, A. and Halpern, J. P. 2007, GCN 6162

Misra, K. 2006, GCN 4742

Misra, K., Kamble, A. P. and Pandey, S. B. 2005, GCN 3130

Misra, K., Kamble, A. P. and Pandey, S. B. 2005, GCN 3175

Mitrofanov, I. G. & Sagdeev, R. Z. 1990, *Astron. Zh.*, 68, 590

Monfardini, A., Kobayashi, S., Guidorzi, C. et al. 2006, *ApJ*, 648, 1125

Muaoz Maran, V., Sabater, J., Castro-Tirado, A. J. et al. 2005, GCN 7291

Muehleger, M., Duscha, S., Stefanescu, A. et al. 2006, GCN 5404

Mundell, C. G., Melandri, A., Guidorzi, C. et al. 2007, *ApJ*, 660, 489

Munz, F., Terra, F., Greco, G. et al. 2008, GCN 7563

Nemiroff, R. J. 1994, *Comments on Astrophysics*, 17, 189

Nishiura, S., Tomita, H., Urata, Y. et al 2007, GCN 6308

Novak, R. 2005, GCN 4027

Nysewander, M., Reichart, D. E., Crain, J. A. et al. 2009, *ApJ*, 693, 1417

Oates, S. R., Mundell, C. G., Piranomonte, S. et al. 2006, *MNRAS*, 372, 327

Oesch, P. A., Bouwens, R. J., Illingworth, G. D. et al. 2010, *ApJ*, 709, L16

Ofek, E. O., Cenko, S. B., Soderberg, A. M. and Fox, D. B. 2006, GCN 4691

Oksanen, A. and Hentunen, V. P. 2008, GCN 7657

Olivares, F., Yoldas, A. K., Greiner, J. et al. 2009, GCN 9245

Olivares, F., Kruehler, T., Greiner, J. et al. 2009, GCN 9303

Olofsson, G. and Fynbo, J. P. U., GCN 8425

Pavlenko, E., Efimov, Y., Shlyapnikov, A. et al. 2005, GCN 3744

Pavlenko, E., Rumyantsev, V. and Pozanenko, A. 2009, GCN 9179

Pavlenko, E., Shlyapnikov, A., Efimov, Y. et al. 2005, GCN 3783

Perley, D. A., Cenko, S. B., Bloom, J. S. et al. 2009, *ApJ*, 138, 1690

Piran, T. 1999, *Physics Reports*, Vol 314, Issue 6, 575

Piranomonte, S., Calzoletti, L., D'Avanzo, P. et al. 2005, GCN 3953

Piranomonte, S., Magazzu, A., Mainella, G. et al. 2005, GCN 4032

N. Pirzkal et al., STScI-PRC07-31

Pozanenko, A., Shulga, A., Volnova, A. et al. 6407

Price, P. A., Minezaki, T., Cowie, L. and Yoshii, Y. 2005, GCN 3312

Price, P. A., Minezaki, T., Cowie, L. L. et al. 2006, GCN 4854

Racusin, J. L., Karpov, S. V., Sokolowski, M. et al. 2008, *Nature*. 455, 183

Rau, A., Kasliwal, M. M. and Cenko, S. B. 2007, GCN 6436

Rhoads, J. E. and Malhotra, S. 2001, *ApJ*, 563, L5

Rhoads, J. E., Dey, A., Malhotra, S. et al. 2003, *ApJ*, 125, 1006

Rhoads, J. E., Xu, C., Dawson, S. et al. 2004, *ApJ*, 611, 59

Rhoads, J. E., Panagia, N., Windhorst, R. A. et al. 2005, *ApJ*, 621, 582

Rhoads, J. E., Malhotra, S., Pirzkal, N. et al 2009, *ApJ*, 697, 942

Richards, G. T., Strauss, M. A., Fan, X. et al. 2006, *ApJ*, 131, 2766

Rol, E., Guidorzi, C., Gomboc, A. et al. 2008, GCN 7801

Rol, E., Wijers, R. A. M. J., Kouveliotou, C. et al. 2005, *ApJ*, 624, 868

Rossi, A., Afonso, P. and Greiner, J. 2009, GCN 9395
 Rossi, A., Clemens, C., Greiner, J. et al. 2008, GCN 8296
 Rossi, A. and Greiner, J. 2009, GCN 8849
 Rossi, A., Kruehler, T., Greiner, J. et al. 2008, GCN 8266
 Ruiz-Velasco, A. E., Swan, H., Troja, E. et al. 2007, ApJ, 669, 1
 Rummyantsev, V., Antonyuk, K., Andreev, M. and Pozanenko, A. 2008, GCN 8645
 Rummyantsev, V., Antoniuk, K., Pozanenko, A. et al. 2009, GCN 9320
 Rummyantsev, V., Biryukov, V., Pozanenko, A. et al. 2005, GCN 3939
 Rummyantsev, V., Biryukov, V. and Pozanenko, A. 2006, GCN 4610
 Rummyantsev, V., Biryukov, V., Pozanenko, A. and Ibrahimov, M. 2005, GCN 4094
 Rummyantsev, V. and Pozanenko, A. 2008a, GCN 7857
 Rummyantsev, V. and Pozanenko, A. 2008b, GCN 8667
 Rummyantsev, V., Pozanenko, A., Ibrahimov, M. and Asfandyarov, I. 2006, GCN 5306
 Rummyantsev, V., Shakhovkoy, D., Sergeev, S. et al. 2008, GCN 8630
 Salvaterra, R., Della Valle, M., Campana, S. et al 2009, Nature, 461, 1258
 Sanchawala, K., Wu, W. L., Huang, K. Y. et al. 2005, GCN 3334
 Sarugaku, Y., Miura, N., Zheng, Z. W. et al. 2006, GCN 5634
 Schady, P., Page, M. J., Oates, S. R. et al. 2009, MNRAS 401, 2773
 Schaefer, B. E. 1999, ApJ, 511, L79
 Schmidt, B., Peterson, B. and Lewis, K. 2006, GCN 5258
 Sharapov, D., Abdullaeva, G., Ibrahimov, M. et al. 2005, GCN 3897
 Sharapov, D., Augusteijn, T., Pozanenko, A. et al. 2006, GCN 5263
 Sharapov, D., Ibrahimov, M., Karimov, R. et al. 2005, GCN 3124
 Sharapov, D., Ibrahimov, M., Pozanenko, A. and Rummyantsev, V. 2005, GCN 4185
 Sharapov, D., Ibrahimov, M., Pozanenko, A. and Rummyantsev, V. 2005, GCN 4308
 Sharapov, D., Ibrahimov, M., Pozanenko, A. and Rummyantsev, V. 2006, GCN 4902
 Shakhovskoy, D., Rummyantsev, V., Biryukov, V., and Pozanenko, A. 2007, GCN 6485
 Sorensen, P. and Azzaro, M. 2002, <http://catserver.ing.iac.ex/staralt/>
 Spergel, D. N., Verde, L., Peiris, H. V. et al. 2003, ApJ, 148, 175
 Stacy, A., Greif, T. H. and Bromm, V. 2010, MNRAS, 403, 45
 Starling, R. L. C., Rol, E., van der Horst, A. J. et al. 2009, MNRAS, 400, 90
 Steidel, C. C., Giavalisco, M., Dickinson, M. and Adelberger, K. L. 1996, AJ, 112, 3525
 Steidel, C. C., Adelberger, K., Giavalisco, M. et al. 1999, ArXiv Astrophysics e-prints
 Steidel, C. C., Adelberger, K., Giavalisco, M. et al. 1999, ApJ, 519, 1
 Steidel, C. C., Pettini, M. and Adelberger, K. 2001, ApJ, 546, 665
 Steidel, C. C., Adelberger, K., Shapley, A. E. et al. 2003, ApJ, 592, 728
 Stefanescu, A., Duscha, S., Kanbach, G. et al. 2007, GCN 6723
 Tanvir, N. R., Fox, D. B., Levan, A. J. et al. 2009, Nature, 461, 1254
 Tanvir, N. R., Levan, A. J., Rol, E et al. 2008, MNRAS, 388, 1750
 Tanvir, N., Rol, E., and Hewett, P. 2006, GCN 5216
 Tanvir, N. R., Rol, E., Stephens, A. et al. 2008, GCN 7488

Trenti, M. & Stiavelli, M. 2009, *ApJ*, 694, 879

Trenti, M., Stiavelli, M. & Shull, M. 2009, *ApJ*, 700, 1679

Tristram, P., Castro-Tirado A. J., de Ugarte Postigo, A. et al. 2007, GCN 6312

Thoene, C. C., Fynbo, J. P. U. and Jakobsson, P. 2006, GCN 5747

Thoene, C. C., Fynbo, J. P. U., Jakobsson, P. et al 2006, GCN 5812

Thoene, C. C., Fynbo, J. P. U., de Ugarte Postigo, A. et al. 2008, GCN 7658

Thoene, C. C., Kann, D. A., Augusteijn, T. and Reyle-Laffont, C. 2007, GCN 6154

Thoene, C. C., Kann, D. A. and Augusteijn, T. 2007, GCN 6142

Thoene, C. C., Malesani, D., Fynbo, J. P. U. et al. 2006a, GCN 5799

Thoene, C. C., Malesani, D., Fynbo, J. P. U. et al. 2006b, GCN 5807

Thoene, C. C., Malesani, D., Fynbo, J. P. U. et al. 2008, GCN 7878

Uemura, M., Arai, A. and Uehara, T. 2007, GCN 6171

Updike, A. C., Hartmann, D. H. and Rumstay, K. S. 2007, GCN 7084

Updike, A. C., Hartmann, D. H. and Rumstay, K. et al. 2007, GCN 6317

Updike, A. C., Williams, G. G., Milne, P. A. and Hartmann, D. H. 2008, GCN 7288

Updike, A., Rau, A., Kruehler, T. et al 2009, GCN 9773

Usov, V. 1992, *Nature*, 357, 472

van der Horst, A. J., Kouveliotou, C., Gehrels, N. et al. 2009, *ApJ*, 699, 1087

van Paradijs, J., Groot, P. J., Galama, T. et al. 1997, *Nature*, 386, 686

Vreeswijk, P. M., Fynbo, J. P. U., Malesani, D., GCN 8191

Wang, X. F., Li, J. Z., Feng, Q. C. et al. 2008, GCN 7550

Watson, D., Fynbo, J. P. U., Ledoux, C. et al. 2005, *ApJ*, 652, 1011

Waxman, E. and Draine, B. T. 2007, *ApJ*, 537, 796

Willingale, R., O'Brien, P. T., Osborne, J. P. et al. 2007, *ApJ*, 662, 1093

Willingale, R., 2008, private communication

Willott et al. 2010, *AJ*, 139, 906

Wozniak, P. R., Vestrand, W. T., Wren, J. et al. 2006, GCN 4687

Xin, L.P., Feng, Q. C., Zhai, M. et al. 2008, GCN 7814

Xin, L. P., Meng, X. M., Zhai, M. et al. 2008, GCN 7371

Xin, L. P., Wang, X. F., Zheng, W. K. et al. 2009, GCN 9142

Xin, L. P., Zhai, M., Qiu, Y. L. et al. 2007a GCN 6416

Xin, L. P., Zhai, M., Qiu, Y. L. et al. 2007b GCN 6962

Xu, D., Leloudas, G., Malesani, D. et al. 09, GCN 9755

Yanagisawa, K., Toda, H., and Kawai, N. 2005, GCN 3489

Yanagisawa, K., Toda, H., and Kawai, N. 2006, GCN 4517

Yang, M., Huang, K. Y., Ip, W. H. et al. 2006, GCN 4631

Yoshioka, T., Chen, C. W., Nishiura, S. et al. 2005, GCN 3120

Zheng, W. K., Deng, J. S. and Wang, J. 2009, *Research in Astron. Astrophys.*, 9, 1103

Zheng, W. K., Zai, M., Qiu, Y. L. et al. 2006, GCN 4802